The Investigation of Nitrite Accumulation and Biological Phosphorus Removal in an Intermittently Aerated Process Combining Shortcut Nitrogen Removal and Sidestream Biological Phosphorus Removal

Kathryn Elizabeth Printz

Thesis submitted to the faculty of Virginia Polytechnic Institute and State University in partial fulfillment of the requirements for the degree of

Masters of Science
In
Civil Engineering

Amy J. Pruden
Jason He
Charles B. Bott

October 16th, 2019
Blacksburg VA

Keywords: Post-anoxic denitrification, RAS fermentation, sidestream fermentation, partial denitrification, deammonification

The Investigation of Nitrite Accumulation and Biological Phosphorus Removal in an Intermittently Aerated Process Combining Shortcut Nitrogen Removal and Sidestream Biological Phosphorus Removal

Kathryn Elizabeth Printz

Technical Abstract

The research in this thesis was conducted at the Hampton Road Sanitation District's biological nutrient removal pilot, located at the Chesapeake-Elizabeth WWTP in Virginia Beach, VA. The pilot is operated in an A/B process with a high-rate, carbon-diverting A-stage, followed by a biological nitrogen removal B-stage containing four intermittently aerated CSTRs, followed by an anammox polishing MBBR. The goal of this research was to successfully combine short-cut nitrogen removal with sidestream enhanced biological nutrient removal (EBPR) in the most efficient way possible, specifically aiming to decrease cost and energy requirements, divert the most amount of carbon possible before B-stage, and to achieve low effluent nitrogen and phosphorus concentrations.

A RAS fermenter (SBPR) and an A-stage WAS fermenter that feeds VFA into the SBPR (the supernatant of the fermenter is called fermentate) were implemented in order to enhance biological phosphorus removal. About 8 months after the RAS and WAS fermenter implementation, there was a 28 day consecutive period of low B-stage effluent OP <1 mg/L, with an average of 0.5 ± 0.1 mg/L OP. Following this low effluent OP period, bio-P became more unstable and there was high nitrite accumulation in the B-stage effluent for 106 days with concentrations ranging from 1.1-5.9 mg/L NO_2. The nitrite accumulation was not due to NOB out-selection, confirmed by AOB & NOB maximum activity tests. It was determined that the nitrite accumulation was due to partial denitrification of nitrate to nitrite by bacteria using internally stored carbon, because profiles and activity tests showed anoxic nitrite accumulation at the end of the aerobic process. Post-anoxic denitrification using internally stored carbon compounds has been observed in other EBPR systems (Vocks, Adam, Lesjean, Gnirss, & Kraume, 2005).

Fermentate addition was then halted, and nitrite accumulation and bio-P activity ceased all together, linking the fermentate addition to both bio-P activity and nitrite accumulation. Fermentate was then controlled to dose at 60% of the sCOD/OP (fermentate sCOD g/day / total OP- fermentate + influent - g/day) of the first low effluent OP period. During this fermentate dosing period where the average sCOD/OP was 15.6 ± 3.0 g/g, no nitrite accumulation was observed, but another consecutive low effluent OP period was observed with an average of 0.6 ± 0.2 mg/L OP.

Linear correlation analysis shows that the highest r^2 values relating the low effluent OP periods and the COD loads to the SBPR for both periods were between VFA g/day vs OP effluent mg/L, at r^2=0.18 for the first low effluent OP period and r^2=0.65 for the second. There were also high tCOD r^2 values for the second low effluent OP period showing that COD hydrolysis in the SBPR could have impacted bio-P activity. However, the VFA r^2 value was higher than any tCOD r^2 value, concluding that the fermentate dosing mainly worked to enhance biological phosphorus removal by increasing the VFA load in g VFA as acetate/day. Since no nitrite was observed in a period with a lower VFA/OP dose, then the probable VFA load needed to provide enough internal storage to produce nitrite accumulation by partial denitrification is between 5-9 (g VFA as acetate/ g total OP). If sidestream EBPR systems could be studied further to promote nitrite accumulation and bio-P activity to produce low effluent OP, then short-cut nitrogen removal and EBPR could be successfully combined in an efficient way.

The Investigation of Nitrite Accumulation and Biological Phosphorus Removal in an Intermittently Aerated Process Combining Shortcut Nitrogen Removal and Sidestream Biological Phosphorus Removal

Kathryn Elizabeth Printz

General Audience Abstract

It is important to reduce nitrogen and phosphorus concentrations in wastewater treatment effluent in order to both protect the environment from eutrophication and to meet the increasingly stringent nutrient effluent discharge limits imposed by the EPA. Conventional biological nitrogen removal is achieved through nitrification and denitrification converting ammonia to nitrogen gas, where nitrogen gas is volatile and leaves the system naturally. Phosphorus removal can be achieved through either chemical addition or through biological phosphorus removal, where phosphorus is taken up in cells and removed from the system by the subsequent solids wasting of these cells. The combination of biological nitrogen and phosphorus removal can be improved to increase energy efficiency, reduce costs including aeration and chemical addition costs, increase system capacity and reduce tank sizes, and reduce biomass production, all while achieving low effluent N and P concentrations.

Short-cut nitrogen removal can increase the efficiency of biological nitrogen removal. Deammonification, the combination of partial nitritation and anammox, has the potential to reduce wastewater treatment plant (WWTP) aeration costs by 63%, carbon requirements by 100%, and biomass production by 80% (Nifong, Nelson, Johnson, & B. Bott, 2013). Deammonification is the combination of partial nitritation and anammox. Anaerobic ammonia oxidation (anammox) is a useful class of bacteria that converts ammonia and nitrite straight to nitrogen gas in anaerobic conditions, which is a more direct pathway than the conventional nitrification-denitrification pathway. Anammox requires a nitrite supply, which can supplied by partial nitratation of ammonia to nitrite, performed by ammonia oxidizing bacteria (AOB) aerobically in the deammonification process. In order for partial nitratation to work, there needs to be nitrite oxidizing bacteria (NOB) out-selection so that the nitrite produced by AOB does not get oxidized to nitrate.

Enhanced biological phosphorus removal (EBPR) is accomplished by the taking up and storing of orthophosphate (OP) by phosphorus accumulating organisms (PAOs). These organisms require an anaerobic carbon-storage phase followed by an aerobic growth phase where the internally stored carbon is used for growth. During the cell growth phase of PAOs in aerobic conditions, PAOs are able to take up more OP than they previously released in anaerobic conditions, creating a net OP removal from the system. There has been recent success in recycle activated sludge (McIlroy et al.) fermentation to enhance biological phosphorus removal, which

works to promote hydrolysis, fermentation, and EBPR enhancement (Houweling, Dold, & Barnard, 2010). A portion of the RAS is introduced to an anaerobic zone before returning to the main process, allowing for extra VFA production and adsorption by PAOs. RAS fermentation solves the issue of carbon needed for EBPR in VFA/carbon limited systems without having to add too much additional carbon, creating a carbon efficient EBPR system.

The research outlined in this study was done at the Hampton Road Sanitation District's (HRSD) pilot plant located within HRSD's Chesapeake-Elizabeth WWTP in Virginia Beach VA. The pilot is run in an A/B process that works in two separate steps: the A-stage is the first step that works to remove carbon by oxidation, and by adsorption so it can potentially be diverted, and the B-stage is the second step where biological nitrogen removal (BNR) is done. The BNR phase consists of an anaerobic selector followed by four completely stirred tank reactors (CSTRs) that are intermittently aerated to provide aerobic and anoxic phases. The pilot also has an anammox polishing step following B-stage. The nitrogen removal goal for this research was short-cut nitrogen removal via deammonification, by producing partial nitritation in B-stage and polishing with anammox. A B-stage RAS fermenter, along with an A-stage waste activated sludge (WAS) fermenter that feeds VFA into the RAS fermenter, was implemented to the existing pilot to enhance biological phosphorus removal. The overall goal of this study was to successfully combine short-cut nitrogen removal with sidestream EBPR to achieve low effluent N and P concentrations in the most energy and carbon efficient way possible.

EBPR was achieved about eight months after the implementation of the RAS and WAS fermenter to the pilot. A period of B-stage effluent OP that was consistently below 1 mg/L OP was observed right before an unexpected period of high nitrite in the B-stage effluent. The high effluent nitrite lasted for 106 days and ranged from 1.1-5.9 mg/L of effluent nitrite during this time. The nitrite accumulation was unexpected because weekly maximum activity tests for AOB and NOB showed that NOB out-selection was not occurring. The first phase of this research investigates the cause of the nitrite accumulation. Based on profiles taken in the reactors in the aerobic and anoxic phases, and based on denitrification activity tests, it was determined that the nitrite accumulation was due to partial denitrification of nitrate to nitrite. Because this partial denitrification was happening in the reactor anoxic times where external should have been used up, it was determined that the source of the partial denitrification was from a bacteria using internally stored carbon during anoxic periods as the electron supply for partial denitrification. Research has showed that EBPR systems promote bacteria that are capable of storing carbon internally and keeping that carbon stored through an aerobic phase and then using that stored carbon for denitrification following an aerobic phase (Vocks et al., 2005), like observed in this research.

The second phase of this research sought to link the nitrite accumulation and bio-P activity to the VFA added to the RAS fermenter. The VFA addition was decreased in phases, and with that a

decrease in nitrite in the effluent was observed. The bio-P activity became more unstable after the nitrite accumulation occurred, but all bio-P activity ceased after VFA addition to the RAS fermenter ceased. It was concluded, unsurprisingly, that the VFA added to the RAS fermenter was the source of the internally stored carbon that caused the nitrite accumulation, and necessary for bio-P enhancement.

The third phase of this research sought to recreate the low effluent OP period and the nitrite accumulation by controlling the VFA dose to the RAS fermenter. The average soluble chemical oxygen demand (sCOD) per OP (fermenter sCOD g/day / total OP-fermenter + influent- g/day) of the period of low effluent OP was calculated, and the dose from the WAS fermenter was controlled to meet 60% of the calculated value. The calculated dose was 13.6 gC/gP, but the actual average dose from controlling the load during this period was 15.6 ± 3.0 gC/gP. The average VFA/OP (g VFA as acetate/ g total OP) dose for the first low effluent OP period was 9.4 ± 3.6 g/g, and the average dose for the third phase of research was 5.5 ± 1.3 g/g. No nitrite accumulation occurred in this phase, but another consistent low effluent OP period did occur. From linear correlation analysis, the highest r^2 values relating the low effluent OP periods and the COD loads to the RAS fermenter for both periods were between VFA g/day vs OP mg/L, at r^2=0.18 for the first period and r^2=0.65 for the second. This shows that effluent OP < 1 mg/L can be achieve at 5.5 or 9.4 (g VFA as acetate/ g total OP). Since no nitrite was observed in phase 3, than the probable VFA load needed to provide enough internal storage to produce nitrite accumulation by partial denitrification is probably between 5.5-9.4 (g VFA as acetate/ g total OP).

This research was significant because the link between nitrite accumulation and bio-P enhancement with sidestream RAS and WAS fermentation was confirmed. Partial denitrification of nitrate to nitrite could be used as an alternative source of nitrite for anammox, instead of NOB out-selection and partial nitritation of ammonia to nitrite by AOB, in combined EBPR and short-cut nitrogen removal systems. If sidestream EBPR systems could be used to promote nitrite accumulation and bio-P activity to produce low effluent OP and nitrogen removal efficiently than short-cut nitrogen removal and EBPR could be successfully combined in an efficient way. Future work needs to be done on the organism that is capable of nitrite accumulation and if that organism can be enhanced in conjunction with EBPR organisms to promote both nitrite accumulation and low effluent OP simultaneously.

Acknowledgements

I would like to thank my entire committee, Dr. Amy Pruden, Dr. Charles Bott, and Dr. Jason He. My committee has been generous with their time and support. I would especially like to thank HRSD and Dr. Charles Bott for not just providing me with funding, but for providing me with the opportunity to learn and grow as a scientist, engineer, and person. I am grateful for the incredible opportunity to work at HRSD.

Special thanks to Dr. Stephanie Klaus for taking time to answer questions, provide research and writing guidance, and generally pushing me to learn and grow to the maximum. Without Dr. Klaus this thesis would not have been possible.

My research peers have worked hard and tirelessly to make this research possible. Special thanks to:

Kester McCullough
Lindsey Ferguson
Cody Campolong
Sarah Schoepflin
Kyle Malin
Tyler Robinson
Kaitlyn Greene

Special thanks to my colleagues and friends, Lindsey Ferguson and Samantha Hogard, for their emotional support that made my time as an HRSD intern fulfilling and possible.

Finally, thank you to all of my family and friends for supporting me endlessly on my graduate school journey. From helping me look for apartments to answering every phone call, this thesis partly belongs to my parents, Cindy and David Printz. Thank you to my sister, Emily Printz, for all the added emotional support and joy. Thank you to my best friend, Kaley Brady, for encouraging me to go back to school and for constantly inspiring me to follow my passions. It is because of my incredible support system that I was able to grow emotionally and mentally enough in order to get the most out of my experience.

Table of Contents

Technical Abstract ii
General Audience Abstract iv
Acknowledgements vii
List of Figures x
List of Tables xii
Abbreviations xiii
1. Introduction 1
1.1 Project motivation 2
1.2 Research objectives 3
2. Literature Review 4
2.1 Nitrification 4
2.2 Denitrification 5
2.3 Anammox 6
2.4 Short-cut nitrogen removal 7
2.4.1 Nitritation/denitritation- nitrite shunt 7
2.4.2 Deammonification: partial nitration and anammox 8
2.4.3 Partial denitrification + anammox 9
2.5 NOB out-selection 9
2.5.1 Different DO control strategies for NOB out-selection purposes 10
2.6 Phosphorus removal 12
2.6.1 Glycogen Accumulating Organisms: nuisance organisms in EBPR systems 15
2.6.2 Sidestream EBPR 17
2.6.3 Denitrifying PAOs and GAOs 20
2.7 Post-anoxic denitrification in EBPR systems 22
3. Methodology 25
3.1 A-stage 25
3.2 B-stage 26
3.3 A-stage WAS fermenter 27
3.4 Sidestream biological phosphorus remover (SBPR) 27
3.5 Data analysis 27
3.6 Sampling 28

3.7 AOB/NOB activity measurement 28
3.8 PAO/dPAO activity measurement 28
3.8.1 PAO 29
3.8.2 dPAO 29
3.9 ISCD activity measurement 29
3.10 Profile measurement 30
3.11 Central Environmental Laboratory (CEL) sampling 30
3.12 EA_ANX and EA_EICD tests 30
3.12.1 EA_ANX: system endogenous decay 31
3.12.2 EA_EICD: system internally stored carbon denitrification 31
3.13 Statistical analysis 31
4. Results and Discussion: 33
4.1 Determining the cause of the nitrite accumulation 36
4.2 Decreased fermentate addition / SBPR HRT maximization experiment 39
4.2.1 Operational phase 2A 40
4.2.2 Operational phase 2B 41
4.2.3 Operational phase 2C 42
4.3 Dosing experimental setup- operational phase 3 42
4.4 Operational phase 3 & result phase 3 43
4.4.1 Success in controlled fermentate load 43
4.4.2 Fermenter performance variation 45
4.4.3 Bio-P results 47
4.4.4 PAO activity and profile data also show bio-P activity 53
4.4.5 Negative effects of the high tCOD load to B-stage 55
4.4.6 ISCD activity, endogenous decay, and nitrite accumulation 56
4.4.7 AOB & NOB activity 61
5. Conclusions 63
References 64

List of Figures

Figure 1- AOB and NOB Monod kinetics for Nitrospira dominated system ……...11
Figure 2- General metabolic diagram of a PAO……..…..13
Figure 3- A2/O process flow diagram……...……14
Figure 4- UCT process flow diagram……..……..14
Figure 5- JHB process flow diagram……..…15
Figure 6- 5-S Bardenpho process flow diagram……...……...……..15
Figure 7- General metabolic diagram of a GAO…….…..16
Figure 8- A2O process with RAS fermentation process flow diagram…….……17
Figure 9- Examples of different sidestream flow processes to accomplish bio-P ……....…..19
Figure 10- Theorized metabolism of Tetraspharea working with general PAOs…….……20
Figure 11- Theorized nitrite loop where dPAOs/dGAOs provide a nitrite source for NOB to thrive……..……21
Figure 12- Post anoxic denitrification process flow diagram adapted from Vock's study…..…..23
Figure 13- HRSD's BNR pilot process flow diagram- updated on November 2017……....25
Figure 14- B-stage instrumentation and PID control…….27
Figure 15-: B-stage effluent nitrite (mg NO2-/L) shown on the left y-axis and OP (mg OP/L) shown on the right y-axis for the entire duration of research……..…….…35
Figure 16- Cyanide measured in the influent composite …….…….…...……..…36
Figure 17- B-stage effluent nitrite (mg NO2-/L) is displayed on the left y-axis and NOB/AOB maximum rate test fractions are displayed on the right y-axis …….37
Figure 18- Profile taken in the last CSTR over time on day 320……..…….38
Figure 19- Internally stored carbon denitrification test using MLSS from the last CSRT on day 312. ……..……..……..……..38
Figure 20- B-stage effluent OP (mg OP/L), SBPR HRT (hours), RAS mass split % going into the SBPR, and the fermentate addition into the SBPR (L/min) are displayed over the entire operational phase 2……..……..40
Figure 21- SBPR effluent VFA concentration (mg VFA as acetate/L) and VFA consumed in the SBPR (mg VFA as acetate/L)……..……41
Figure 22- Operational phase 3 (OP3) C/P load and the OP3 load goal along with the fermentate addition used to control the C/P load ……...…..……..…44
Figure 23- C/P and VFA/P throughout the duration of the experiment ……...……..…45
Figure 24- Fermenter VFA yields……..…46
Figure 25- Fermenter soluble COD yields…….....46
Figure 26- B-stage effluent OP (mg OP/L) and nitrite (mg NO2/L). ……..……..…47
Figure 27- Total influent + fermentate COD (g COD/day) and B-stage effluent OP (mg OP/L) ……..……..48

Figure 28 Total influent + fermentate pCOD (g COD/day), total influent + fermentate sCOD (g COD/day), and B-stage effluent OP (mg OP/L)……..……..49
Figure 29- The % of total pCOD addition to B-stage that comes from fermentate and influent, and B-stage effluent OP (mg OP/L)…….....……49
Figure 30- Fermentate load into the SBPR (g VFA as acetate/day) and B-stage effluent OP (mg OP/L)……..…50
Figure 31- Fermentate mass added to system divided by mainstream flow for COD, sCOD, and OP……..……....……...….52
Figure 32- PAO maximum activity rates from weekly tests……...53
Figure 33- System OP uptake and release from profile data ……54
Figure 34- SBPR sCOD consumption from profile data……...…..……...55
Figure 35- B-stage MLSS (mg TSS/L), B-stage influent COD (mg COD/L), and fermentate COD/mainstream flow (mg/L)……...……56
Figure 36- Endogenous decay rates (EA_ANX)……...……57
Figure 37- Internally stored carbon denitrification rate (EA_EICD)……..…57
Figure 38- ISCD maximum activity test rates for NO3 removed, OP released, and NO2-removed ……..…..……..……58
Figure 39 Linear correlation trend between the VFA added to the SBPR (g VFA as acetate/day) and B-stage effluent nitrite (mg NO2-/L).……...…….....…60
Figure 40- : VFA addition to the SBPR (g VFA as acetate/day) and B-stage effluent nitrite (mg NO2-/L)…….……..……...…….61
Figure 41- AOB and NOB maximum specific activity rates and B-stage aerobic fraction ……...….62

List of Tables

Table 1- Pilot influent and effluent characteristics……..……..33
Table 2- Operational phases of research……..…….34
Table 3- Result phases of research……..……..34
Table 4- Dosing control phases based off of the C/P in result period 1……..…….43
Table 5-Result period 1 linear correlation analysis……...……51
Table 6-Result period 3 linear correlation analysis……...……51
Table 7-Linear correlation analysis continued for result period 1&3…….……..52
Table 8- PAO activity rate averages…….54
Table 9- ISCD activity rate averages……..……..59

Abbreviations

A/B- Adsorption/Bio-oxidation
A2O- Anerobic, Anoxic, Oxic
AER- Aerobic
AMX- Anaerobic Ammonia Oxidation
ANA- Anaerobic
ANX- Anoxic
AOB- Ammonia Oxidizing Bacteria
AR- Aerobic Recycle
AS- Anaerobic Selector
AvN- Ammonia vs. NOx
Bio-P- Biological phosphorus
BNR- Biological Nitrogen Removal
BPR- Biological Phosphorus Removal
CEL- Central Environmental Laboratory
CN- Cyanide
COD- Chemical Oxygen Demand
CSTR- Completely Stirred Tank Reactor
CWA- Clean Water Act
dGAO- Denitrifying Glycogen Accumulating Organism
DO- Dissolved Oxygen
dPAO- Denitrifying Polyphosphate Accumulating Organism
EBPR- Enhanced Biological Phosphorus Removal
EPA- Environmental Protection Agency
SRT- Solids Retention Time
FA- Free Ammonia
ffCOD- Floc-filtered Chemical Oxygen Demand
GAO- Glycogen Accumulating Organism
HRAS- High Rate Activated Sludge
HRSD- Hampton Roads Sanitation District
HRT- Hydraulic Retention Time
IMLR- Internal Mixed Liquor Recycle
ISCD- Internally Stored Carbon Denitrification
JHB- Johannesburg
MBBR- Moving Bed Biofilm Reactor
MLR- Mixed Liquor Recycle
MLSS- Mixed Liquor Suspended Solids
MLVSS- Mixed Liquor Volatile Suspended Solids
NOB- Nitrite Oxidizing Bacteria

NPDES- National Pollutant Discharge Elimination System
OHO- Ordinary Heterotrophic Organism
OP- Orthophosphate
ORP- Oxidation Reduction Potential
PAO- Polyphosphate Accumulating Organism
pCOD- Particulate Chemical Oxygen Demand
PdN- Partial denitrification
PHA- Polyhydroxyalkanoates
PHB- Polyhydroxbuturate
PHV-Poly-3-hydroxyvalerate
PID- Proportional-Integral Derivative
PLC- Programmable Logic Controller
Poly-P- Polyphosphate
RAS- Return Activated Sludge
rbCOD- Readily Biodegradable Chemical Oxygen Demand
SBPR- Sidestream Biological Phosphorus Remover
sCOD- Soluble Chemical Oxygen Demand
tCOD- Total Chemical Oxygen Demand
TIN- Total Inorganic Nitrogen
TMDL- Total Maximum Daily Limit
TN- Total Nitrogen
TP- Total Phosphorus
TSS- Total Suspended Solids
UCT- University Cape Town
VFA- Volatile Fatty Acids
VIP- Virginia Initiative Plant
VSS- Volatile Suspended Solids
WAS- Waste Activated Sludge
WWTP- Wastewater Treatment Plant

1. Introduction

Eutrophication is excess algal growth of natural waterways leading to dissolved oxygen depletion and ecosystem destruction. This phenomenon is caused by an overabundance of the limiting nutrients nitrogen and phosphorus, allowing algae to grow exponentially. Approximately 25% of all water-body impairments are nutrient-based causes since wastewater treatment effluent can be high in nitrogen and phosphorus and discharges into natural waterways, efforts have been made to reduce wastewater effluent concentrations of nutrients. The United States regulates WWTP effluent under the National Pollutant Discharge Elimination System (NPDES) and the Clean Water Act (CWA) (Hendriks & Langeveld, 2017). These WWTP regulations focus on limiting effluent levels of nitrogen and phosphorus, usually increasing the limitation over time (Hendriks & Langeveld, 2017).

Biological nutrient removal (BNR) uses microorganisms present in wastewater to removal total nitrogen (TN) and total phosphorus (TP). BNR uses alternating aerobic, anoxic, and/or anaerobic reactors to expose single-sludge systems to different biochemical environments. BNR was developed in the 1970s and is an expansion of the activated sludge process developed in Manchester in 1914.In BNR, microorganisms are enhanced to carry out nitrification, denitrification, and/or phosphorus accumulation in addition to carbon oxidation (Grady, Daigger, Love, & Filipe, 2011).

Nitrogen is removed biologically through nitrification and denitrification, converting ammonia (NH_4^+) to nitrogen gas (N_2), causing nitrogen to leave the water.. Nitrification requires oxygen and therefor requires an aerobic environment, while denitrification is accomplished in the absence of oxygen in anoxic environments. Nitrogen removal is accomplished by either aerobic zones followed by anoxic zones, or pre-anoxic zones with recycled, aerated mixed liquor. Phosphorus is removed biologically through microbial accumulation, and it exits the system through solids wasting. This is accomplished by anaerobic zones, necessary for phosphorus release and carbon uptake, followed by aerobic zones for phosphorus uptake. To combine nitrogen and phosphorus removal there needs to be adequate aerobic/anoxic zones for nitrogen and anaerobic/aerobic for phosphorus.

There are many different flow processes for combined biological nitrogen and phosphorus removal, including the A2O, UCT, VIP, JHB, and 5-stage Bardenpho processes. There is a need to intensify combined bio-P and bio-N removal systems, meaning creating systems that are better, cheaper, faster, and that have less of an ecological and environmental impact while still achieving low effluent N and P concentrations. Efforts are specifically needed to reduce tank size, lower aeration cost, and improve carbon efficiency so that carbon can be diverted for energy recovery.

1.1 Project motivation

The Chesapeake Bay watershed expands 64,000 square miles and has been over-polluted with nitrogen, phosphorus, and sediment ("Chesapeake Bay TMDL Document," 2010). On May 12, 2009, President Obama issued Executive Order 13508 in order to restore and protect the Chesapeake Bay watershed ("Chesapeake Bay TMDL Document," 2010). The Chesapeake Bay Total Maximum Daily Load (TMDL) was then established in 2010, aiming to fully restore the bay by 2025, with 60% of the actions towards restoration completed by 2017 ("Chesapeake Bay TMDL Document," 2010). With this goal, wastewater treatment effluent limits in the bay watershed region have been decreased and will continue to decrease, creating a greater need for efficient and effective nitrogen and phosphorus removal from wastewater.

A pilot facility was constructed in 2011 on the Chesapeake-Elizabeth plant's facility to explore the European A/B process. The A/B process is a two-sludge system that focuses on carbon adsorption and capture in the A-stage, and biological nitrogen removal in the proceeding B-stage. The A-stage is a high-rate system with an HRT of 30 minutes, an SRT of <1 day, and DO concentrations of <0.5 in the aerobic reactors. The first stage efficiently captures carbon and removes it from the system and it also provides stable influent COD/N control for B-stage. It also provides potential for carbon diversion for other nutrient removal processes or for energy recovery processes. The second stage is composed of multiple CSTRs in series that perform nitrification and denitrification for efficient bio-N removal. The B-stage can be run at different SRTs and HRTs to best enhance nitrogen removal, but currently runs at a 7-9 day SRT and a 5 hour HRT. The B-stage is followed by an anammox polishing MBBR.

The A/B process has shown to increase efficiency by effectively removing and controlling carbon, reducing aeration requirements, and reducing tank volume sizes (less carbon in B-stage = less biomass production). A side-stream RAS fermenter and an A-stage WAS fermenter were added to the B-stage in order to enhance bio-P removal. The goal of the RAS fermenter and A-stage WAS fermenter was to start achieving biological phosphorus removal in a system with established short-cut biological nitrogen removal, all while efficiently using carbon.

1.2 Research objectives

Specific objectives of this research were to:

1. Determine the fermentate carbon addition amount that promotes successful bio-P enhancement that drives the effluent OP below 1 mg/L. Use this point for limited carbon addition for intensification purposes.
2. Determine the fermentate carbon addition amount that caused the likely population shift to the internally stored carbon denitrification bacteria that caused the nitrite accumulation. Determine if nitrite accumulation from partial denitrification and good OP removal from bio-P can exist simultaneously in the same system
3. Observe the relationship between bio-P, nitrite accumulation, and fermentate addition.
4. Investigate how NOB out-selection is effected by fermentate addition and bio-P enhancement.
    a. Determine if the COD needed for bio-P impedes NOB out-selection controls in the pilot
    b. Determine if nitrite accumulation from partial denitrification of nitrate to nitrite could be an alternate reliable source of nitrite for anammox over NOB out-selection
5. Conclude if shortcut nitrogen removal and sidestream bio-P enhancement can be successfully combined in a system that uses carbon efficiently

2. Literature Review

2.1 Nitrification

Nitrification involves the chemical transformation of ammonia (NH_4^+/NH_3) to nitrate (NO_3^-) by two separate reactions performed by nitrifiers: ammonia (NH_4^+/NH_3) to nitrite (NO_2^-), and nitrite (NO_2^-) to nitrate (NO_3^-). Ammonia oxidizing bacteria (AOB) are primarily responsible for the first step in nitrification, termed nitritation: the oxidation of ammonia to nitrite. AOB are considered chemolitho-autotrophs and obligate aerobes, and are dominated in wastewater by the two geneses Nitrososomas and Nitrosospira (Kowalchuk & Stephen, 2001). AOB use two enzymes in the ammonia oxidation; ammonia monooxygenase (AMO) and hydroxylamine oxidoreductase (HAO), with hydroxylamine formed as an intermediate (Kowalchuk & Stephen, 2001).

The conversion of nitrite (NO_2^-) to nitrate (NO_3^-), termed nitratation, is performed by nitrite oxidizing bacteria (NOB). NOB are also chemiolitho-autotrophs, and typically grow in the same environments as AOB. Predominate wastewater NOB species include the genus Nitrobacter and the genus Nitrospira (Grady et al., 2011). NOB use an enzyme called nitrite oxidoreductase (NXR) for nitrite oxidation. NOB activity usually depends on AOB activity for nitrite production, making it useful to combine the AOB and NOB stoichiometry for total nitrification.

Total nitrification involves the transfer of 8 electrons from NH_4^+-N(-III) to NO_3^--N(+V) using oxygen as the electron acceptor. The oxygen required is 4.24 mg O_2/mg NH_4^+-N removed, of that 3.22 mg O_2 is used by AOB (~76%) and 1.11 by NOB (~25) (Grady et al., 2011). Biomass is not generally a concern when designing for nitrification because of the low yield, especially when compared to heterotrophic biomass yield. A large amount of alkalinity is consumed during nitrification: 6.708 mg HCO_3^-/mg NH_4^+-N removed, or 7.14 mg CaCO3/mg NH4+-N removed (Grady et al., 2011). Nitrifiers have an optimal pH range from 7-8, and since they consume alkalinity there may be a need for alkalinity addition in order to stay in the optimal pH range. Free nitrous acid (FNA) inhibits both AOB and NOB, but AOB have shown to have a higher tolerance. NOB inhibition is observed at 0.023 mg HNO_2-N/L, while AOB inhibition has been observed over the ranges of 0.40-2.81 mg HNO_2-N/L ((Vadivelu, Yuan, Fux, & Keller, 2006), (Nan et al., 2019)).

The Monod equation can be used to predict growth rates for AOB and NOB, assuming that ammonia is the limiting nutrient for AOB and nitrite for NOB. For AOB, û=0.014-0.092/hr with the typical assumed value of 0.032/hr, and for NOB û= 0.021-0.042/hr. Both AOB and NOB have been observed as the faster growing nitrifier in different studies (Blackburne, Vadivelu, Yuan, & Keller, 2007; Grady et al., 2011). It is also important to note that growth rates for denitrifying bacteria (0.13/hr) are much higher than nitrifying bacteria, which can make

nitrification the limiting factor in nitrogen removal systems when growth is an important factor, like in start-up systems. The K_s for AOB = 0.5-1.0 mg/L NH_4^+-N and the K_s for NOB = ~1.3 mg/L NO_2^--N, which favors AOB growth at lower substrate concentrations (González-Cabaleiro, Curtis, & Ofițeru, 2019). Since nitrifiers are not inhibited by oxygen like denitrifiers, oxygen can be used in the Monod equation as an additional limiting substrate.

$$\mu = \hat{\mu}\left(\frac{S_1}{K_{s1}+S_1}\right)\left(\frac{S_2}{K_{s2}+S_2}\right) \quad (1)$$

For AOB S_1=NH_4^+ and S_2=DO, and for NOB S_1=NO_2^- and S_2=DO. The K_{s2}, also known as K_O, is the oxygen half saturation coefficient, usually between 0.74-0.99 mg/L DO for AOB (Grady et al., 2011). The K_O for NOB in literature is 1.4-1.75 mg/L DO (Grady et al., 2011). There has been recent research to suggest that the K_O values for AOB and NOB are more complex than previously thought, and might be dependent on the dominate autotrophic species present in a system (Blackburne et al., 2007; Regmi et al., 2014).

2.2 Denitrification

Denitrification refers to the reduction of nitrate (NO_3^-) to nitrogen gas (N_2) through a series of intermediates. Heterotrophic organisms are responsible for denitrification in wastewater, and they do so in anoxic environments using organic carbon as the electron donor and nitrite/nitrate as the election acceptor. The release of N_2 gas from denitrification effectively removes nitrogen from the treated water.

Heterotrophs responsible for denitrification are known as denitrifiers. Most known denitrifiers are chemoorgano-heterotrophs, gaining their electron supply from organic carbon sources (Huijie Lu, Chandran, & Stensel, 2014). Most are also facilitative anaerobes, using nitrate as an electron acceptor in the absence of oxygen (Huijie Lu et al., 2014). Different nitrogen reductases catalyze each step of the denitrification pathway in order for denitrifiers to use each form of oxidized nitrogen as an electron acceptor in their metabolic energy-generating reactions (in order: nitrate reductase (Nar), nitrite reductase (Nir), nitric oxide reductase (Marques et al.), and nitrous oxide reductase (Nos)) (Miao & Liu, 2018).

Heterotrophic denitrification of domestic wastewater consumes hydrogen ions, and therefore produces alkalinity. The total alkalinity produced is 3.354 mg HCO_3^-/NO_3-N removed, or 3.57 mg $CaCO_3$/NO_3-N removed. When heterotrophic denitrification is combined with nitrification, the overall alkalinity consumed is reduced by 50% because of the alkalinity produced in denitrification. When nitrification and denitrification are combined in the same system the total alkalinity loss is approximately 3.57 mg $CaCO_3$/N-removed. It takes 2.86 g COD/g N to reduce nitrate to nitrogen gas, and when considering biomass production and assimilation it can take

around 5-6 g COD/ g N (Grady et al., 2011). Considering the average COD/N of municipal wastewater is 7-12, and considering carbon consumption in other metabolic cycles, external carbon addition might be necessary for denitrification.

Optimal pH needed for denitrification is between 7-9 and the optimal temperature is between 20-30°C (Huijie Lu et al., 2014). Anoxic conditions required for proper heterotrophic denitrification are usually between <0.2-0.5 mg/L DO. Denitrification can be inhibited over the required DO conditions because oxygen will be available as the preferred electron accepter over nitrate (Huijie Lu et al., 2014).

The Monod equation can be used to predict growth rates for heterotrophic bacteria growing anoxically with COD as the limiting nutrient; the û= 0.13/hr and the K_s= 76 mg/L COD (Grady et al., 2011). Heterotrophic bacteria also grow similarly under aerobic conditions, with the values û= 0.14/hr and the Ks= 67 mg/L COD (Grady et al., 2011). Anoxic heterotrophic growth can also be inhibited by low nitrate concentrations or high oxygen concentrations. To consider multiple inhibition and/or limiting factors for growth, the multiple Monod equation is used (Equation 2 below).

$$\mu = \hat{\mu}\left(\frac{S_s}{K_s+S_s}\right)\left(\frac{S_{NO3}}{K_{NO3}+S_{NO3}}\right)\left(\frac{K_{IO}}{K_{IO}+S_O}\right) \quad (2)$$

In this instance, K_s = COD and K_{NO3} is the half-saturation coefficient for nitrate, and K_{IO} is the inhibition coefficient for oxygen. Using this equation, the values commonly accepted in most models are K_{NO3}=0.1-0.2 mg/L of NO_3-N and K_{IO}=0.2-2.0 mg/L DO (Grady et al., 2011). Since nitrate is a limiting substrate, a minimum of 0.1-0.2 mg/L NO_3-N is needed, but since oxygen is an inhibitor there can be no more than 0.2-2 mg/L DO in order for denitrification to occur.

2.3 Anammox

The 1995 discovery of anaerobic ammonium oxidation (anammox) has been making great advances in BNR (Mulder, Vandegraaf, Robertson, & Kuenen, 1995). Anammox is a bacterium that thrives in anaerobic environments and is able to convert ammonia to nitrogen gas using nitrite as an electron acceptor, bypassing nitrification and denitrification. Since its discovery, anammox has been widely studied in wastewater processes because of its potential to lower aeration costs, efficiently remove nitrogen, lower sludge yields, and decrease overall operational costs (Wang et al., 2018).

$$NH_4^+ + 1.32NO_2^- + 0.066HCO_3^- + 0.13H^+ \rightarrow 1.02N_2 + 0.26NO_3^- + 0.066CH_2O_{0.5}N_{0.15} + 2.03H_2O \quad (3)$$

Anammox has been successfully implemented in side-stream treatments with high free ammonia (FA) concentrations, such as landfill leachate and sludge digestion liquid (Wang et al., 2018). Anammox thrive at a temperature above 20°C, which can be implemented in side-stream treatment much easier than in mainstream processes (O'Shaughnessy, 2016). Another reason why side-stream anammox technologies have been successful is because the slow growth rate of anammox, û= 0.0027/hr, requires a long SRT which is easier to implement in the side-stream. Anammox have been successfully retained in attached growth systems such as biofilters, but suspended growth systems (flocs or granules) need an SRT of 30-45 days in order to prevent wash out (O'Shaughnessy, 2016). The success of suspended growth systems largely depends on good settling to accurately control the SRT, which can be enhanced by cyclones separating out biomass mechanically based on density.

Currently, most applications of anammox in municipal wastewater treatment are treating small portions of flow in the side-stream. Implementing side-stream anammox processes does increase the overall efficiency of a BNR wastewater plant by decreasing the overall carbon, DO, and tank size requirements for nitrogen removal, but efficiency could be further increased if it could be implemented in the mainstream. As previously discussed, SRT, FA, and temperature are limiting factors in the mainstream. Another major factor is NOB out-selection, meaning the ability to promote AOB species over NOB species so there is enough nitrite produced for anammox but not too much consumed by NOB.As shown in Equation 15, anammox need ammonia and nitrite inputs but not nitrate, which NOB produces by oxidizing nitrite.

2.4 Short-cut nitrogen removal

Advances are being made to improve the traditional nitrification/denitrification pathways for nitrogen removal in order to improve efficiency and cost. If aeration requirements, tank sizes, and alkalinity requirements decrease, then overall cost will decrease. If less carbon is required for nitrogen removal then carbon can be diverted and used for other BNR processes or for energy recovery, increasing the overall energy efficiency of the system. Several promising short-cut pathways are being explored and developed.

2.4.1 Nitritation/denitritation- nitrite shunt

Since nitrite is an intermediate in nitrification and denitrification, the nitrite shunt process aims to shorten the nitrification/denitrification pathway by jumping to denitritation (reduction of nitrite to nitrogen gas) after ammonia oxidation to nitrite.

$$NH_4^+ + 1.5O_2 + 2HCO_3^- \rightarrow NO_2^- + 3H_2O + 2CO_2 \quad (4)$$

$$NO_2^- + 0.5CH_3OH + 0.5CO_2 \rightarrow 0.5N_2 + HCO_3^- + 0.5H_2O \quad (5)$$

By skipping nitrite oxidation and nitrate denitrification, an overall electron transfer of six electrons is needed instead of eight. This pathway can reduce oxygen requirements by 25% and carbon requirements by 40% (Grady et al., 2011). A 40% reduction in biomass is also possible, due to the decreased use of heterotrophic bacteria that have a much higher biomass yield than autotrophic bacteria (Hellinga, Schellen, Mulder, van Loosdrecht, & Heijnen, 1998). NOB out-selection is required in order for nitritation/denitritation to occur.

2.4.2 Deammonification: partial nitration and anammox

Deammonification refers to the combination of partial nitration, where approximately half of present ammonia is oxidized to nitrite by AOB, and anammox oxidation of ammonia to nitrogen gas using nitrite. Deammonification theoretically requires no carbon, which could greatly improve the cost and total efficiency of BNR if all carbon can be diverted before deammonification (Hellinga et al., 1998). Alkalinity consumption can potentially be reduced from the reduction of AOB activity required, and also because of the small production of alkalinity by anammox. This pathway saves even more aeration costs than the nitrite shunt, and up to 63% less than conventional nitrification (Nifong et al., 2013). Biomass production can be reduced by 80% due to elimination of heterotrophic bacteria. Nearly 100% of the total carbon can be diverted before the deammonification step to be used for other BNR processes or for energy recovery, creating potential for energy-neutral WWTPs.

Aeration is required in order to achieve partial nitritation. Oxygen requirements for AOB make combining the two deammonification steps in the same reactor an issue since anammox can be inhibited at certain DO concentrations. Some promising studies have shown no significant decrease in anammox activity at DO concentrations of 2-3 mg/L O_2 (Siegrist, Salzgeber, Eugster, & Joss, 2008) and other studies show that AOB can be successfully implemented with anammox at low DO of 0.1-0.2 on granules and biofilms (Huynh et al., 2019). Deammonification can occur in single-stage processes or in two-stage systems. Single-stage systems have been successful in side-stream implementation and have shown promise in efficiency, cost reduction, and easier operation and maintenance. Examples of single-step side-stream processes already used in WWTPs are DEMON, AnitaMox, and ANAMMOX (Nifong et al., 2013; B. Wett, 2006).

Side-stream technologies only treat a portion of the wastewater treated at full-scale plants, usually high ammonia streams like digester effluent, but if the process could be modified to perform in more dilute ammonia influent conditions then the benefit of the process would increase exponentially. Mainstream deammonification is a challenge because of dilute ammonia influent conditions, anammox retention issues, and NOB out-selection challenges (See chapter

2.5 for NOB out-selection challenges). Not only do higher COD/N mainstream influent conditions take away the benefits of anammox enhancement and NOB out-selection, but too much COD is a problem for heterotrophic consumption of nitrite. Mainstream deammonification has not been successful implemented in full-scale systems but continues to be a focus of research.

2.4.3 Partial denitrification + anammox

Partial denitrification (PdN) combined with anammox works by using partial denitrification of nitrate to nitrite by heterotrophic bacteria to supply nitrite to anammox. This requires an external carbon addition source for the PdN. This mechanism acts as a nitrite source for anammox, and can improve the overall anammox efficiency since anammox produces nitrate (see Equation 6). When combining PdN with anammox, nitrate production can be eliminated (see Equation 6) improving the TIN efficiency of anammox from 75-80% (O'Shaughnessy, 2016) to >95% (Wu, Li, Zhao, Liang, & Peng, 2018). PdN can improve the overall COD/TIN efficiency if nitrite production from supplemental carbon is reliable so less carbon is needed for conventional nitrification/denitrification.

$$NH_4^- + 1.06NO_2^- + 0.021C_6H_{12}O_6 \rightarrow 1.02N_2 + 0.066CH_2O_{0.5}N_{0.15} + 0.066HCO_3^- + 2.03H_2O \quad (6)$$

2.5 NOB out-selection

The suppression of NOB over AOB would greatly enhance the conditions necessary for anammox by providing a nitrite supply. Since AOB and NOB grow in the same environments under similar conditions, promoting one species over the other is difficult to do. NOB out-selection has been successfully implemented in side-stream treatment because of high free ammonia (FA) concentrations usually present in side-stream treatment (usually exceeding 100 mg NH_3). High FA inhibits NOB between 0.1-1 mgN/L, but does not inhibit AOB until 10-150 mgN/L (Anthonisen, Loehr, Prakasam, & Srinath, 1976). Side-stream applications contain higher FA amounts because of their higher temperatures and pH.

Applying NOB out-selection is more difficult to achieve in mainstream processes mostly due more dilute ammonia concentrations and lower temperatures and pH. Success has been shown for NOB out-selection in the mainstream by seeding AOB from the side-stream, controlling a short aerobic SRT, and controlling DO concentrations. Side-stream processes can produce AOB-rich biomass which can be seeded back into the mainstream to bioaugment AOB and increase AOB/NOB (Al-Omari et al., 2015). Bioaugmenting AOB can decrease SRT requirements for the

same nitrogen removal, due to increased AOB activity (Al-Omari et al., 2015). Aerobic SRT control works to flush out NOB, which are shown in practice to have slightly slower growth rates than AOB at certain DO concentrations (Regmi et al., 2014). Since there is only a small difference in growth rates the aerobic SRT control needs to be strictly monitored (Regmi et al., 2014). Aerobic SRT is also directly related to DO control strategies.

2.5.1 Different DO control strategies for NOB out-selection purposes

2.5.1.1 Continuous low Do

Some studies have shown that AOB out-compete NOB at low continuous DO conditions (<0.25 mg/L DO) due a higher oxygen affinity for AOBs and/or excess ammonia remaining from incomplete ammonia oxidation (Sliekers, Haaijer, Stafsnes, Kuenen, & Jetten, 2005). Most success in continuous low DO operation comes from biofilm and granular studies that can create anoxic zones for anammox retention and can promote AOB over NOB in the right conditions. Success with NOB out-selection in biofilms operating at less than 1.2 mg/L O_2 has been observed (Laureni et al., 2019). There has been success in granular sludge studies with continuous low DO <4 mg/L, again due to ammonia availability due to partial ammonia oxidation (Courtens et al., 2015). Granular studies differ from floc studies because the granules themselves are specific niche environments. With successful granule studies, AOB grow on the outside where they can receive oxygen and anammox grow on the inside shielded from oxygen and in direct supply of ammonia and nitrite from partial ammonia oxidation.

2.5.1.2 Intermittent aeration

Intermittent aeration is implemented by alternating periods of aeration and no aeration in the same reactors, creating transient anoxia in aerated reactors. This essentially creates different biochemical environments in the same reactor instead of separate aerated and anoxic reactors, which is another transient anoxia mechanism. Intermittent aeration has been proven to enhance NOB out-selection, and there are several theories as to why including enzymatic lag, substrate inhibition, and substrate availability. Enzymatic lag refers to creating shorter aeration times so that AOB can oxidize ammonia with the available oxygen before NOB can oxidize nitrite, relying on AOB's greater affinity (lesser K_O value) for oxygen than NOB (Kornaros, Dokianakis, & Lyberatos, 2010). Studies have shown that nitric oxide acts as an inhibitor for NOB, so increasing partial denitrification of nitrite to nitrogen gas would increase the exposure of NOB to NO (Courtens et al., 2015). Hydroxylamine, an ammonia oxidation intermediate, has also been shown to inhibit NOB activity (Park & Chandran, 2016). Substrate availability is also thought to be a factor because if nitrite produced by AOB is consumed in anoxic periods by heterotrophs before it is available for aerobic uptake by NOB, then NOB will suffer as a result (Chandran &

Smets, 2000). This mechanism directly shows the role of heterotrophs in NOB out-selection, relying on them for denitrification of nitrite. Since decreasing substrate availability depends on heterotrophs, adequate COD for denitrification is a key factor and could be limiting for this mechanism. All three theorized mechanisms could play a role in different NOB out-selection systems, but the key to intermittent aeration is the specific aeration duration and DO concentrations used to during aeration.

More recent studies have shown success with high DO (>1.5) during air-on times ((Regmi et al., 2014), (Bernhard Wett, 2007)). This shows that the accepted K_O values for AOB and NOB might not be as reliable as previously thought. Recent studies show in abundance that Nitrospira are the dominating NOB species in wastewater BNR processes instead of the previously thought Nitrobacter ((Juretschko et al., 1998), (Dytczak, Londry, & Oleszkiewicz, 2008)). Nitrobacter has been shown to have a higher K_O than AOB (Dytczak et al., 2008), so determining the dominate NOB species could drastically effect the DO value needed for NOB out-selection if Nitrospira and Nitrobacter have widely differing values. In a Nitrospira dominated pilot-scale system, the K_O for AOB was determined to be 1.14 mg O_2/L, and the K_O for NOB was determined to be 0.16 mg O_2/L using modeled Monod kinetics, displayed below in Figure 1 (Regmi et al., 2014). This system ran at an intermittent aeration approximate DO = >1.5 mg/L (Regmi et al., 2014). Further research has proved NOB out-selection success using high DO control intermittent aeration, concluding that Nitrospira is the dominate NOB and it's K_O values are more relevant than previously discovered literature values (Jiang et al., 2018).

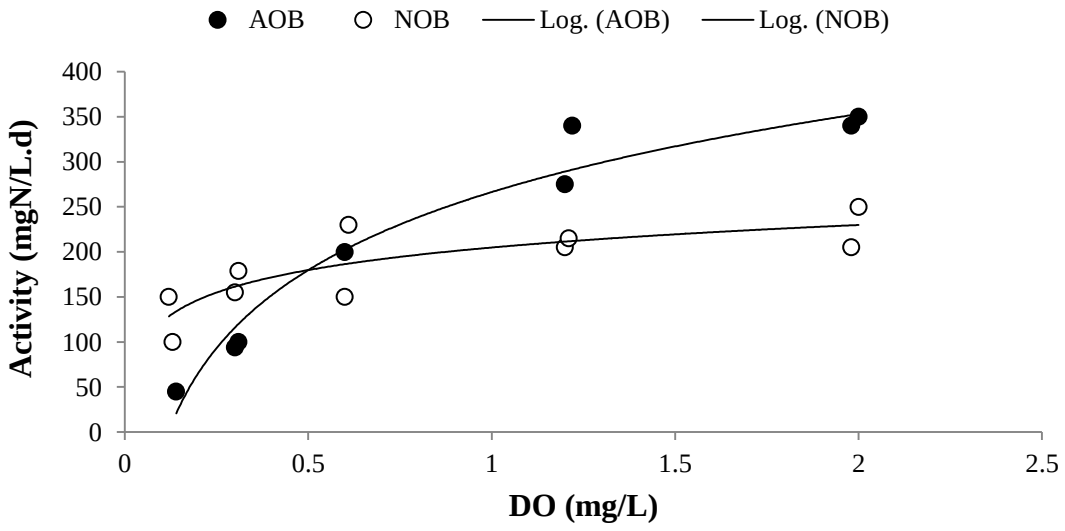

Figure 1: AOB and NOB Monod kinetics for Nitrospira dominated system. Graph adapted from (Regmi et al., 2014). Model rates taken from pilot system at 25 °C.

2.5.1.3 AvN aeration control

A novel aeration strategy was developed to enhance the intermittent aeration process by basing the aeration times on effluent ammonia/NOx (nitrite + nitrate) values (Regmi et al., 2014). If aeration is controlled to an effluent ratio of nitrogen, then aeration effectively controls how much nitrification, and consequently denitrification, occurs. AvN only nitrifies enough ammonia for subsequent denitrification to occur, efficiently using COD for nitrogen removal. If COD is used efficiently then more can be diverted before aeration reactors for redistribution or energy recovery purposes, therefor making the whole system more carbon and energy efficient.

AvN control has shown to be a useful NOB out-selection tool at 20°C, in addition to being an efficient aeration strategy. Leaving ammonia residual in the effluent has shown to help with NOB out-selection, so operating with an NH_4/NO_x ratio of 1:1 can promote AOB over NOB (Regmi et al., 2014; Bernhard Wett & Rauch, 2003). It is also thought that is COD is not being completely used up by controlling intermittent aeration with AvN than more COD will be available during anoxic periods to consume nitrite so there is less available for NOB to thrive on.

2.6 Phosphorus removal

Bio-P is accomplished by the accumulation of phosphorus in phosphorus accumulating organisms (PAOs) and the subsequent solids wasting of these organisms, displayed below in Figure 2. It is thought that *Candidatus Accumulibacter phosphatis* (ca. Accumulibacter), and more generally the genus Accumulibacter, dominates bio-P activity (Hesselmann, Werlen, Hahn, Van der Meer, & Zehnder, 1999) ((Yunhong, Nielsen, & Nielsen, 2004). These bacteria are betaproteobacteria, and are closely related to Rhodocyclus (Hesselmann et al., 1999). It has also been shown that gammaproteobacteria are contributing PAOs (Menes, Viera, Farías, & Seufferheld, 2011).

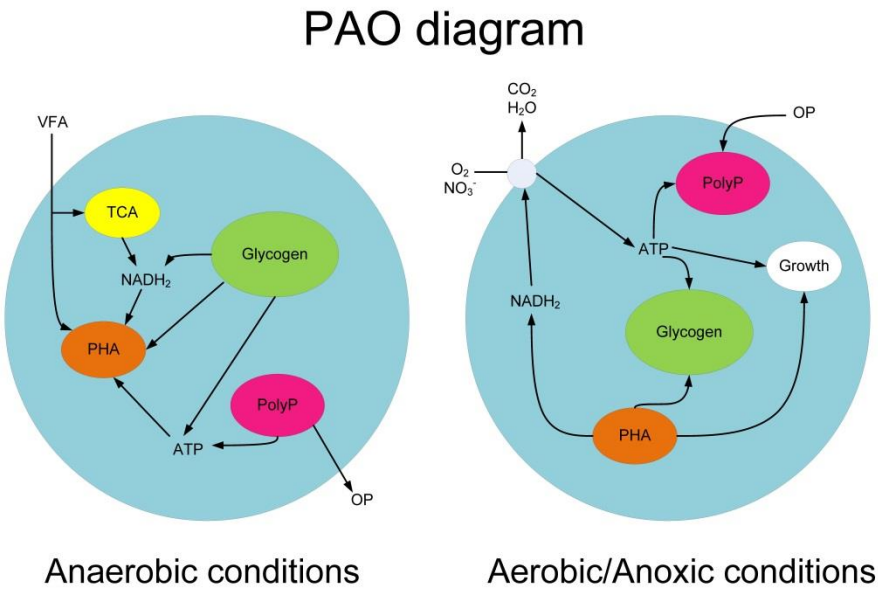

Figure 2: General metabolic diagram of a PAO. Adapted from (Yuan, Pratt, & Batstone, 2012)

During anaerobic conditions, PAOs cleave polyphosphate (Poly-P) which releases phosphate and allows for the uptake of volatile fatty acids (VFAs). The uptake of VFAs during this phase is important because PAOs store VFAs as poly-B-hydroxyalkanoate (PHA) for energy. In aerobic conditions, PAOs metabolize PHA for growth, and form Poly-P by up-taking phosphorus. PAOs are able to take up all of the phosphorus released anaerobically plus additional phosphorus, thereby achieving overall phosphorus removal.

Sufficient organic matter is needed for proper PAO enhancement and phosphorus uptake. The COD/P required is determined by PAO activity and by the amount of denitrification that the BNR process requires, since COD is also needed for denitrification. In a system with no denitrification or little heterotroph interference a tCOD/P ratio of 26-34 is needed, but that required ratio can rise above 43 for systems that also perform denitrification (DeBarbadillo, 2018). An rbCOD/TP of at least 15 is needed for successful bio-P enhancement in normal wastewater conditions (Kobylinski, 2008).

The optimal SRT required for bio-P enhancement is usually around 2-3 days, which does overlap with the SRT range for nitrification of 2-15 days depending on the process, so it is possible to combine these processes. Bio-P enhancement requires lower SRT values because long overall SRTs will decrease the overall phosphorus removal since wasting is the mechanism in which phosphorus is removed from the system. Long aerobic SRTs may also result in a complete oxidation of stored intracellular organic matter in PAOs, which will result with reduced phosphorus uptake. In addition, endogenous decay occurs more with longer SRTs, which produces additional phosphorus release.

Enhanced biological phosphorus removal (EBPR) requires an anaerobic zone at the beginning of the process in order for PAOs to have time to uptake VFA and release phosphorus without too much interference from heterotrophs using carbon for denitrification. Examples of EBPR processes are listed below:

A2/O process

This involves an anaerobic zone, an anoxic zone, then an oxic (aerobic) zone in series. RAS is recirculated to the anaerobic zone and internal mixed liquor recycle (IMLR) is recycled from the aerobic to anoxic zones. Good nitrogen and phosphorus removal can be achieved in this process, but phosphorus removal is effected by the amount of nitrate in the RAS.

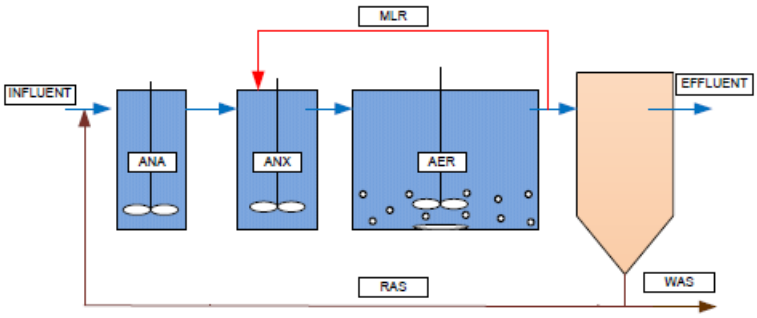

Figure 3: A2/O process flow diagram

University Cape Town (UCT)

This process improves on the A2O process by directing RAS to the anoxic zone, eliminating nitrate interference with PAOs. More advanced phosphorus removal is usually observed, but nitrogen removal is usually moderate. This also adds an anoxic recirculation (AR) step, which requires another pump.

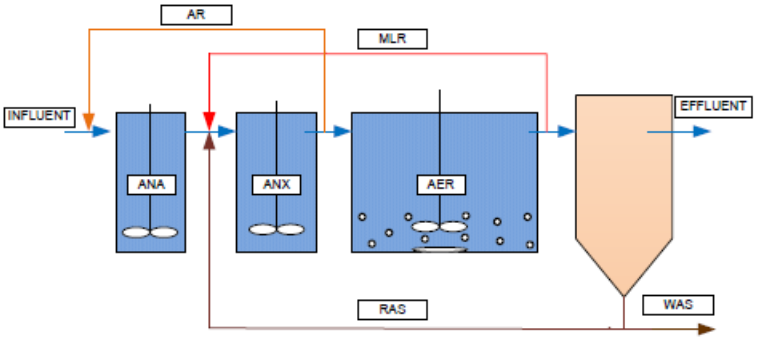

Figure 4: UCT process flow diagram

Virginia Initiative Plant (VIP)
This process is extremely similar to the UCT process, with the only differences being staged anoxic and anaerobic steps, a plug-flor system for the aerobic reactors, and short SRTs.

Johannesburg (JHB)
This process provides a mechanically simpler solution to eliminate RAS before the anaerobic zone by providing an additional anoxic zone, before the anaerobic zone, where the RAS is recycled to. While this also succeeds in aiding phosphorus removal, nitrogen removal usually stays moderate.

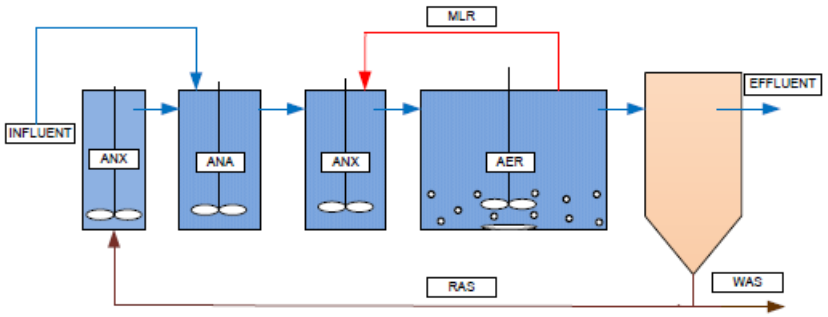

Figure 5: JHB process flow diagram

Five-stage bardenpho
This involved the classic 4-stage bardenpho process with an initial anaerobic zone added. This process greatly improves nitrogen removal but usually produces moderate phosphorus removal. Although effective, it involved large reactor volumes and can be impractical for that reason. The long SRTs that come with the larder tank volumes limit bio-P.

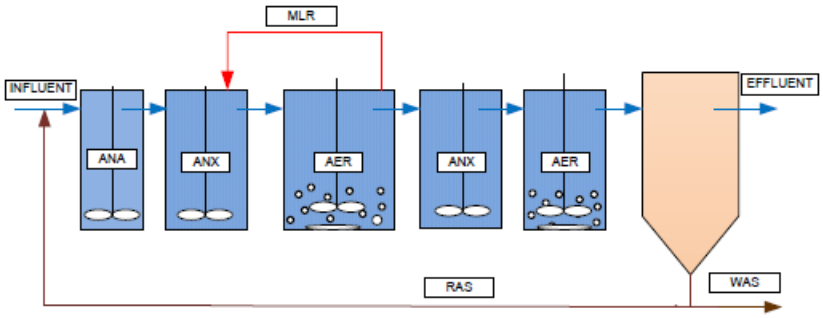

Figure 6: 5-S Bardenpho process flow diagram

2.6.1 Glycogen Accumulating Organisms: nuisance organisms in EBPR systems

A crucial factor in bio-P enhancement is competition with glycogen accumulating organisms (GAOs). GAOs have very similar metabolisms to PAOs but they accumulate glycogen and do

not store polyphosphate or uptake phosphorus (see Figure 7 below). In anaerobic conditions they hydrolyze glycogen for energy and take up VFA for PHA storage, and in aerobic conditions they grow by oxidizing PHA and up-taking glycogen. GAOs are usually present in bio-P systems and compete with PAOs for VFA, potentially causing VFA limitation for PAOs.

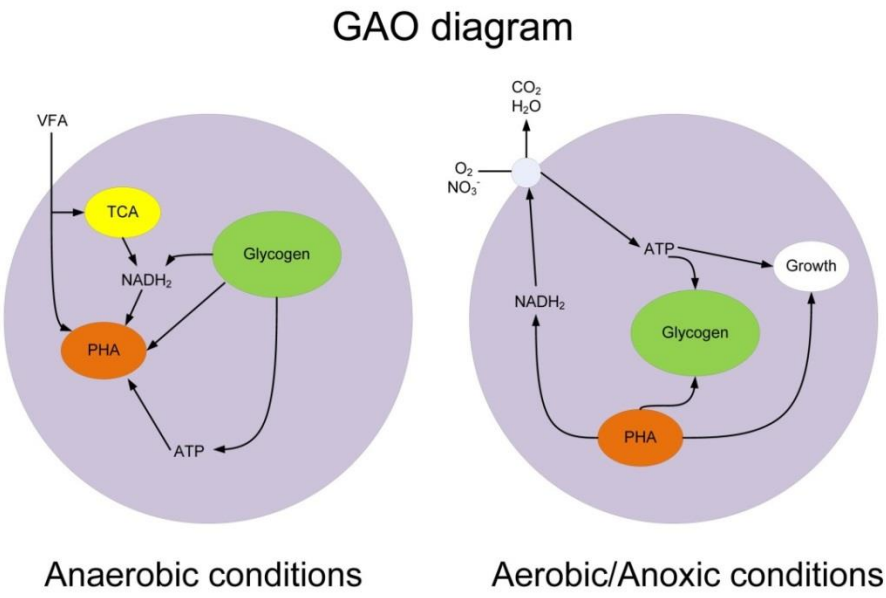

Figure 7: General metabolic diagram of a GAO. Adapted from (Zeng, van Loosdrecht, Yuan, & Keller, 2003)

Many operating parameters can have influence on PAO vs. GAO competition, including temperature, carbon/VFA source and availability, and pH. Studies show that temperatures below 20°C promote PAOs over GAOs, and temperatures above 20°C promote GAOs over PAOs (Wende, Weiguang, Hui, & Zheng, 2010). PAOs are shown to have a competitive advantage over GAOs at higher pH values. GAOs tend to have an advantage below the critical pH of 7.25, and PAOs tend to have the advantage above the pH of 7.25 (Filipe, Daigger, & Grady, 2001). The carbon source available for uptake is another critical factor; the most successful carbon sources for PAO promotion are acetate and propionate, over others such as butyrate and valerate (Wende et al., 2010). Lots of research has shown success in varying ratios of acetate and propionate, but generally more studies have shown that the promotion of propionate is the most directly successful in PAO promotion over GAOs (Oehmen, Teresa Vives, Lu, Yuan, & Keller, 2005). Studies have also shown that alternating the carbon sources can be successful in out-competing GAOs (Huabing Lu, Oehmen, Virdis, Keller, & Yuan, 2006). Influent VFA concentrations above 8.33 C-mol/P-mol have also shown to promote PAOs over GAOs (Schuler & Jenkins, 2003). Research has also been done on SRT effects, showing promotion of PAOs at lower SRT values because GAOs have longer growth rates (Whang, Filipe, & Park, 2007).

2.6.2 Sidestream EBPR

Side-stream EBPR involves an anaerobic zone where RAS is fed before being returned to the mainstream process of an activated sludge system (example of a sidestream EBPR process is shown below in Figure 8). Sidestream EBPR has been around since the development of the pho-strip process in 1972 (Levin, Shaheen, Topol, & Tarnay, 1974), and the improvement of that process by adding VFA addition to the "stripping" or sidestream tank in 1975 (Fuhs & Chen, 1975). The use of sidestream EBPR was recognized and studied further by James Barnard in 1985, where he noted the important difference of nitrate interference with EBPR between sidestream and mainstream anaerobic zones (Barnard, 1985). Nitrates act as an alternative electron acceptor to oxygen which can deplete carbon and make less available for PAO uptake. The added SRT and HRT of a sidestream EBPR tank allows time for nitrate reduction and VFA production via fermentation then the uptake of VFA by PAOs.

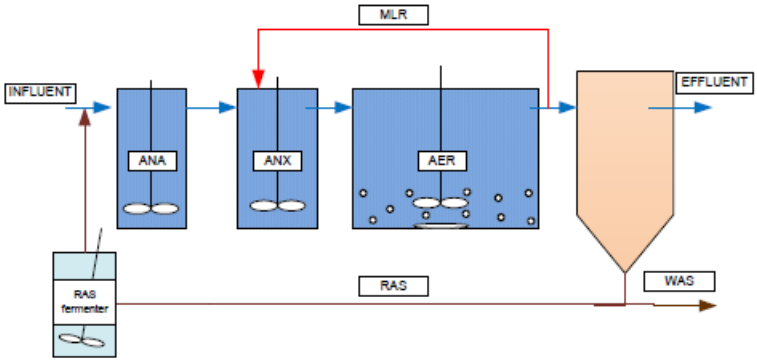

Figure 8: A2O process with RAS fermentation process flow diagram

It is thought that sidestream SBPR systems work to promote hydrolysis, fermentation, and BPR enhancement. Hydrolysis, which involves the breaking down of more complex molecules into less complex molecules by the incorporation of water, is an important process needed for EBPR in order to turn complex carbons into readily biodegradable COD (Houweling et al., 2010). Once carbon is in the form of rbCOD, acetogenesis-the final step of the fermentation process-is needed to produce VFA from the rbCOD (Houweling et al., 2010). Both hydrolysis and complete fermentation are needed to produce VFA for PAO uptake, and both require time in an anaerobic environment to do so. An extended anaerobic period is also important to maximize OP release in PAOs, in order to maximize VFA storage and to therefor maximize OP uptake in a following aerobic phase (López-Vázquez, Hooijmans, Brdjanovic, Gijzen, & van Loosdrecht, 2008). Sidestream also enhances PAOs over GAOs due to the lower decay rate of PAOs than GAOs in extended anaerobic conditions (Tooker et al., 2017). This phenomenon of GAO decay to enhance PAO/GAO relative populations has been observed in many sidestream processes, and could possibly be a source of hydrolysis and fermentation (Hao, Wang, Cao, & van Loosdrecht, 2010).

There are several different configurations of sidestream treatment that can be used to induce hydrolysis, fermentation, and EBPR enhancement, shown in Figure 9 below. There are several different types of fermentation, including primary fermentation (part B of Figure 9), WAS/RAS fermentation (part A of Figure 9), and MLSS fermentation (part C of Figure 9) that can be used in some combination to provide the three steps necessary for EBPR (Tooker et al., 2017). Primary fermentation can be used in conjunction with a RAS fermenter to provide VFA so that the RAS fermenter can have a shorter HRT for just p-release purposes, and there for a smaller tank size (Tooker et al., 2017).

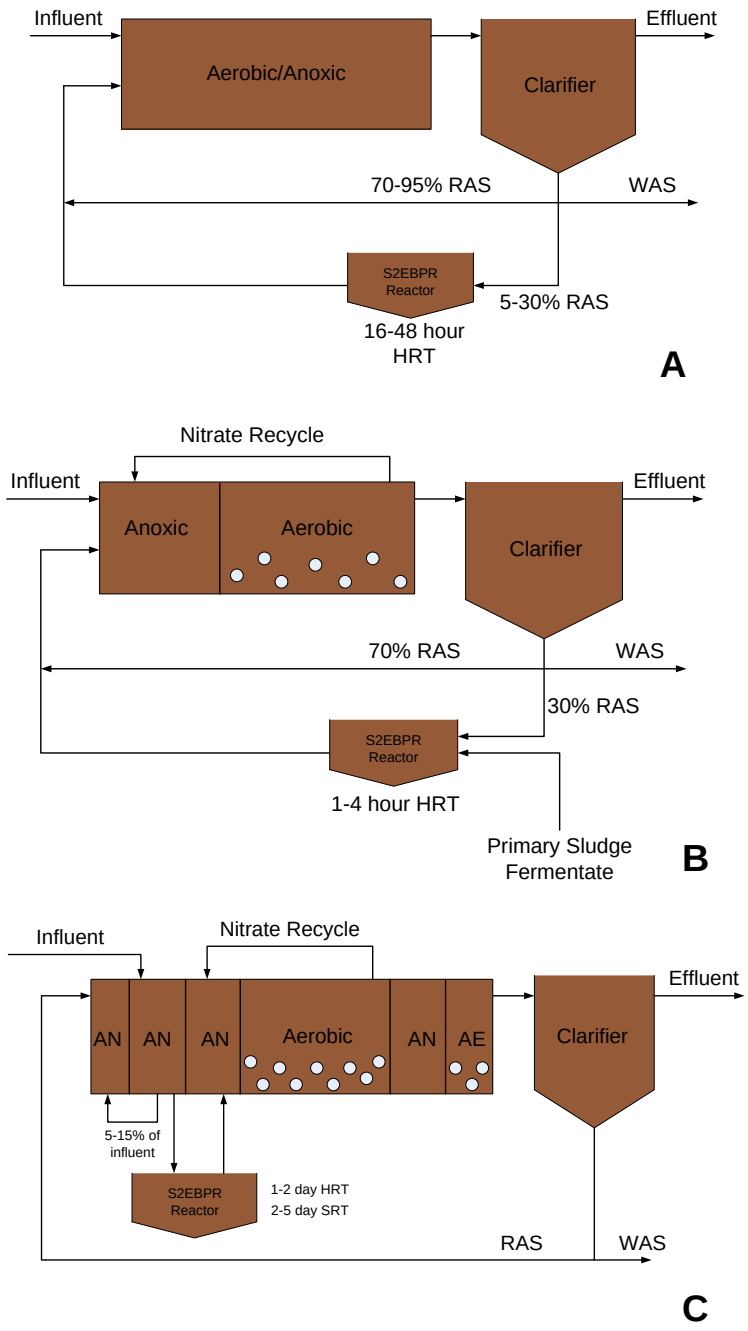

Figure 9: Examples of different sidestream flow processes to accomplish bio-P. Adapted from Tooker et al., 2017)

There has been recent renewed interest in sidestream EBPR systems because of success in bio-P enhancement by implementing side-stream RAS fermenters. These systems have produced low effluent OP concentrations, most <1 mg/L OP and some <0.01 mg/L OP, with little cost of implementation and maintenance (Barnard, Dunlap, & Steichen, 2017). Most of the established RAS fermenters can be easily added to existing BNR& BPR systems (see Figure 8 above for an example of a RAS fermenter added to an A2O process). The theory behind the success of these side-stream processes is that the RAS fermenter promotes *Tetrasphaera* by providing an

anaerobic zone maximum oxidation-reduction potential (ORP) of -300 mV (Barnard et al., 2017). Operational conditions of RAS fermenters should involve minimal mixing in order to keep conditions strictly anaerobic for *Tetrasphaera*, and long SRTs between 30-40 hours & HRTs between 1.5-2 days to provide time for fermentation (Barnard et al., 2017).

Tetrasphaera uptakes phosphorus aerobically to form poly-P, and might actually be capable of up taking a greater amount of phosphorus then Accumulibacter, but they do not store VFA as PHA anaerobically ((Marques et al., 2017), (Kong, Nielsen, & Nielsen, 2005)). Tetrasphaera are fermenting PAOs that digest carbohydrates and amino acids and produce fermentation products anaerobically, which means that they could potentially provide VFA for Accumulibacter to thrive alongside of them (Bernard et. al 2017). The general theorized metabolic diagram for how Tetrasphaera promotes bio-P enhancement by working alongside PAOs is displayed below in Figure 10.

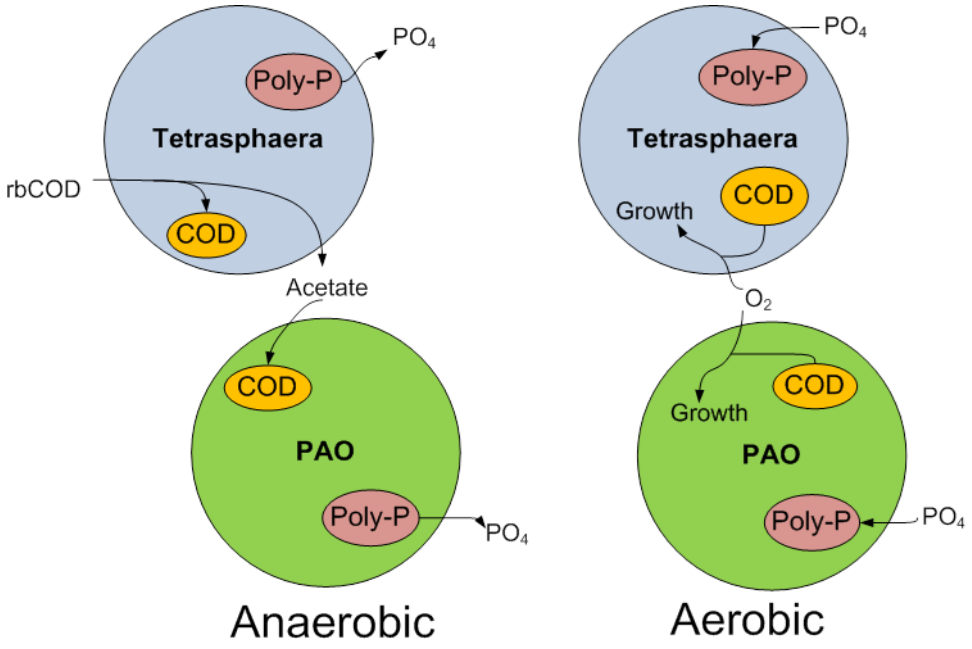

Figure 10: Theorized metabolism of Tetraspharea working with general PAOs. Adapted from (Barnard et al., 2017)

2.6.3 Denitrifying PAOs and GAOs

2.6.3.1 dPAOs

PAOs that can use nitrate in anoxic conditions are referred to as denitrifying PAOs (dPAOs) since they reduce nitrate or nitrite in addition to up taking phosphorus. Some PAOs possess

denitrifying capabilities as an adaptation in order to grow in the absence of oxygen (Camejo et al., 2016). There are several advantages for having dPAOs in a system including reducing the overall oxygen requirement, decreasing the COD need for denitrification, overall less biomass production, and overall increased efficiency of nitrogen and phosphorus removal (Zhang, Li, Zhang, Sang, & Jiang, 2018). When anaerobic/anoxic conditions are used instead of anaerobic/aerobic for phosphorus removal, the overall COD requirement is reduced by 50%, the oxygen requirement by 30-50%, and the biomass production by 20-30% (Kuba, VanLoosdrecht, & Heijnen, 1996).

2.6.3.2 dGAOs

GAOs that can use nitrate/nitrite as an electron acceptor instead of oxygen are referred to as denitrifying GAOs (dGAOs). Studies have shown that dGAOs are more likely to use nitrate as an electron acceptor and dPAOs are more likely to use nitrite as an electron acceptor, linking dGAOs over dPAOs to nitrite accumulation due to partial denitritation (Rubio-Rincón, Lopez-Vazquez, Welles, van Loosdrecht, & Brdjanovic, 2017). While nitrite accumulation through partial denitrification of nitrate to nitrite would benefit short-cut nitrogen removal systems by supplying nitrite for anammox, dGAOs and dPAOs could negatively affect short-cut nitrogen removal by interfering with NOB out-selection. The "nitrite loop" theory was developed in a study that found excess NOB growth with COD addition in aerobic granular sludge (Winkler, Bassin, Kleerebezem, Sorokin, & Loosdrecht, 2012). This theory essentially involves dGAOs and dPAOs partially denitrifying nitrate to nitrite and supplying more substrate for NOB to thrive, essentially impeding NOB out-selection (displayed below in Figure 11).

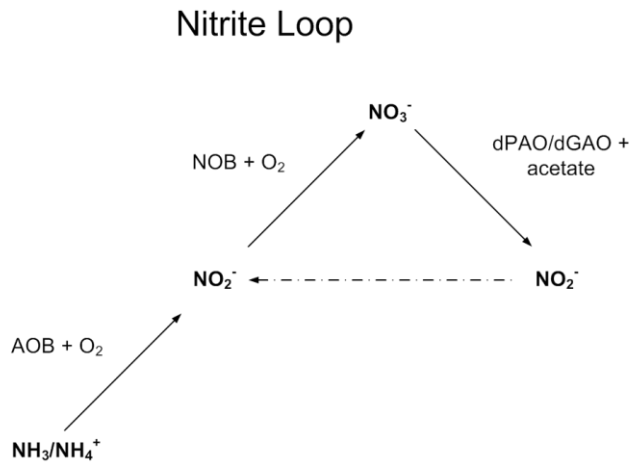

Figure 11: Theorized nitrite loop where dPAOs/dGAOs provide a nitrite source for NOB to thrive. Adapted from ((Winkler et al., 2012)

It is difficult to determine the difference between active PAOs, GAOs, dPAOs, and dGAOs in a system. Studies show above 0.5 g P-uptake/g COD consumed indicates PAO promotion over GAOs; however this fraction is based off of stoichiometry of PAOs and GAOs, which is debated (Welles et al., 2015). Maximum substrate activity tests can show PAO and dPAO activity by measuring OP uptake and release.

2.7 Post-anoxic denitrification in EBPR systems

Recent studies have observed and investigated denitrification above endogenous rates in anoxic zones following aeration zones in systems with bio-P enhancement. Since the external carbon in these systems should be oxidized by the time the biomass reaches the anoxic environment, the post-anoxic denitrification is likely due to an internally stored carbon compound supplying the necessary electrons. Also, since this phenomenon has been observed in EBPR systems with preceding anaerobic tanks, the carbon used for this denitrification is most likely being stored during the anaerobic period. A study showed that a 45% reduction in post-anoxic denitrification happened when the anaerobic zone before the aeration zone in a system was removed, linking the anaerobic zone to internally stored carbon denitrification (Vocks et al., 2005). The process schematic for this study where the post-anoxic denitrification was observed is displayed below in Figure 12. This study compared washed and unwashed batch tests to rule out external carbon as the source for denitrification.

Studies have shown that endogenous decay rates are commonly assumed higher than what they actually are, and that cell lysis does not happen quickly enough to produce the COD needed for adequate denitrification (Van Loosdrecht & Henze, 1999). This supports the post-anoxic denitrification by internally stored carbon theory because these denitrification rates are usually less than denitrification with external carbon rates, but is still above rates you would expect to see from denitrification using COD from cell lysis. The Vocks study displayed post-anoxic denitrification rates of 0.47-1.17 $mgNO_3/gVSS/hr$ (in the anoxic zone in Figure 12 below) (Vocks et al., 2005), which is above the referenced endogenous decay rates of 0.2-0.6 $mgNO_3/gVSS/hr$ (Kujawa & Klapwijk, 1999) so it can be assumed the denitrification was not due to COD produced by cell lysis.

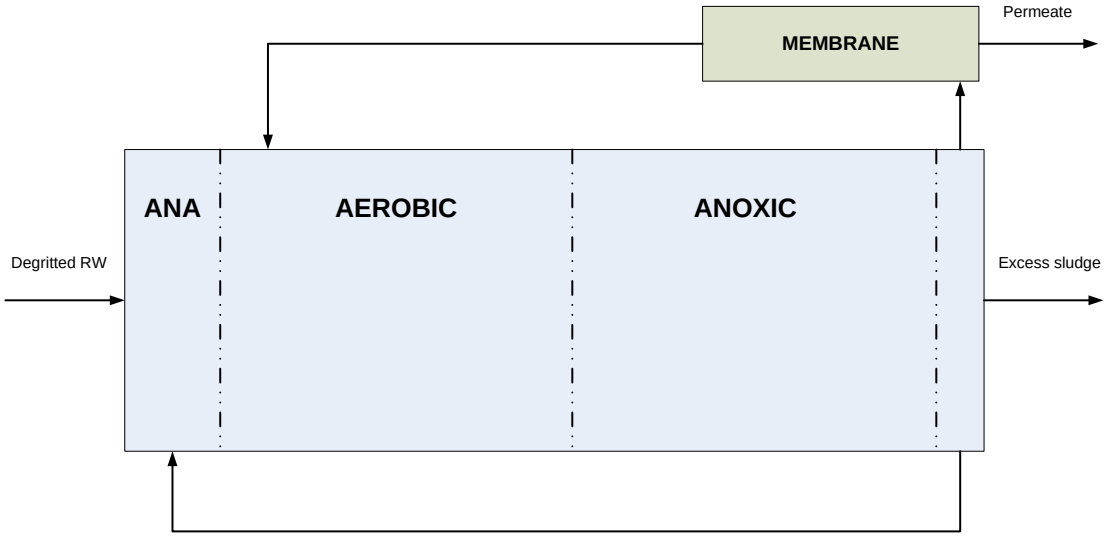

Figure 12: Post anoxic denitrification process flow diagram adapted from Vock's study (Vocks et al., 2005)

The internally stored carbon compound used for denitrification after aeration has been theorized to be polyhydroxyalkanoate (PHA), polyhydroxybutyrate (PHB), glycogen or some combination of the three. Some studies have linked post-anoxic denitrification to PHA and glycogen (Coats, Mockos, & Loge, 2011; Vocks et al., 2005), but there is an abundance of studies linking it to PHB (Bernat & Wonjnowska-Baryla, 2007; Bernat, Wonjnowska-Baryla, & Dobrzynska, 2008; Chen et al., 2013). One study showed aerobic denitrification rates at 4.54 mgN/L after the sludge used accumulated 0.35 g PHB/ g VSS (Bernat & Wonjnowska-Baryla, 2007). Another similar study linked aerobic denitrification to PHB storage, observing a denitrification rate that doubled when the PHB intercellular storage increased from 0.23 – 0.40 g PHB/ gVSS (Bernat et al., 2008). Although aerobic denitrification is not the same as post-anoxic denitrification, it is interesting that these studies observed PHB storage for denitrification purposes, and the same organisms could be linked to post-anoxic denitrification if they are able to store carbon internally for denitrification purposes.

The bacteria thought to conduct post-anoxic denitrification are PAOs and GAOs, since they are enhanced within EBPR systems and they are both capable of storing carbon internally. One study shows that GAOs are more closely linked to post-anoxic denitrification than PAOs because GAOs keep their glycogen stores through aeration longer than PAOs keep their internal carbon stores (Zhao et al., 2019). This study also attributes partial denitrification producing nitrite accumulation to GAOs using internally stored carbon (Zhao et al., 2019). This could be due to evidence that GAOs have a greater affinity for NO_3^- reduction than NO_2^- reduction, while PAOs are the opposite (Rubio-Rincón et al., 2017). There is also research showing other types of bacteria capable of internal carbon storage and post-anoxic denitrification, like a study that highlights the bacterium *Paracoccus denitrificans* capable of both phosphate accumulation and denitrification using internal carbon storage in the form of PHB (Barak & Rijn, 2000).

More research needs to be conducted to determine the internal carbon storage compound for post-anoxic denitrification and to determine which bacteria are capable of this phenomenon. Post-anoxic denitrification has the potential to increase the efficiency of BNR & BPR systems by providing a very low carbon input source of denitrification while also providing bio-P. The potential for post-anoxic denitrification to intensify processes is great.

3. Methodology

This research was conducted at HRSD's BNR pilot, located at the Chesapeake-Elizabeth WWTP in Virginia Beach, VA. The BNR pilot is runs in an A/B process consisting of a high rate A-stage for carbon removal followed by a B-stage for nitrogen removal (pilot schematic shown in Figure 13 below). The pilot also includes an A-stage WAS fermenter and a sidestream RAS fermenter for biological phosphorus removal, and an anammox polishing step following B-stage. The anammox polishing moving bed biofilm reactor (MBBR) is used along with B-stage to accomplish shortcut nitrogen removal.

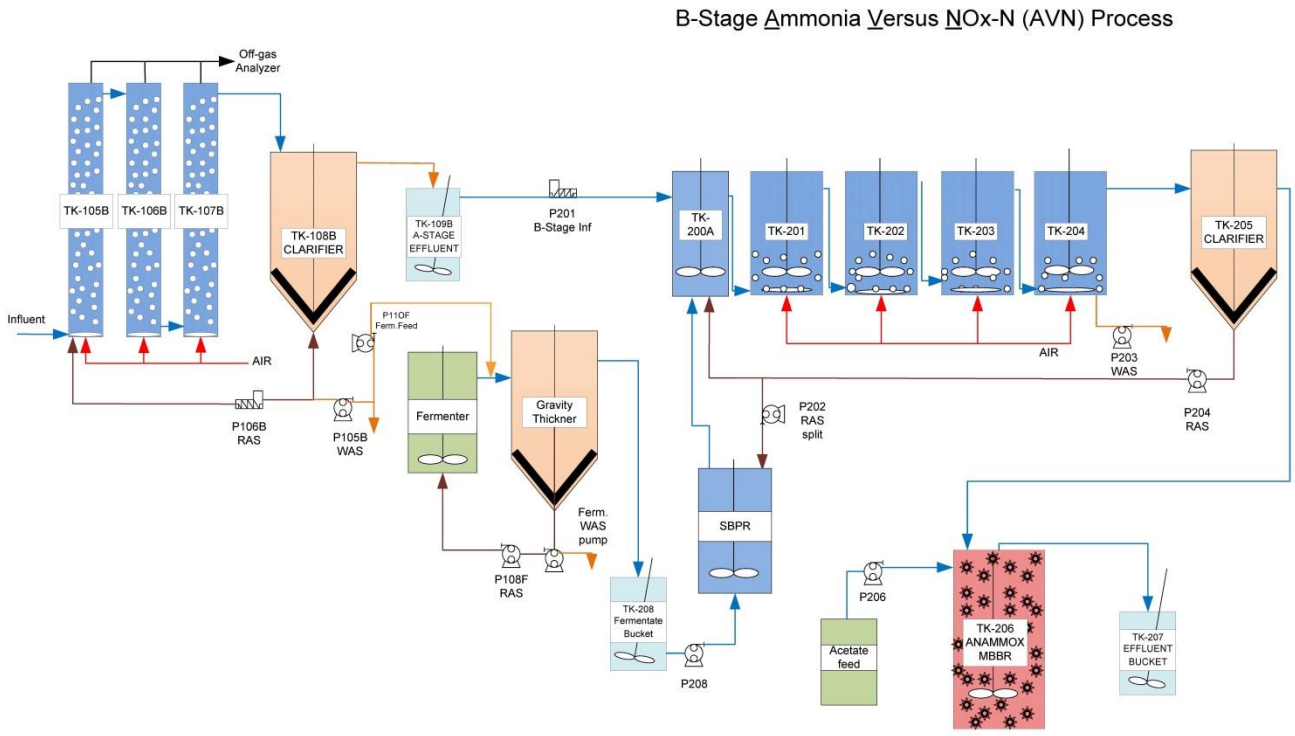

Figure 13: HRSD's BNR pilot process flow diagram- updated on November 2017

3.1 A-stage

The influent for the pilot is taken from the main plant influent after it is screened and degritted. The pilot influent is first pumped into a grit removal tank (removed grit by settling) then through a screen with 2.4 mm openings using a progressive cavity pump (Seepex, Somerset, UK). After the screen, the flow goes into a temperature control tank that regulates the water temperature to stay at 20°C using a heater and a chiller alternatively. The heater and chiller are controlled by a

programmable logic controller (PLC) (Allen Bradly, Milwaukee, WI) that uses a signal from a thermocouple in the temperature control tank to regulate the tank temperature based on a user-set temperature range. The temperature-controlled flow is then pumped into the A-stage reactors using another progressive cavity pump (Seepex, Somerset, UK).

There are three high-rate A-stage reactors in series, with a total volume of 511 L. After the reactors, the flow goes to a cone-bottom clarifier, and then the supernatant of the clarifier is fed as influent for the B-stage. RAS is returned from the bottom of the clarifier to the first A-stage reactor in series using another progressive cavity pump (Seepex, Somerset, UK). The MLSS in A-stage is controlled via the PLC using a TSS sensor (s::can, Austria) to measure the MLSS in A-stage, and a programmable digital peristaltic pump (Cole-Parmer, Vernon Hills, IL) to control wasting from the bottom of the clarifier to reach the desired MLSS value set manually in the PLC.

3.2 B-stage

The B-stage consists of an anaerobic selector with a volume of 53 L, followed by four CSTRs in series that have a total volume of 600 L. Once the B-stage influent is pumped into the anaerobic selector, the system is gravity fed through the CSTRs and then into a cone-bottom clarifier. The RAS is pumped from the bottom of the clarifier, using a programmable digital peristaltic pump (Cole-Parmer, Vernon Hills, IL), back into the anaerobic selector, except for a portion of the RAS which is pumped into the side-stream RAS fermenter, called the Sidestream Biological Phosphorus Remover (SBPR), using an additional programmable digital peristaltic pump (Cole-Parmer, Vernon Hills, IL). After the clarifier, gravity flow continues further into the anammox polishing step, comprised of a 340 L MBBR made up of K3 biofilm carriers (AnoxKaldness, Sweden).

B-stage instrumentation includes pH (Foxboro/Invensys, UK), dissolved oxygen (Hach LDO, CO, USA), ammonium (WTW VARiON, Germany), nitrate and nitrite (s::can Spectro::lyser, Austria), and nitrous oxide (Unisense, Denmark). The placement of the listed instrumentation is displayed in Figure 14 below. The CSTRs are intermittently aerated via a proportional-integral-derivative (PID) controller. The aeration times are determined through AvN control, with two separate PID loops. The first loop depends on the NH_4/NO_x ratio of sensor values in the effluent to control a solenoid valve determine the aerobic fraction. The second loop controls the motor operated valve to meet a programmable set point of 2.0 mg/L of DO when the air is on. The pH in B-stage is controlled to remain around 6.8 by the addition of sodium bicarbonate to TK-203, the third CSTR in series where the pH probe is also located, by a peristaltic pump (Cole-Parmer, Vernon Hills, IL).

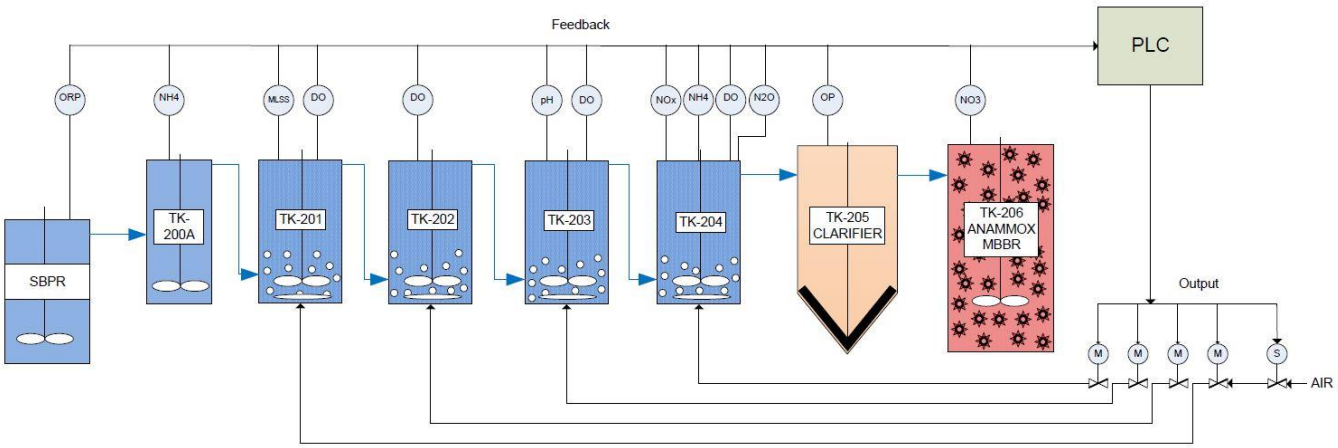

Figure 14: B-stage instrumentation and PID control

3.3 A-stage WAS fermenter

The A-stage WAS fermenter consists of a completely mixed fermenter and a gravity thickener. The influent to the fermenter is A-stage WAS and comes into the gravity thickener. The solids at the bottom of the gravity thickener are pumped into the fermenter by a programmable digital peristaltic pump (Cole-Parmer, Vernon Hills, IL), and the fermenter is fed back in to the gravity thickener by gravity for a total SRT of 3-5 days. Solids are wasted from the bottom of the thickener to maintain the SRT. The supernatant of the gravity thickener, the fermentate, is captured in a 5 gallon bucket then pumped into the SBPR by a programmable digital peristaltic pump (Cole-Parmer, Vernon Hills, IL).

3.4 Sidestream biological phosphorus remover (SBPR)

The SBPR is fed by B-stage RAS and by fermentate both by a programmable digital peristaltic pump (Cole-Parmer, Vernon Hills, IL). A programmable digital peristaltic pump is used to feed the SBPR into the anaerobic selector of B-stage. The SBPR is mixed for a 10 minute duration every 3 hours. The SBPR operates at a 4-7 day SRT and a HRT of about 4 hours

3.5 Data analysis

Total suspended solids (TSS) and volatile suspended solids (VSS) were analyzed using 2540D and 2540E in Standard Methods (APHA, 2005), respectively. Total chemical oxygen demand (COD), soluble COD (sCOD), and floc-filtered COD (ffCOD) which is also known as readily-biodegradable COD (rbCOD), were measured via HACH TNT 820, 821, and 822 kits and a HACH DR2800 spectrophotometer (HACH Loveland, CO). All COD, TSS, and VSS samples use a 1.5 µm glass microfiber filter. Orthophosphate (OP), NH_4^+-N, NO_3^--N, NO_2^-N, and cyanide (CN) were measured by first filtering the sample through a 0.45 µm cellulose acetate

filter then HACH TNT 846, 830, 831, 832, 835, 836, 839, 840 kits were used along with the spectrophotometer, respectively (HACH Loveland, CO).

3.6 Sampling

Composite samples are drawn daily to help analyze the overall pilot performance. These samples are 24-hour composites that extract 250 mL aliquots every hour using automated samplers (ISCO, Lincoln, NE). The samplers are set to sample A-stage influent and effluent (A-stage effluent = B-stage influent), B-stage effluent, and B-stage polished effluent after the anammox polishing step. Composite samples are measured daily for TSS, VSS, COD, soluble COD, OP, NH_4^+-N, NO_3^--N, and NO_2^-N. Floc-filtered COD is measured weekly.

Additionally, some samples are taken daily for measurement directly from the process, usually between 7 AM-8 AM on the day of analysis. The fermentate (product of the fermenter that is fed into the SBPR) is taken daily and analyzed for TSS, VSS, COD, sCOD, OP, NH_4^+-N, and VFA. The SBPR was tested daily, before and after mixing, for TSS. The fermenter was also tested daily for TSS, used for accurate SRT calculations of the fermenter. A-stage WAS (fed into the fermenter) is grabbed daily and tested for TSS, VSS, COD and sCOD. MLSS from A-stage and B-stage are both grabbed daily and tested for TSS and VSS, and used for accurate, daily SRT calculations.

3.7 AOB/NOB activity measurement

A 4-liter MLSS sample from TK-204 in B-stage is taken to the bench and measured for AOB and NOB activity weekly. The MLSS is aerated between 3-5 mg/L of DO, completely mixed using a submersible pump, and regulated to maintain a pH around 7 using acid and base addition. The sample is aerated for 10 minutes before it is spiked with around 10 mg/L of NH_4^+-N and 2 mg/L NO_2^--N, to make sure the test is not limited in substrate or oxygen. A sample is taken after spiking and every 15 minutes following the first sample, for a total of 1 hour. All samples are analyzed for NH_4^+-N, NO_2^--N, and NO_3^--N concentrations. AOB maximum rates are calculated based on NO_x accumulation over time ($mgNO_x$/L/hr) and normalized to the MLSS measurement ($mgNO_x$/gVSS/hr). NOB maximum rates are calculated based on NO_3^- accumulation over time ($mgNO_3$/L/hr) and also normalized to ($mgNO_3$/gVSS/hr).

3.8 PAO/dPAO activity measurement

A 4-liter sample of MLSS from TK-204 is grabbed and placed on the bench for testing. The test is completely mixed, and DO and pH are measured throughout the test, with pH control around 7 using acid and base addition.

3.8.1 PAO

The first part of the PAO test involves anaerobic OP release, so no aeration is added and the test is covered with Styrofoam to prevent air-transfer. Between 150-300 mg/L of acetate as COD is spiked at time 0 of this test and samples are taken every 10-30 minutes. All samples in this part of the test are measured for OP, NO_3^-, NO_2^-, NH_4^+, and sCOD. Anaerobic OP release rates are measured using mg/L of OP over time (mgOP/L/hr), and are normalized with the VSS of the test to mgOP/gVSS/hr. The COD uptake is measured by mg/L of sCOD over time, and is sometimes calculated around the NO_3^- denitrification rates throughout the test to determine the accurate OP release/COD uptake.

The second part of the PAO test involves aerobic OP uptake, so the styrofoam cover is removed and the test is aerated between 4-6 (mg DO/L). Samples are taken every 10-30 minutes and analyzed for OP. The OP release rates are measured using mg/L of OP over time (mgOP/L/hr) and are normalized with the VSS of the test.

3.8.2 dPAO

The dPAO test is performed after the anaerobic portion of the PAO test. Usually, the bench scale MLSS is split into two containers after the anaerobic portion so that the anoxic dPAO test can be done along with the aerobic part of the PAO test. The styrofoam cover is kept on, pH and DO are measured throughout the test, and the MLSS remains completely mixed using a submersible pump. About 20 mg/L of NO_3^- is spiked, and 1-2 mg/L of NO_2^- is spiked, and samples start after spiking and are taken every 15 minutes until 1 hour. Samples are analyzed for OP, NO_2^-, NO_3^-, NH_4^+, and sCOD. Activity is indicated by anoxic OP uptake, so dPAO activity is measured by OP uptake in mg/L over time (mgOP/hr/L). To indicate dPAO activity over normal denitrification, sCOD is measured to insure no additional COD uptake is used throughout the test. Denitrification is measured using NO_3^-, NO_2^-, and NO_x reduction in concentration over time.

3.9 ISCD activity measurement

The internally stored carbon denitrification (ISCD) test starts by taking a 4-liter sample of MLSS from TK-204 and bringing it to the bench. The goal of this test is to determine post-anoxic denitrification rates of internally stored carbon compounds after aeration in the process (the MLSS has been through aeration once it is in TK-204). The test is anoxic, and is covered by styrofoam and monitored to insure there is no DO throughout the test. The MLSS is completely mixed using a submersible pump and the pH is monitored. The test starts by spiking about 30 mg/L of NO_3^- and 1-5 mg/L of NO_2^-, and samples are taken every 10 minutes up to 1 hour. All samples are analyzed for NH_4^+, OP, NO_2^-, NO_3^-, and sCOD. NO_3^- and NO_2^- denitrification rates

are measured by observing the NO_3^- and NO_2^- decrease or increase over time (NO_x/L/hr). OP is monitored to ensure no dPAO activity is occurring, and sCOD is measured to insure that the denitrification is due to internally stored carbon and not due to uptake of external carbon.

3.10 Profile measurement

In-space profiles are taken in B-stage twice a week to analyze the OP uptake and release throughout the system. Profiles samples are pulled from the SBPR (both before and after mixing), the anaerobic selector, and TK-201, 202, 203 and 204 (intermittently aerated CSTRs). Samples are pulled approximately two hours after the SBPR has mixed (it mixes every 3 hours for a 10 minute duration) at the end of an air-on period in the CSTRs. The SBPR is mixed manually after the profile is pulled to compare the before and after mixed SBPR sample. Samples are analyzed for OP, NH_4^+, NO_3^-, NO_2^-, and sCOD. OP uptake in the system is measured by subtracting TK-204 OP (mg/L) from AS OP (mg/L). OP release in the SBPR is calculated by taking the concentrations of the SBPR before and after mix and multiplying by their effective times, then subtracting the fermentate OP (added into the SBPR) out. Soluble COD consumed in the SBPR is calculated by using the fermentate COD that goes into the SBPR in g/day and subtracting out either after-mix or before-mix sCOD from the profile in g/day.

3.11 Central Environmental Laboratory (CEL) sampling

Samples from the pilot process are sent bi-weekly to the HRSD laboratory for analysis. Samples sent twice a week include A-stage WAS, 208 (fermentate), and SBPR (after mix). Samples sent only once a week are the A-stage and B-stage mixed liquor.

The VFA is measured for A-stage WAS, 208 fermentate, and the SBPR. The VFA is analyzed with the distillation method, which measures the overall VFA concentration as acetic acid in COD mg/L. In this analysis method, all VFA in a sample was steam-distilled then measured using titration of 0.1 N NaOH, following the procedures for distillation from Standard Methods (APHA, 2005).

3.12 EA_ANX and EA_EICD tests

Bench tests were done on day 582 to determine the actual endogenous decay rate in B-stage. Mixed liquor was taken from TK-204 of B-stage and set on the bench on day 581 to be aerated overnight before the tests, to deplete any external carbon and internal carbon storage. The MLSS was then split into two different tests performed on day 582.

3.12.1 EA_ANX: system endogenous decay

This test was completely anoxic for 360 minutes in order to determine the endogenous decay rate in B-stage. The goal of this test was to determine the actual endogenous decay rate in the system by ensuring that all internal and external carbon was used up so that the denitrification rates observed must only be due to cell decay. The test was covered with a Styrofoam cover in order to reduce oxygen transfer, and the DO was monitored to ensure that it remained at 0 mg/L. Nitrite was spiked at the beginning of this test (it was not necessary to spike nitrate because the test had been aerating for about 15 hours so all ammonia should have been converted to nitrate) at a concentration of 1 mg/L NO_2^- -N. Samples were taken throughout the duration of the test, filtered through a 0.45 µm cellulose acetate filter, and measured for NH_4^+, OP, NO_2^-, NO_3^-, and sCOD using HACH kits (HACH Loveland, CO). A sample was pulled from this test to measure MLSS and MLVSS. The endogenous rate for the pilot was measured from this test by calculating the NO_x decreasing rates over time through the duration of this test.

3.12.2 EA_EICD: system internally stored carbon denitrification

This test was anaerobic for 120 minutes, and then was washed in order to remove external carbon, and then the test was anoxic for an additional 1108 minutes. The goal of this test was to determine the actual denitrification rate from internally stored carbon by first getting rid of external and internal carbon by over aerating for 15 hours, then by spiking COD and allowing time for cells to store that COD internally, washing the mixed liquor to get rid of any extra external carbon, then by spiking with nitrate and nitrite. After doing all of this, it could be ensured that the only energy source for the denitrification happening in the anoxic time was internally stored carbon. To start the anaerobic part of this test, 210 mg/L of acetate as COD was spiked. There was an hour of washing between the anaerobic part of the test and the anoxic part, and 30 mg/L NO_3^- & 1 mg/L NO_2^- was spiked at the beginning of the anoxic part. Samples were taken intermittently in the anaerobic period and anoxic period and filtered through a 0.45 µm cellulose acetate filter, and measured for NH_4^+, OP, NO_2^-, NO_3^-, and sCOD using HACH kits (HACH Loveland, CO). A sample was pulled from this test to measure MLSS and MLVSS. The internally stored carbon denitrification rate for the pilot was measured from this test by calculating the NOx decreasing rate over time through the duration of the anoxic period of this test. The sCOD measured in the anoxic period ensured that no additional external carbon uptake was interfering with the ISCD rate.

3.13 Statistical analysis

Linear correlation analysis was done on two distinct periods of data. This analysis lists the r^2 values of several different linear regressions in chart form. Each r^2 value represents a single

linear regression relating two different data sets. The rows of the charts display the relation of the r^2 values to the X-axis of the linear regressions, and the columns of the chart display the relation to the Y-axis.

4. Results and Discussion:

The average influent and effluent characteristics for A and B stage (A-stage effluent is B-stage influent) for the entire 0-632 day duration of the research are displayed below in Table 1. All values are included except for NH_4^+, NO_3^-, and NO_2^- during cyanide inhibition periods (days 353-368, 400-445, 486-519, & 542-584). The average TIN % removal for this entire period excluding the cyanide inhibition periods was 47 ± 13 (% removal of TIN) and the average OP % removal of this period was 25 ± 53 (% removal of OP). The average AvN (effluent NO_x/NH_4) of this period was 1.4 ± 5.8 mg/mg.

Table 1: Pilot influent and effluent characteristics

	NH_4^+ (mg N/L)	**NO_2^- (mg N/L)**	**NO_3^- (mg N/L)**	**OP (mg OP/L)**	**COD (mg COD/L)**	**sCOD (mgCOD/L)**
A-stage influent	34 ± 3.7	-	-	4.0 ± 0.9	538 ± 136	176 ± 38
B-stage influent	30 ± 3.8	-	-	2.3 ± 0.7	232 ± 60	97 ± 22
B-stage effluent	7.6 ± 2.6	0.9 ± 1.4	7.1 ± 2.5	1.6 ± 1.0	57 ± 19	31 ± 7.0

The data represented in this research expands from day 0 of research, when the SBPR and fermenter were implemented in the pilot, to day 362. The three main operational phases compared in this research are listed below in Table 2, and the result phases discussed in this experiment are listed below in Table 3.

During the first operational phase, there was no change to operation but there were two result phases observed. Effluent OP was consistently below 1 OP (mg/L) for a period of time described, by result period 1. The effluent nitrite also increased during operational period 1, described by result period 2, where effluent nitrite was above 1 mg/L NO_2^+ the entire time. The specific timing of the low effluent OP period followed by the bio-P failure, then the nitrite accumulation, was unknown since conditions were not changed to induce any system changes. These two result phases are displayed below in Figure 15.

Table 2: Operational phases of research

Phase name		Phase name abbreviation	Duration (days)	Total days	SBPR HRT (hour)	Fermentate addition	Description
Operational phase 1		OP1	227-385	172	3.6	100%	RP1 & RP2- Low effluent OP and high effluent NO2
Operational phase 2	A	OP2-A	385-399	14	3.6	20%	Reduced fermentate addition/SBPR HRT maximization experiment
	B	OP2-B	399-434	35	20.7	10%	
	C	OP2-C	434-482	48	14.2	0%	
Operational phase 3		OP3	482-632	150	3.9	50%	RP3-Fermentate dose experiment

*when fermentate addition = 100% then the maximum load of fermentate that can go into the SBPR is met. When the fermentate addition <100% then the load has been decreased from that maximum

Table 3: Result phases of research

Phase name	Phase name abbreviation	Results		Duration (days)	Total days
Result phase 1	RP1	Effluent OP < 1 mg/L	Average OP = 0.46 ± 0.14 mg/L	264-292	28
Result phase 2	RP2	Effluent NO_2^- > 1 mg/L	NO_2^- = 3.23 ± 1.36 mg/L	295-401	106
Result phase 3	RP3	Effluent OP < 1 mg/L	OP = 0.55 ± 0.17 mg/L	530-549	19

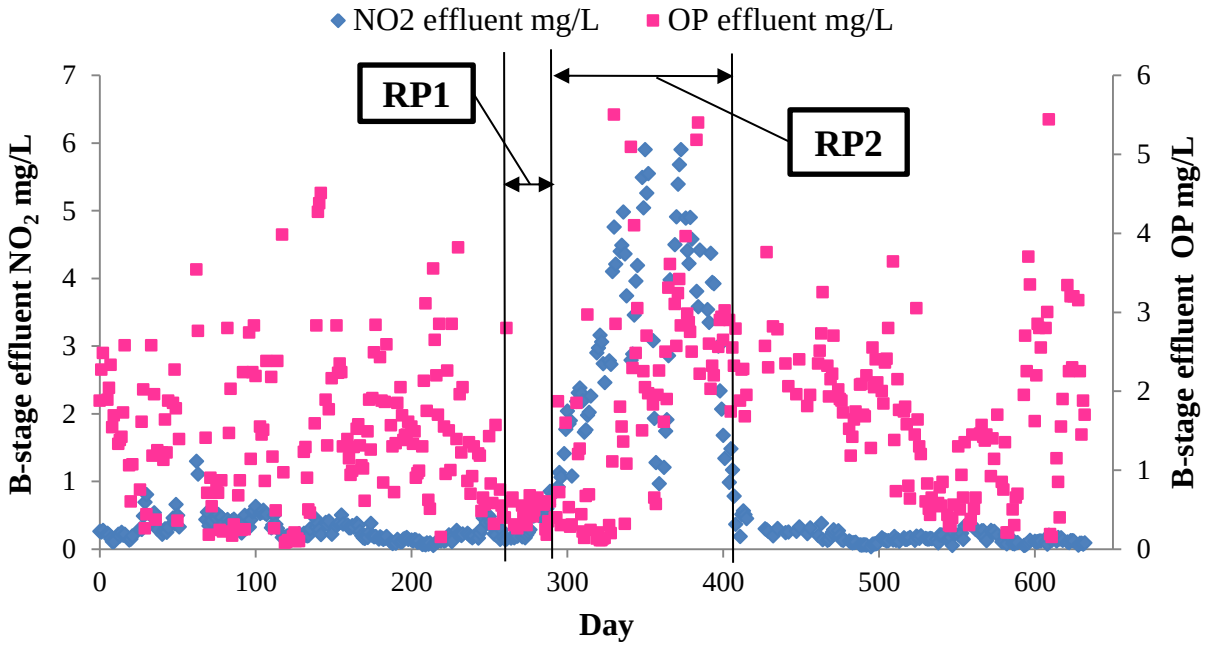

Figure 15: B-stage effluent nitrite (mg NO_2^-/L) shown on the left y-axis and OP (mg OP/L) shown on the right y-axis for the entire duration of research. Result period 1 where effluent OP was <1 (mg OP/L) and result period 2 where effluent NO_2^- >1 (mg NO_2^-/L) are displayed on this graph. The analysis methods for this data are described in section 3.1

It is important to note that the pilot experienced cyanide inhibition during the time of nitrite accumulation, for an unknown duration of time. This was due to some operational failures at the main plant, where recycle centrate streams high in cyanide were being added back into the main plant influent before the pilot influent pump location. Cyanide is a known inhibitor of nitrification at values as low as 0.08 (mg CN/L) at 20°C (Salazar-Benites, 2017). Throughout days 400-600, there was an average of 0.019 ± 0.010 (mg CN/L) detected in the A-stage influent (shown in Figure 16 below), which isn't as high as the 0.08 (mg CN/L) total inhibition value referenced but might have still had a role in inhibiting nitrification to some scale at the pilot. Unfortunately, the influent cyanide was not discovered and measured until day 400, so there is no way of knowing what concentration of cyanide was affecting the pilot around day 350 where the dip in nitrite accumulation occurred. However, the recycle centrate stream that contained the cyanide was measured to have a CN concentration of 1.23 (mg CN/L) on day 415, and conditions were not changed to prevent the flow of this stream until after day 415 so it is likely that cyanide had a big inhibitory effect around day 350.

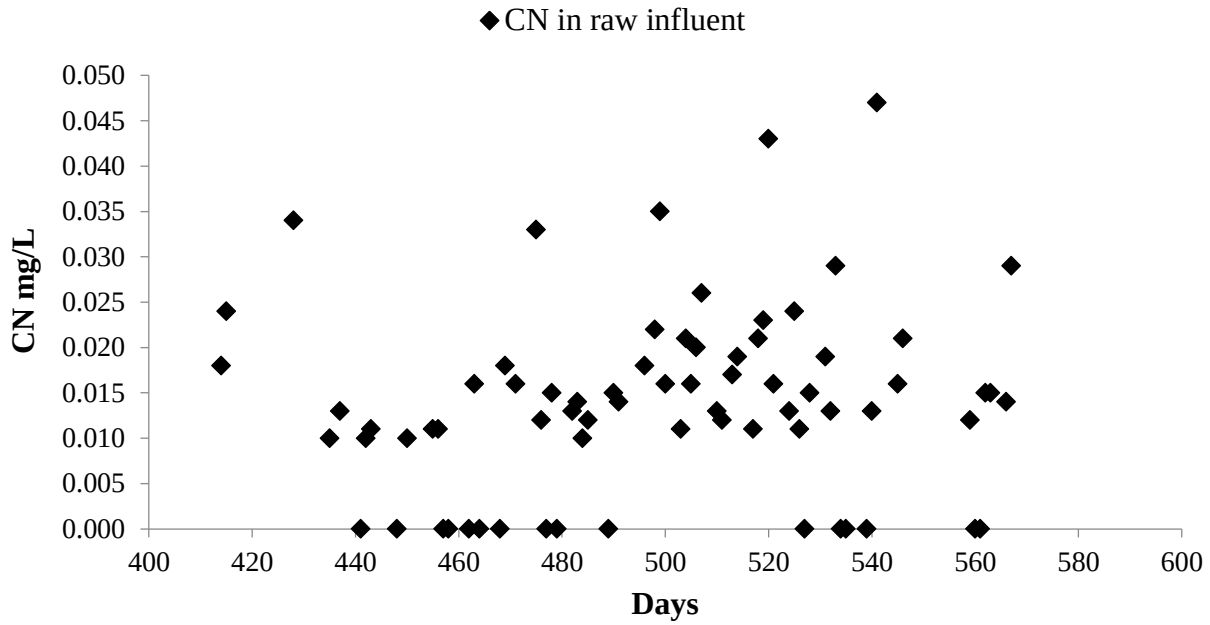

Figure 16: Cyanide measured in the influent composite, described in section 3.2, (mg CN/L) is displayed on the y-axis. All 0 values shown on this graph represent all values <0.002 mg CN/L. The analysis methods for cyanide measurement is described in section 3.1

4.1 Determining the cause of the nitrite accumulation

Result phase 1 was not entirely unexpected since it was the goal of the fermenter and SBPR all along, but result phase 2 was unexpected. The B-stage in the pilot has been successful at NOB out-selection in the past, with the goal to supply a nitrite source for the anammox polishing step (Regmi et al., 2014) . Intermittent aeration duration in the reactors is controlled via effluent ammonia vs NO_x (AvN) control. The AvN was set to a NO_x/NH_4 ratio of 1, which has proved to be a successful ratio for achieving NOB out-selection using growth rate kinetics of AOB and NOB observed at the pilot when the pilot is controlled at 20°C (Regmi et al., 2014). This control was used again starting around day 0 when the SBPR and fermenter were implemented, but NOB out-selection never occurred. One possible explanation is that the increased carbon added to B-stage via the SBPR and fermenter increased heterotrophic denitrification, which may have supplied a NO_2^- source for NOB to thrive (Winkler et al., 2012). This is shown in weekly AOB & NOB rate tests; NOB rates were higher than AOB for most of the experiment duration (see Figure 17 below).

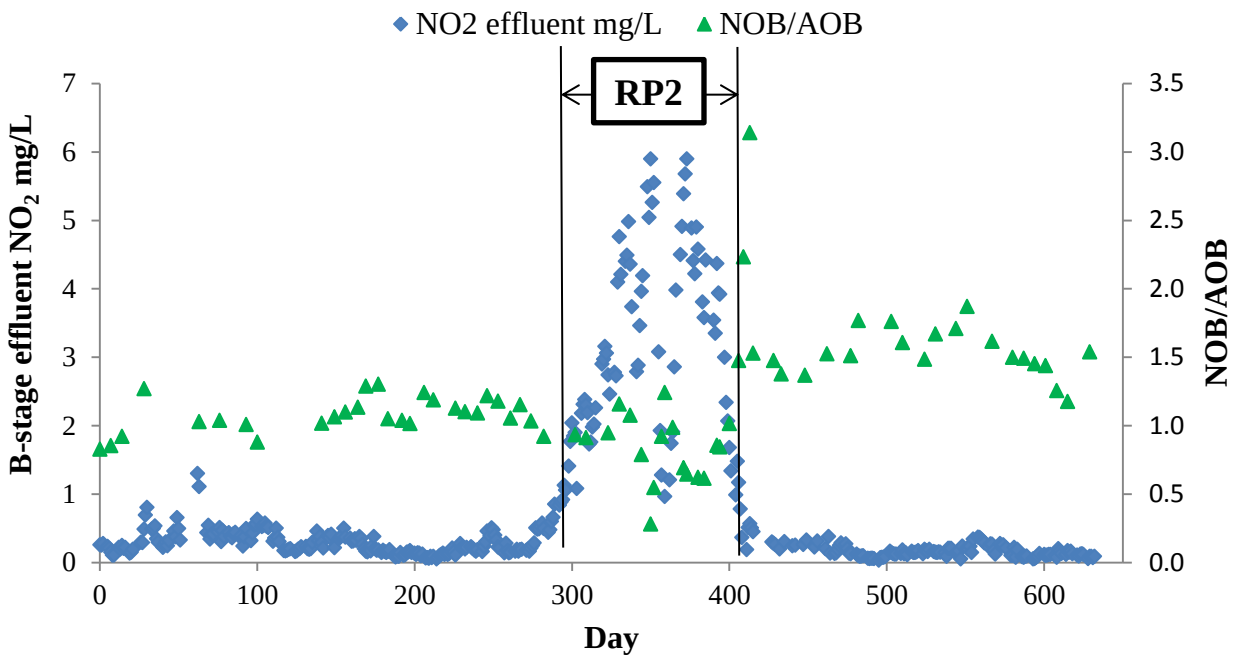

Figure 17: B-stage effluent nitrite (mg NO_2^-/L) is displayed on the left y-axis and NOB/AOB maximum rate test fractions are displayed on the right y-axis. Result period 2 where effluent NO_2^- >1 (mg NO_2^-/L) is displayed on this graph. The analysis methods for NO_2^- are described in section 3.1, and the AOB&NOB activity test methods that produce the weekly maximum substrate AOB and NOB rates are described in section 3.3

Several tests were done to determine the cause of the unexpected nitrite accumulation. In-situ profiles of the CSTRs were taken over time to explore what was happening during the aerobic and anoxic periods (example profile Figure 18 below). These profiles showed that nitrite accumulation was happening during the anoxic periods, ruling out NOB out-selection as the cause. Since the nitrite accumulation was happening during the anoxic periods in the intermittently aerated CSTRs, ruling out NOB out-selection as the source, it was theorized that the source of the nitrite accumulation was partial denitrification of NO_3^- to NO_2^-. Since this was happening in aerated reactors where external carbon should not have been available, it was also theorized that the partial denitrification was due to an internally stored carbon compound. In order to determine if this theory was correct, internally stored carbon denitrification tests were done (see example Figure 19 below).

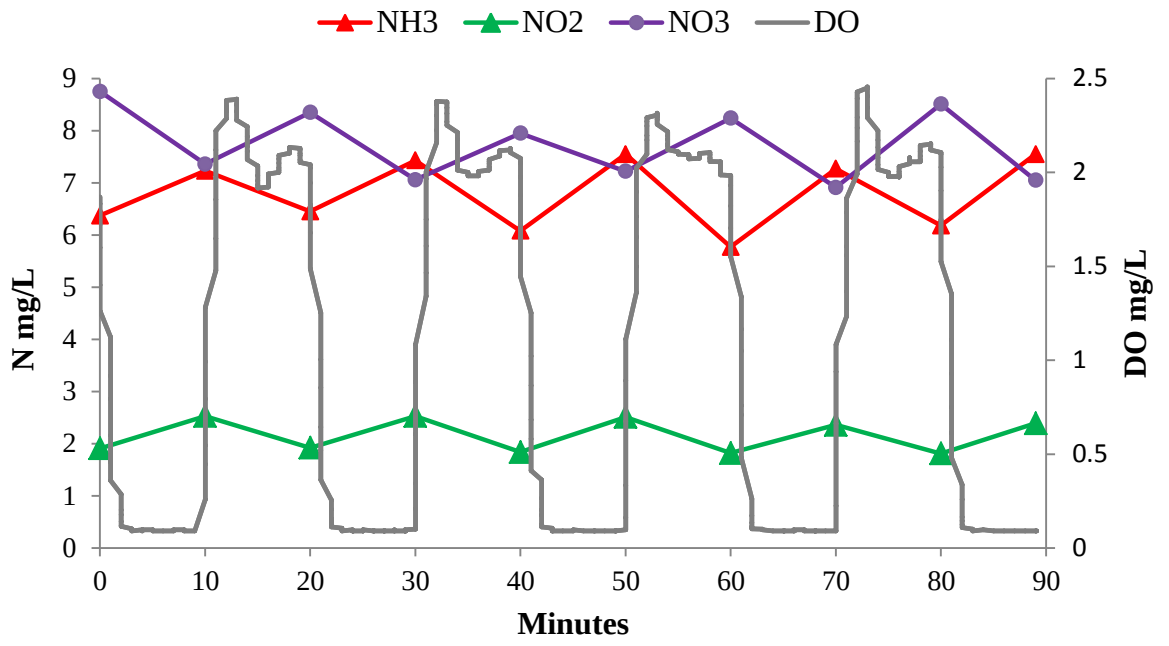

Figure 18: Profile taken in the last CSTR over time on day 320. This data shows nitrite accumulation in the CSTR during the air-off times. The methods for profiles are described in section 3.6

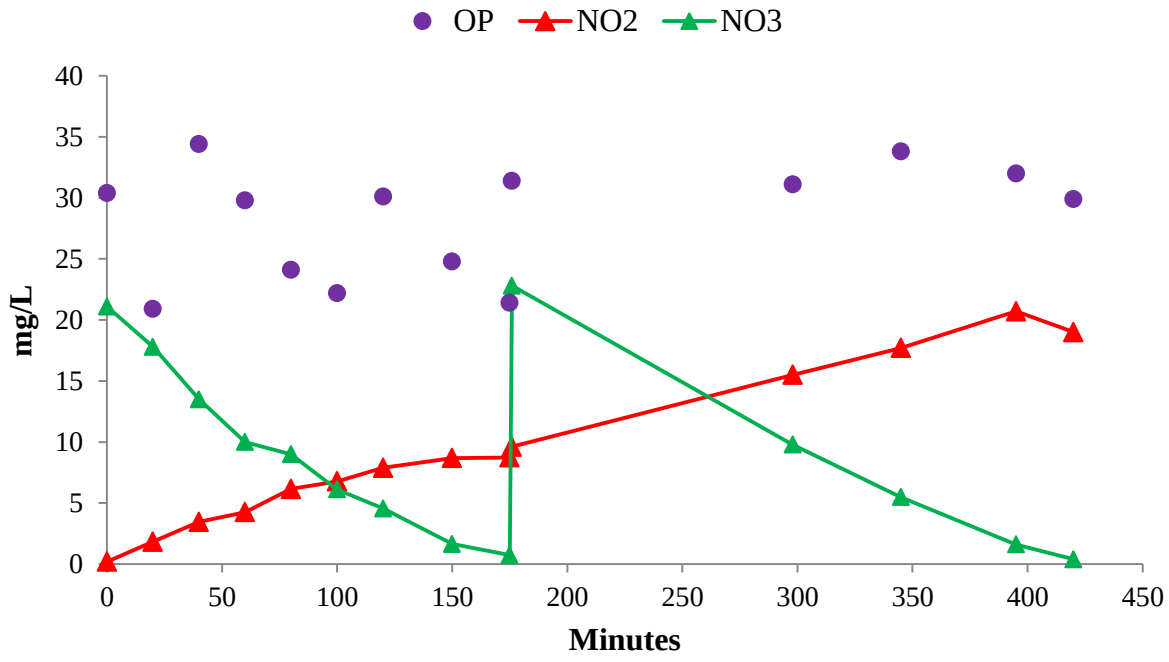

Figure 19: Internally stored carbon denitrification test using MLSS from the last CSRT on day 312. This test shows nitrite accumulation due to partial denitrification of nitrate to nitrite using internally stored carbon. The methods for ISCD tests are described in section 3.5

This ISCD test in Figure 19 used mixed liquor from the last aeration reactor, where there should be no external carbon available for uptake. The denitrification rates in this sample were observed on the bench in a completely anoxic state after spiking with NO_3^-. The test showed NO_3^- denitrification and subsequent NO_2^- accumulation, with NO_2^- accumulation ceasing when NO_3^- ran out, showing that partial denitrification of NO_3^- was the source of the nitrite accumulation. The OP was measured throughout the test and no additional OP uptake observed shows that the partial denitrification was not being performed by dPAOs, who uptake phosphorus when using NO_3^-/ NO_2^- as the electron acceptor in anoxic environments. Although not displayed in Figure 19, the sCOD was measured throughout the test and stayed around 45 (mg COD/L) throughout the duration of the test, further showing that no external carbon was being used as the electron source for the displayed denitrification. Since the denitrification rates observed were higher than usual endogenous denitrification rates (Kujawa & Klapwijk, 1999), the best explanation for the denitrification observed in this test would be the use of internally stored carbon to supply the electron source necessary for denitrification. This test was repeated several times throughout result phase 2 and after, shown below in Figure 38 in the results section.

Although it was theorized that the nitrite accumulation was due to partial denitrification of NO_3^- to NO_2^- using internally stored carbon compounds, the bacteria responsible for this phenomenon and the source of the internally stored carbon remained unknown. Certain studies have shown that dGAOs can be linked to nitrite accumulation since they have a higher affinity to use NO_3^- over NO_2^- as an electron acceptor (Rubio-Rincón et al., 2017). If dGAOs were the bacteria causing the nitrite accumulation then it would also explain the poor bio-P performance after the nitrite accumulation started, since dGAOs would be competing with PAOs for VFA. Studies have also shown links to post-anoxic denitrification in EBPR systems, where implementing EBPR leads to internally stored carbon that can be saved during aeration and used after aeration for denitrification (Vocks et al., 2005). This led to the theory that the SBPR and fermenter were supplying the source of the internally stored carbon, and possibly hosting the bacteria responsible for the partial denitrification.

4.2 Decreased fermentate addition / SBPR HRT maximization experiment

To explore the theory that the fermentate (supernatant of the fermenter that is added to the SBPR) was the source of the internally stored carbon that caused the nitrite accumulation, the fermentate addition into the SBPR was reduced. The SBPR HRT was also maximized following the fermentate reduction, to explore if the SBPR could operate efficiently to produce low effluent OP without the fermentate source. These changes made are described in Table 2 under operational phase 2. The operational phase 2 was divided into three separate operational phases, operational phase 2-A, B & C, shown in Figure 20.

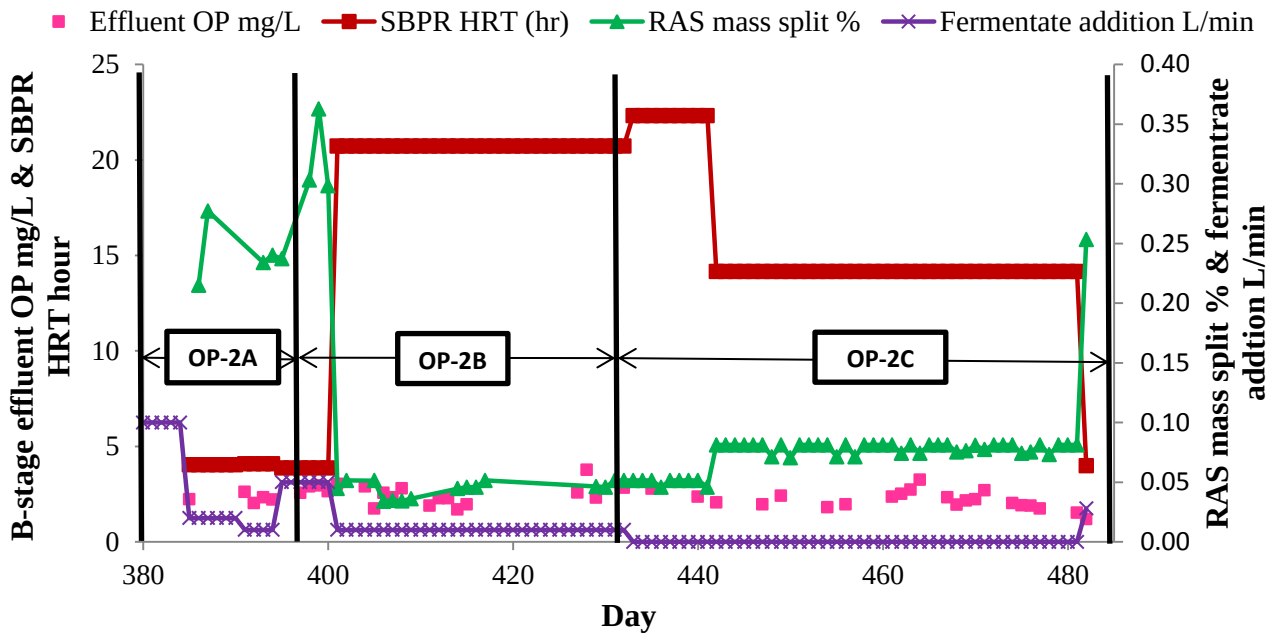

Figure 20: B-stage effluent OP (mg OP/L), SBPR HRT (hours), RAS mass split % going into the SBPR, and the fermentate addition into the SBPR (L/min) are displayed over the entire operational phase 2. This figure displays the HRT maximization during the three different operational phases and 2 sub-phases.

4.2.1 Operational phase 2A

The first fermentate reduction was by 80% on day 385. This fermentate reduction phase lasted until day 399; during this period the fermentate addition was adjusted several times but remained at least 50% less than the operational phase 1 fermentate addition amount. Fermentate reduction coincided with a rapid decline in nitrite accumulation, further linking the fermentate to the carbon source stored internally and used for denitrification. Batch tests using the same methods as the ISCD tests, like the one shown in Figure 19 above, showed the nitrite accumulation rates decreasing around the start of this phase (shown in later results in Figure 38). It should be noted that COD & VFA addition to the SBPR from fermentate was decreasing prior to the fermentate flow reduction because of decreasing concentrations in the fermentate. See Figure 40 for the VFA from the fermentate compared to the nitrite accumulation. It clearly shows that the decrease in VFA added in g/day coincides with the nitrite accumulation decreasing, but it is hard to directly correlate because of cyanide interference likely decreasing VFA production in the fermenter and decreasing nitrite accumulation rates by inhibiting the bacteria responsible for partial denitrification.

4.2.2 Operational phase 2B

The second major fermentate reduction phase was implemented on day 399 and accompanied a HRT increase in the SBPR. The idea was to see if the SBPR could function properly for fermentation and bio-P enhancement without relying on fermentate addition, so the HRT was increased to 20.7 hours. Nitrite accumulation continued to decline until it ceased all together around day 401. The VFA concentration in the SBPR effluent increased, indicating that VFA production was happening in the SBPR at a longer HRT, but overall VFA consumption in the SBPR decreased rapidly (See Figure 21 below). It should also be noted that fermentate addition was still adding VFA to the SBPR, so the VFA production measured is likely a factor of both the VFA added and produced. The negative VFA consumption values during this time indicate that there was some VFA production in the SBPR since more VFA was exiting the SBPR than entering. If VFA was being produced and not consumed at a higher HRT, it is theorized that there were not enough bacteria to consume the VFA produced due to the decreased RAS and fermentate addition into the SBPR. This shows that the SBPR is not large enough to have an HRT long enough for fermentation and to have a large enough incoming RAS mass split % and fermentate flow to provide bacteria in the SBPR to consume the produced VFA.

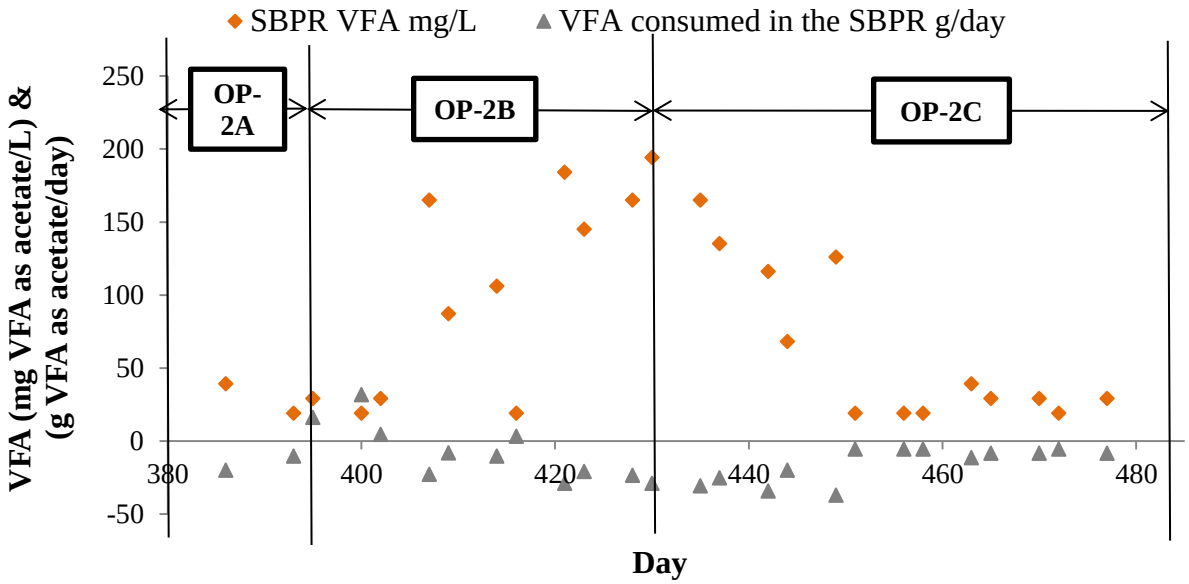

Figure 21: SBPR effluent VFA concentration (mg VFA as acetate/L) and VFA consumed in the SBPR (mg VFA as acetate/L). The VFA consumed was calculated by subtracting the SBPR effluent VFA (mg VFA as acetate/L) from the VFA entering the SBPR via the fermentate (mg VFA as acetate/L). This VFA data comes from the CEL distillation method, described above in section 3.7

4.2.3 Operational phase 2C

The fermentate addition was shut off completely on day 434. The HRT was decreased to 14.2 hours, since the 20.7 hour HRT had produced fermentate but wasn't housing enough bacteria to consume the VFA produced. The thought was to choose a HRT in between the HRT where fermentate was needed because no fermentation in the SBPR was happening and the HRT where only fermentation was happening to see if the SBPR could produce fermentation and consume VFA without relying on the fermenter. This phase went until day 482, and during that time VFA production and consumption in the SBPR halted (see Figure 21 above). There was also no nitrite accumulation during this time and no bio-P activity observed in maximum activity PAO tests. Due to the size of the SBPR in the pilot limiting the SRT, the SBPR is most likely unable to operate to produce bio-P without fermentate addition from the fermenter.

4.3 Dosing experimental setup- operational phase 3

In order to identify the fermentate VFA addition amount that caused the theorized population shift from PAOs to the bacteria that stored carbon internally through the aerobic reactors and caused subsequent nitrite accumulation, a fermentate dosing experiment was set up. The fermentate dose was controlled based on the sCOD of the fermentate and the OP of the fermentate and the influent (see Equation 7 below). The fermentate flow into the SBPR (mL/min) was to be adjusted to meet the desired C/P based on daily fermentate and B-stage influent measurements. The controlling factor, sCOD, was chosen instead of VFA because of possible hydrolysis of colloidal COD impacting bio-P and because of more reliable same-day COD analysis methods. The VFA/P was monitored throughout the experiment for comparison reasons not dosing reasons; see Equation 8.

$$C/P = \frac{sCOD\ fermentate\ \frac{g}{day}}{\left(OP\ fermentate\frac{g}{day}\right)+\left(OP\ influent\frac{g}{day}\right)} \quad (7)$$

$$C/P = \frac{VFA\ fermentate\ \frac{g\ as\ acetate}{day}}{\left(OP\ fermentate\frac{g}{day}\right)+\left(OP\ influent\frac{g}{day}\right)} \quad (8)$$

Using the equation above, the average C/P was calculated for result period 1 at around 23 g/g. The dosing plan, displayed in Table 4 below, was to start dosing fermentate at 60% of the 23 C/P to underdose fermentate, then to increase the dose in phases once conditions stabilized. It was theorized that some C/P value would enhance bio-P performance, and at some C/P value there would be enough internally stored carbon that would lead to nitrite accumulation. There was also interest in overdosing the C/P at a higher value than result period 1 to seeing if that promoted nitrite accumulation further. Although the dosing was not controlled Conditions during each

phase of the dosing experiment were to be compared to result period 1 & result period 2 to make conclusions about the causes of these periods.

Table 4: Dosing control phases based off of the C/P in result period 1

% of C/P phase	C/P	VFA/P
60%	13.6	6.17
100%	22.7	10.3
150%	34.0	15.4

By recreating the conditions of result period 1 in a more controlled way, bio-P activity could be more easily linked to fermentate COD variations. It is clear that fermentate COD addition is the source of the high bio-P activity that caused the low effluent OP and the source for internally stored carbon partial denitrification, but it is unclear how much fermentate COD is needed to cause these results. It is also unclear if nitrite accumulation and biological phosphorus removal can function together at the same time, and in what conditions this would occur. By comparing the more controlled COD dose to result periods 1 & 2, information about the carbon requirements to produce both results can be explored in order to apply the carbon dosing strategy successfully to other sidestream treatment systems.

4.4 Operational phase 3 & result phase 3

4.4.1 Success in controlled fermentate load

Fermenter performance varied, but the five-month dosing period averaged of 15.58 ± 3.00 C/P. The load adjustments to meet the desired 13.6 C/P are displayed below in Figure 22. The load adjustments were originally made based on 2-3 day averages of sCOD and OP measurements, but fermenter variation was higher than expected so the adjustments were switched to daily adjustments approximately 24 days into the experiment. The average percent error of the first 24 days was 24%, which decreased to an average of 13% after dosing was switched to daily adjustments. The average VFA/OP for this five-month period was 5.46 ± 1.26 (g VFA as acetate/g OP).

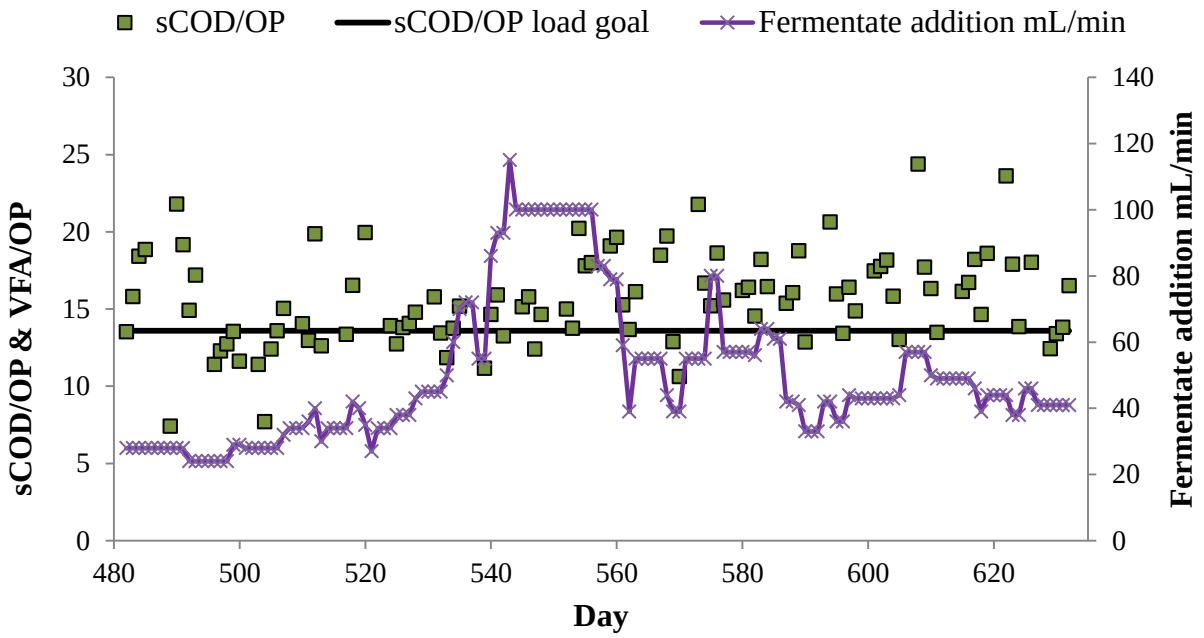

Figure 22: Operational phase 3 (OP3) C/P load and the OP3 load goal along with the fermentate addition used to control the C/P load. The C/P ratio was calculated using equation 7 above.

When the five-month dosing period C/P is compared to the entire duration of the research, it is clear that there was a lot of variation in the ratio, displayed in Figure 23 below. The fermentate addition dose to the SBPR was fairly unchanged for the duration of the experiment leading up to operational period 3, but the fluctuations in OP and VFA concentrations of fermentate drastically changed the loads. This indicates that variation in fermenter performance or incoming COD types and concentrations to the fermenter had a greater effect on the amount of COD and VFA added than previously taken into account.

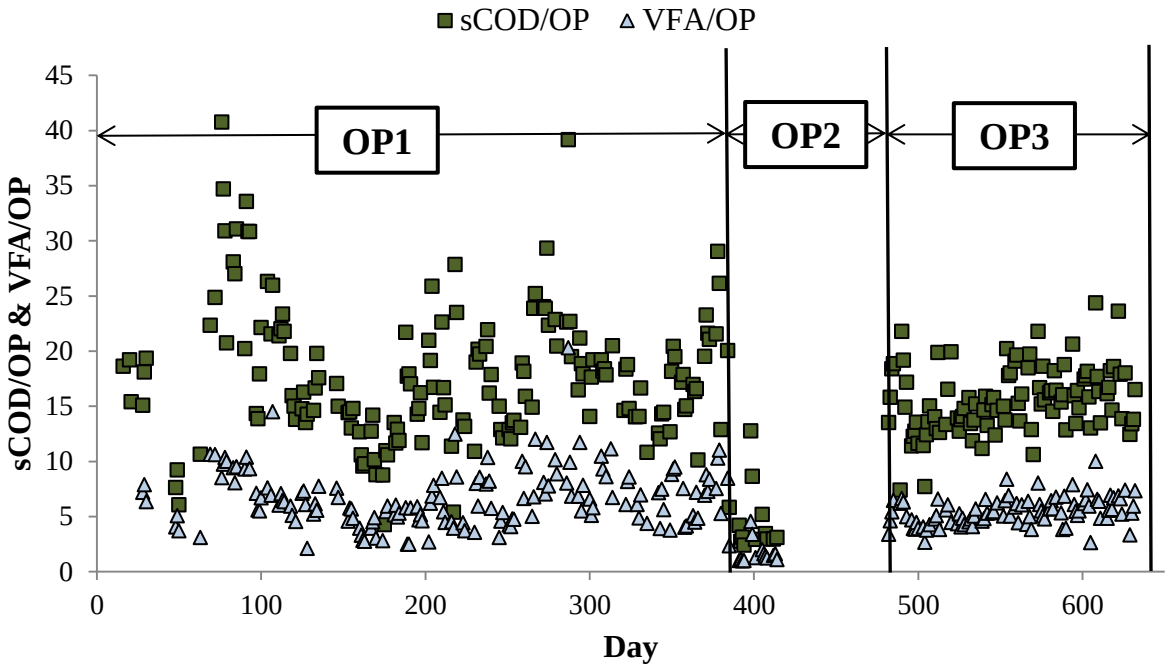

Figure 23: C/P and VFA/P throughout the duration of the experiment. This graph shows the more controlled C/P and VFA/P values during operational phase 3 compared to the more sporadic values through operational phases 1&2. Calculations for C/P are described with Equation 7 above, and the calculations for VFA/P are described with Equation 8 above.

4.4.2 Fermenter performance variation

The fermenter was operated at an unchanged wasting rate and an average pH of 5.38 ± 0.15, temperature of 21.0 ± 1.54 °C, and SRT of 3.26 ± 0.34 days for the entire five-month operational period 3. The VFA yield of the fermenter (Figure 24) and sCOD yield (Figure 25) varied throughout the period, even though conditions remained the same. Some explanations include changes in pilot influent source and changes in A-stage SRT and HRT. The pilot influent includes recycled streams from the main plant, and these recycle streams contained a higher TSS concentration during this time, possibly linked to the main centrifuge in the recycle stream being temporarily out of service.

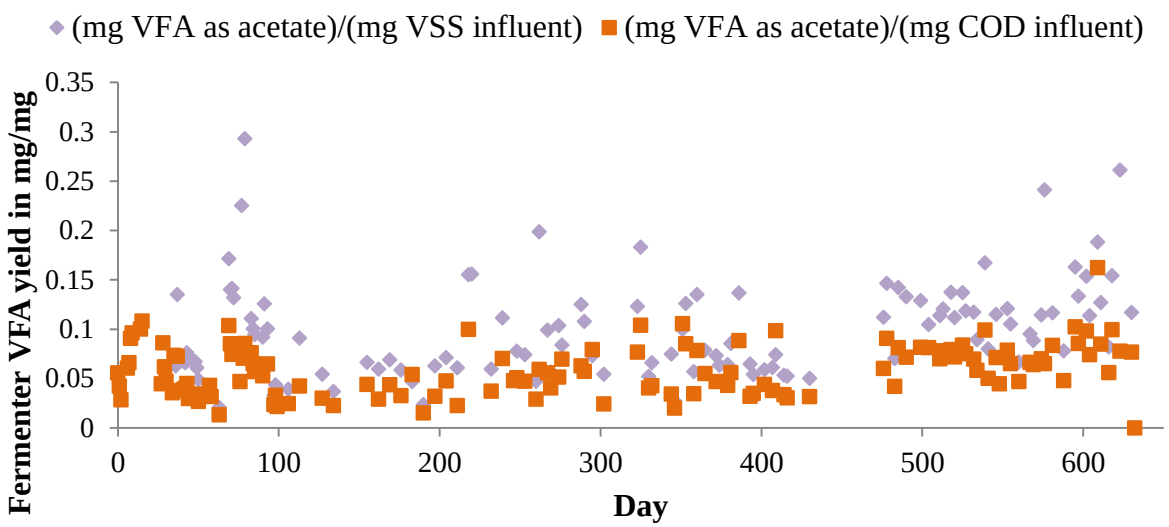

Figure 24: Fermenter VFA yields. The VFA is measured in the fermentate using CEL distillation analysis methods described in section 3.7. The influent measurements refer to measurements of the A-stage WAS that feeds into the fermenter, using analysis methods described in section 3.1.

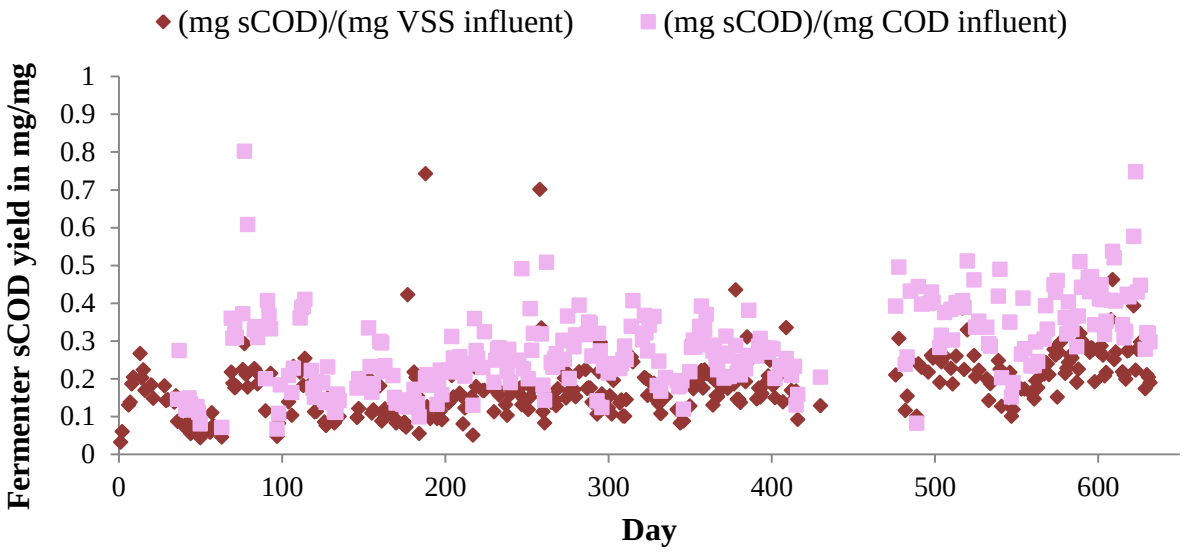

Figure 25: Fermenter soluble COD yields. The sCOD is measured in the fermentate using methods described in section 3.1. The influent measurements refer to measurements of the A-stage WAS that feeds into the fermenter, using analysis methods described in section 3.1.

4.4.3 Bio-P results

The underdosing C/P addition phase, where the C/P load goal was 13.6, lasted for a five-month period. The actual C/P average during this five-month period (operational phase 3) was 15.6 ± 3.0 C/P, and the average VFA/OP was 5.5 ± 1.3 (g VFA as acetate/g OP). During this time, there was a period of enhanced bio-P performance where the effluent OP was again below 1 (mg OP/L) the entire time, referred to in Table C as result period 3 and displayed in Figure 26 below. This 19 consecutive-day period had an average effluent OP of 0.6 ± 0.2 (mg OP/L), which is similar to the average effluent OP of RP1. Result period 3 was significant because fermentate was dosed at a 50% of the fermentate does at result period 1 and still achieved similar low effluent OP concentrations.

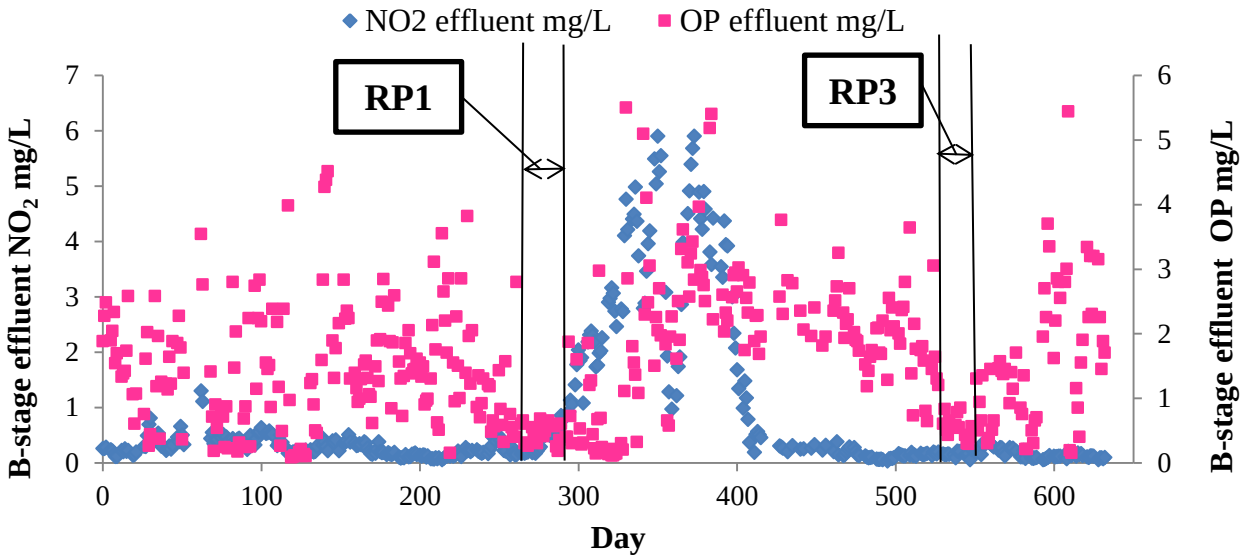

Figure 26: B-stage effluent OP (mg OP/L) and nitrite (mg NO_2/L). Result periods 1&3 where effluent OP <1 (mg OP/L) are displayed on this graph. The analysis methods for this data are described in section 3.1

Result period 3 occurred during the previously described fermentate load increase period. The increased fermentate addition did not dramatically change the amount of sCOD added to the SBPR since the goal was to keep sCOD constant, but did increase the amount of tCOD added. The tCOD (B-stage influent and fermentate) increase coincides with the low effluent OP during this time (see Figure 27 below). It can be shown in Figure 28 below that the total sCOD addition (B-stage influent and fermentate) in g/day remained fairly constant during result period 3, but the total pCOD (B-stage influent and fermentate) in g/day increased. It is further shown in Figure 29 below that the increase in pCOD during RP1 coincides with an increase in pCOD of the fermentate and a decrease in pCOD in the influent. Figures 27, 28, and 29 can be interpreted together to show that the increase in fermentate addition caused the increase in total COD that

coincides with result period 3. It should also be noted that figures 27, 28, and 29 do not show clear trends between COD and effluent OP within result period 1 as clearly as they do within result period 3.

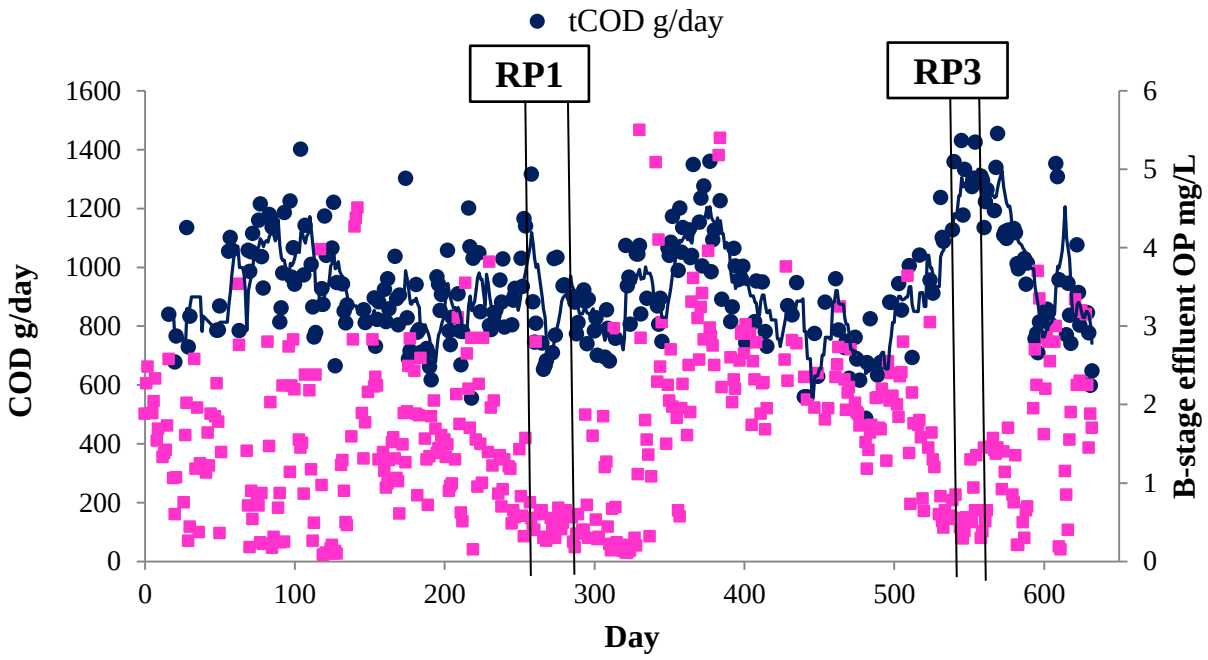

Figure 27: Total influent + fermentate COD (g COD/day) and B-stage effluent OP (mg OP/L). Result periods 1&3 where effluent OP <1 (mg OP/L) are displayed on this graph. The analysis methods for this data are described in section 3.1

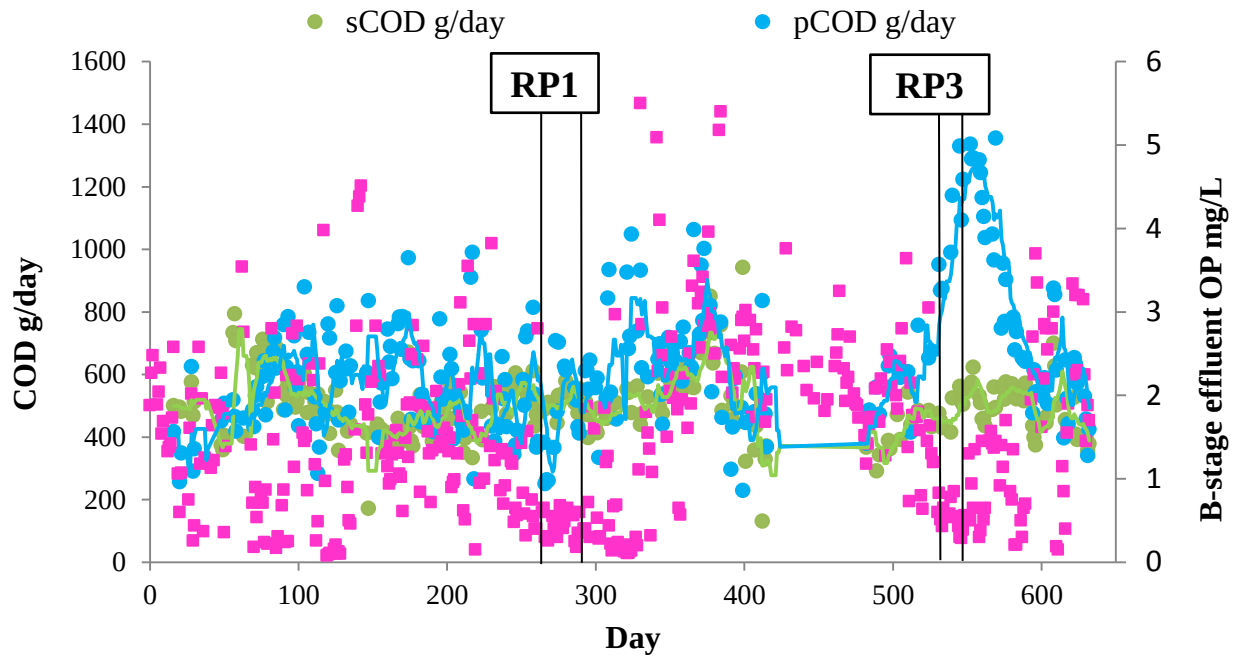

Figure 28: Total influent + fermentate pCOD (g COD/day), total influent + fermentate sCOD (g COD/day), and B-stage effluent OP (mg OP/L). Particulate COD is calculated by subtracting sCOD (g COD/day) from total COD (g COD/day). Result periods 1&3 where effluent OP <1 (mg OP/L) are displayed on this graph. The analysis methods for this data are described in section 3.1

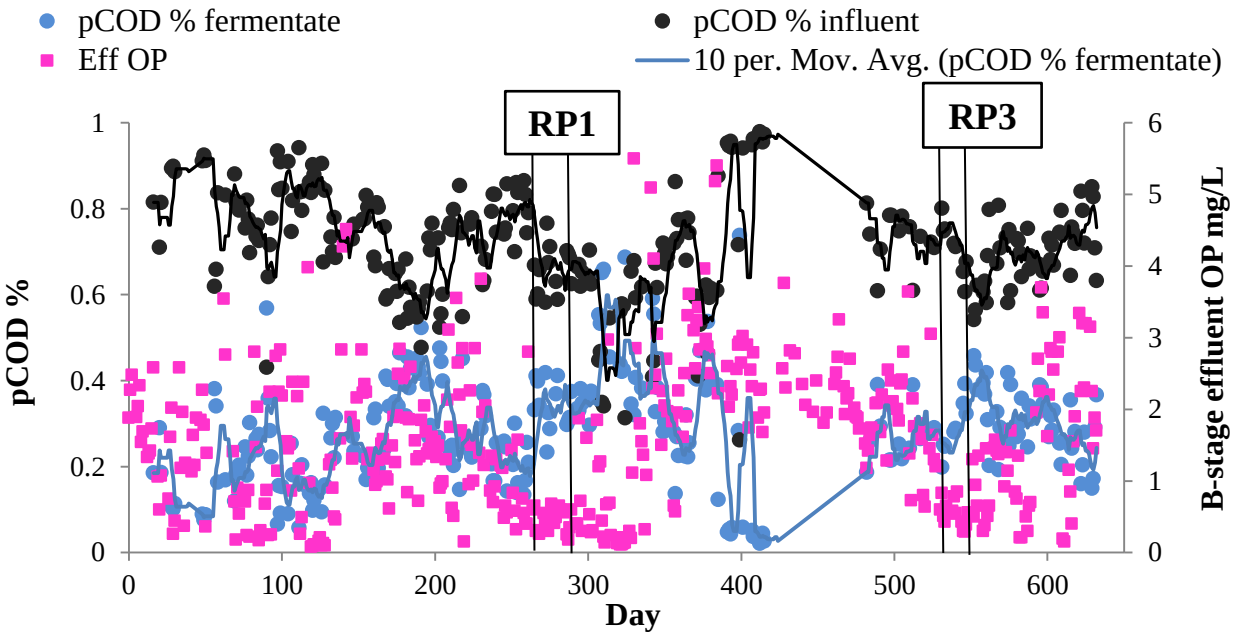

Figure 29: The % of total pCOD addition to B-stage that comes from fermentate and influent, and B-stage effluent OP (mg OP/L). Result periods 1&3 where effluent OP <1 (mg OP/L) are displayed on this graph. The analysis methods for this data are described in section 3.1

Figure 30 below shows that result period 1 correlates with an increase in VFA load to the SBPR (g VFA as acetate/g OP). It is likely that VFA addition also played a significant role in result period 3, since the VFA dose in g/day increased when the fermentate addition increased. This is shown in Figure 30 where an increase in VFA coincides with result period 3. VFA addition during result period 1 is much higher than the second, although both periods coincide with a VFA increase.

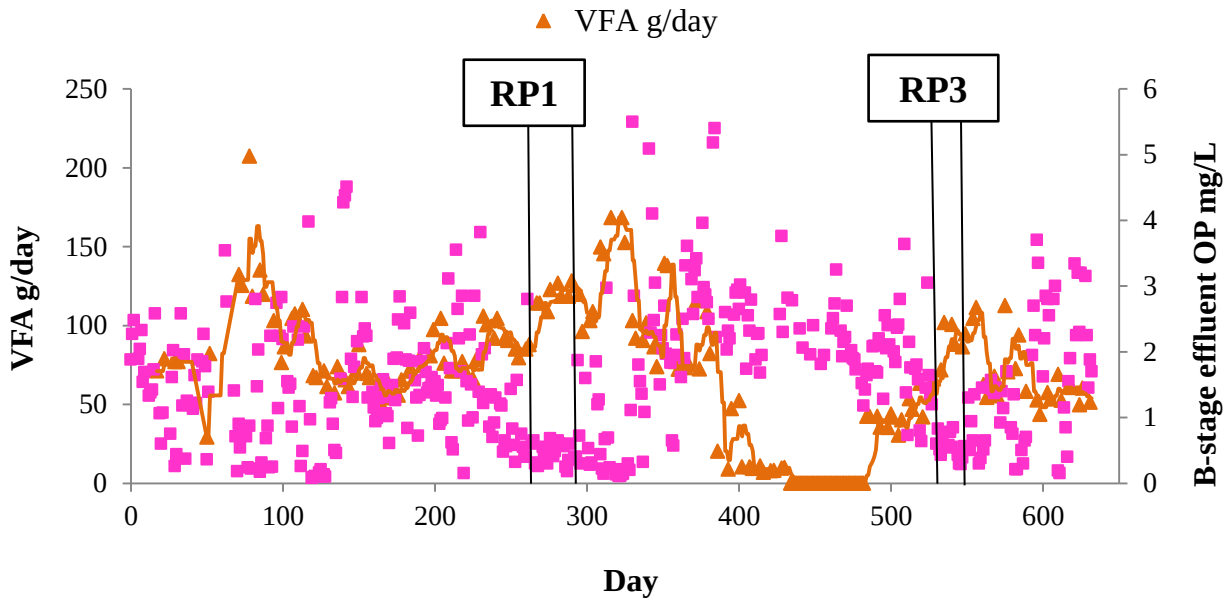

Figure 30: Fermentate load into the SBPR (g VFA as acetate/day) and B-stage effluent OP (mg OP/L). Result periods 1&3 where effluent OP <1 (mg OP/L) are displayed on this graph. The analysis methods for the OP data are described in section 3.1 and the VFA is measured in the fermentate using CEL distillation analysis methods described in section 3.7.

The linear regressions for result period 1 (Table 5) and result period 3 (Table 6) are shown below. The result period 1 linear regression includes data from day 227-354 in order to capture the conditions before and after the low effluent OP period. The result period 3 linear regression does the same by including data values from day 482-362. These linear regressions show a comparison between all COD values vs effluent OP & OP removed, with the COD values including fermentate, influent, and fermentate combined with influent COD loads in g/day. These r^2 values listed in Tables 5 and 6 help relate the low effluent OP periods to the types and amounts of COD introduced to both the sidestream and the mainstream.

The strongest r^2 value for result period 1 was between VFA (g acetate/day) vs B-stage effluent OP (mg OP/L). The strongest r^2 value for result period 3 was between VFA (g acetate/day) vs OP removed (mg OP/L). It is no surprise that the VFA load from the fermentate correlates the strongest with low effluent OP in both periods since VFA is needed for PAO enhancement, so

naturally increasing the amount of VFA available to PAOs in the sidestream would increase PAO activity and therefor increase OP removal. The average VFA load for result period 1 was 119 ± 6.2 (g VFA as acetate/day), and the average VFA load for result period 3 was 91 ± 10 (g VFA as acetate/day), which are both higher than the entire research period average of 59 ± 46 (g VFA as acetate/day).

What is surprising about the correlation analysis is how strong the rest of the COD correlations are for result period 3 compared to the rest of the COD correlations in result period 1. The main difference between result period 1 & 3 is that result period 1 occurred without an increase in fermentate addition, so the VFA load (g acetate/day) increased without drastically increasing the total COD added to the SBPR. In result period 3, the fermentate addition was purposely turned up and more COD was added to the SBPR in addition to adding more VFA. Even though there are some high r^2 values in the table for result period 3, the highest r^2 is still between VFA (g acetate/day) vs OP removed (mg OP/L), which shows that VFA probably had the strongest effect on OP removal during result period 3. The other COD values probably only trended with the low effluent OP during result period 3 because the low effluent OP occurred as a direct result of the increase in VFA load, which also coincided with a COD increase to the sidestream and the mainstream.

Table 5: Result period 1 linear correlation analysis

Linear correlation analysis from day 227-354										
	VFA (g/day)	**tCOD g/day**			**sCOD g/day**			**pCOD g/day**		
		I & F	I	F	I&F	I	F	I&F	I	F
OP (mg/L) in B-stage effluent	0.183	0.000	0.009	0.009	0.000	0.026	0.089	0.011	0.001	0.000
OP removed (mg/L)	0.104	0.061	0.015	0.108	0.032	0.017	0.130	0.088	0.043	0.053

*I = influent and F = fermentate

Table 6: Result period 3 linear correlation analysis

Linear correlation analysis from day 482-632										
	VFA (g/day)	**tCOD g/day**			**sCOD g/day**			**pCOD g/day**		
		I&F	I	F	I&F	I	F	I&F	I	F
OP (mg/L) in B-stage effluent	0.247	0.303	0.198	0.198	0.142	0.009	0.168	0.273	0.205	0.184
OP removed (mg/L)	0.646	0.440	0.363	0.455	0.234	0.056	0.338	0.463	0.361	0.419

*I = influent and F = fermentate

The linear regressions with C/P added vs B-stage effluent OP & OP removed are shown for both result period 1 & 3 in Table G below. A reason that most of these trends were not strong was because the OP added coincides with the COD added since the fermentate was being controlled to regulate both COD and OP parameters. Figure P34 below compares the COD, sCOD, and OP masses in fermentate to the mainstream flow to B-stage, which shows an accurate representation

on the effect of the fermentate addition on the whole system. It is clear in Figure 31 that COD and sCOD increase alongside with OP in the result period 3, which explains the flatter trends linear trends for result period 3 than result period 1 in Table 7.

Table 7: Linear correlation analysis continued for result period 1&3

Linear correlation analysis								
	Days 227-354 (containing RP1)				Days 482-362 (containing RP3)			
	VFA/OP	tCOD/OP	sCOD/OP	pCOD/OP	VFA/OP	tCOD/OP	sCOD/OP	pCOD/OP
OP (mg/L) in B-stage effluent	0.022	0.002	0.025	0.003	0.000	0.048	0.026	0.149
OP removed (mg/L)	0.007	0.054	0.106	0.000	0.001	0.004	0.236	0.113

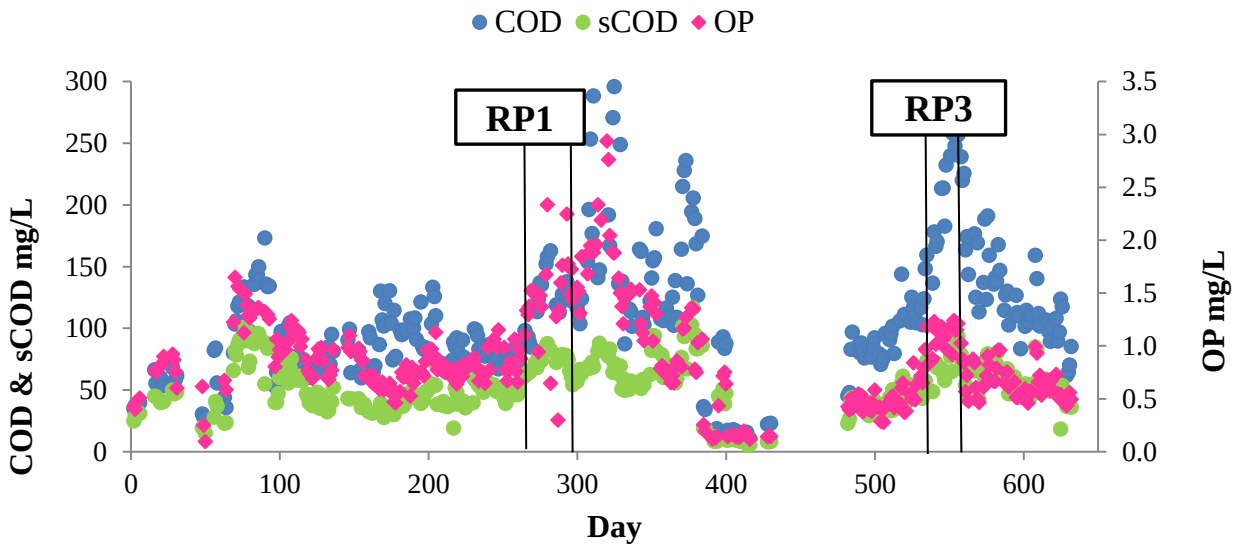

Figure 31: Fermentate mass added to system divided by mainstream flow for COD, sCOD, and OP. These values are calculated by dividing the COD, sCOD, or OP mass added to B-stage (mg) by flow into B-stage (L). Result periods 1&3 where effluent OP <1 (mg OP/L) are displayed on this graph. The analysis methods for this data are described in section 3.1

4.4.4 PAO activity and profile data also show bio-P activity

4.4.4.1 Maximum substrate PAO activity

The PAO activity test results (Figure 32) relate high periods of activity with result period 1 & 3. The maximum activity rates ceased when fermenate addition was turned off on day 434 and began increasing when fermentate addition was added back on day 482. Little dPAO activity was observed throughout the experiment, except for the very end. The last three activity tests showed an average dPAO activity of 1.8 (mgOP/gVSS/hr), which is higher than previously shown but is in an expected range of dPAO activity observed at many full scale bio-P WWTPs (Kuba, Van Loosdrecht, Brandse, & Heijnen, 1997).

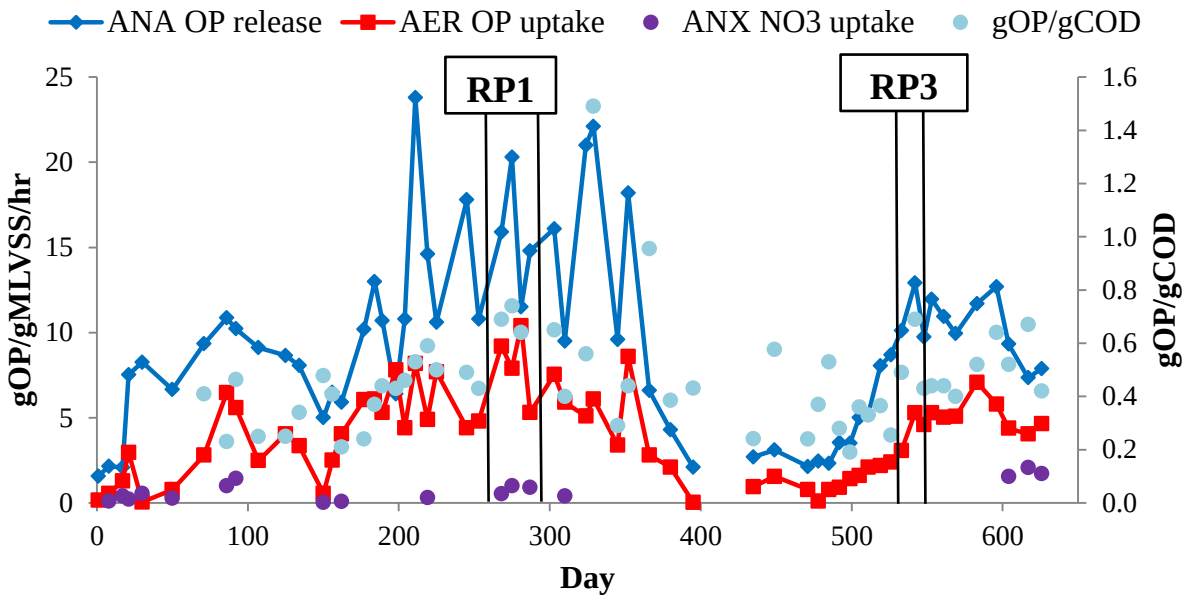

Figure 32: PAO maximum activity rates from weekly tests. Result periods 1&3 where effluent OP <1 (mg OP/L) are displayed on this graph. The analysis methods for this data are described in section 3.4

The PAO activity averages for both result period 1 & 3 are shown below in Table 8. Both periods of low effluent OP show an approximate 50% increase in activity when compared to average PAO activity over the duration of the experiment. Since the values are similar for both periods, it can be concluded that the average value of PAO activity needed for <1 mg/L effluent OP in this process is at least 1.6 (mgOP/gVSS/hr) release and 1.2 (mgOP/gVSS/hr) uptake.

Table 8: PAO activity rate averages

PAO maximum activity rate results				
	OP release		OP uptake	
	mgOP/L/hr	mgOP/gMLVSS/hr	mgOP/L/hr	mgOP/gMLVSS/hr
Entire research period (days 0-632)	30.0	9.03	13.2	3.86
RP1	48.6	15.6	25.8	8.20
RP3	51.6	11.2	21.4	4.56

4.4.4.2 Profile data

The OP release and uptake throughout the system, taken from profile data, is shown in Figure 33 below. The SBPR OP release is calculated by subtracting the OP entering the SBPR (mg OP/L) from the SBPR AM (mg OP/L) profile value. The OP uptake is calculated by subtracting the profile OP value (mg OP/L) from the last CSTR in series from the profile anaerobic selector OP value (mg OP/L). This value allows a representation of the actual OP uptake happening in the system. The sCOD consumed in the SBPR is taken from profile data, and is shown below in Figure 34. The values are calculated by subtracting the fermentate sCOD (g/day) from the before-mix and after-mix SBPR samples pulled in the profile (g/day). This allows for representation of COD consumption in the SBPR. Both the profile OP uptake and release, and SBPR sCOD uptake coincide with the result period 1 & 3. When looking at this profile data and the PAO activity test data with the effluent OP concentrations and OP removals, the low effluent OP periods are clearly due to an increase in bio-P activity stimulated by fermentate addition to the SBPR.

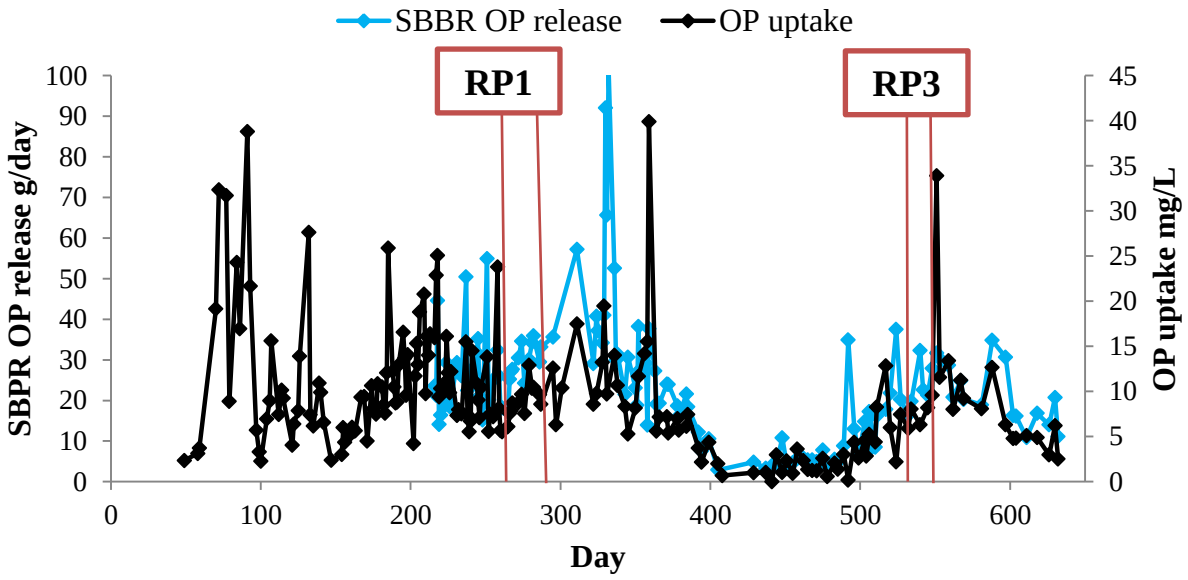

Figure 33: System OP uptake and release from profile data. Result periods 1&3 where effluent OP <1 (mg OP/L) are displayed on this graph. The analysis methods for this data are described in section 3.6

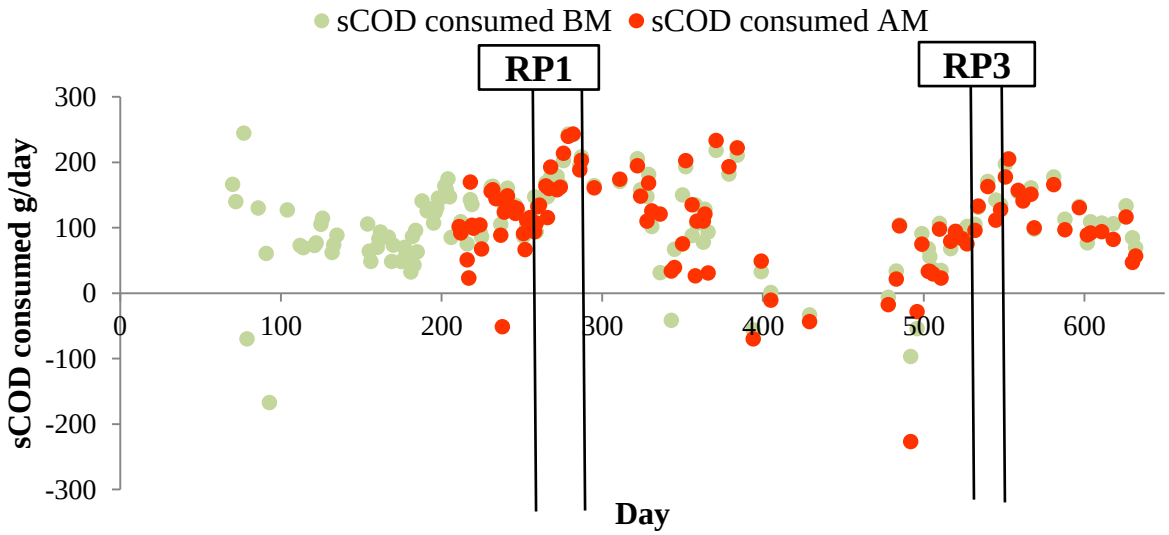

Figure 34: SBPR sCOD consumption from profile data. The data in this graph was calculated by subtracting the sCOD (g COD/day) from profile BM and AM samples from the sCOD from the ferementate (g COD/day) going into the SBPR. Result periods 1&3 where effluent OP <1 (mg OP/L) are displayed on this graph. The analysis methods for this data are described in section 3.6

4.4.5 Negative effects of the high tCOD load to B-stage

It is important to note that mixed liquor in B-stage was very high, between 6000-7000 (mg TSS/L), around the time of result period 3. It is clear when comparing the influent and fermentate COD trends that the MLSS spike was due to not only an increase in influent COD but also due to an increase in fermentate COD (shown in Figure 35 below). Normal maximum MLSS operating conditions are between 5000-4000 (mg TSS/L) and any operation above these parameters causes clogs and settling problems (George Tchobanoglous, 2003). The pilot began to experience some settling and high effluent TSS problems during this period.

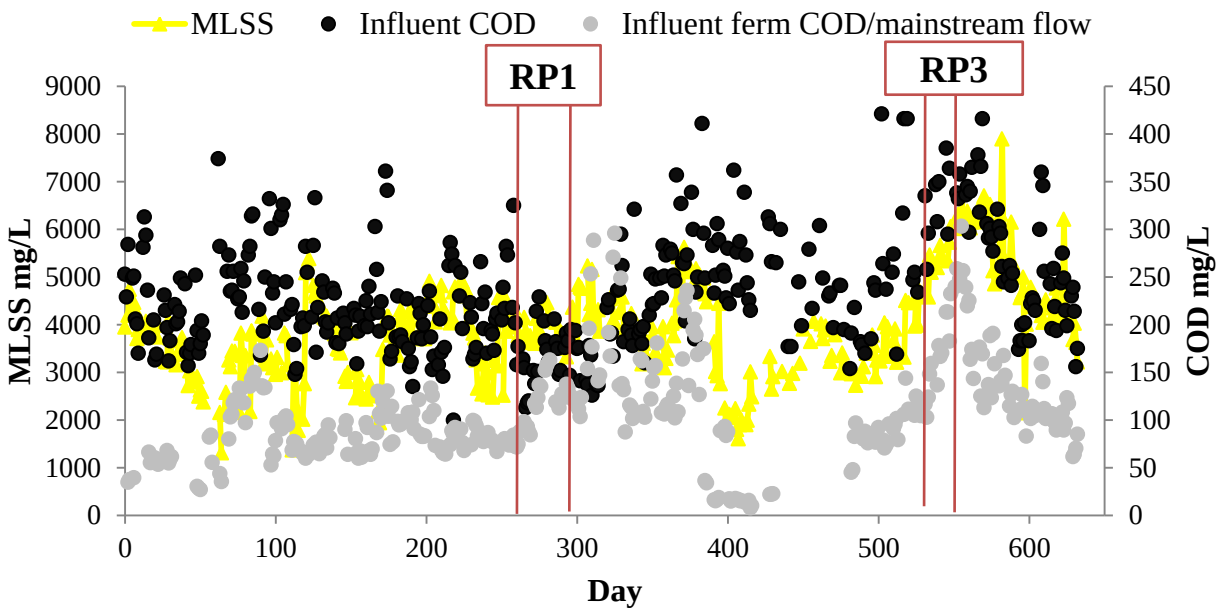

Figure 35: B-stage MLSS (mg TSS/L), B-stage influent COD (mg COD/L), and fermentate COD/mainstream flow (mg/L). Result periods 1&3 where effluent OP <1 (mg OP/L) are displayed on this graph. The analysis methods for this data are described in section 3.1

In addition to the operational problems caused by a high mainstream mixed liquor concentration, the amount of total COD that was added back into B-stage during result period 3 through both the influent and the sidestream impedes the intensification goal of using carbon efficiently. The more carbon that is needed to enhance bio-P is less that can be diverted for redistribution or energy recovery. In addition, more carbon added back into B-stage means more biomass production by heterotrophs, which means lowering the capacity of the system. If fermentation could be improved to produce a higher concentration of VFA in the fermentate, then less fermentate, and therefore total COD, would be needed to enhance bio-P activity.

4.4.6 ISCD activity, endogenous decay, and nitrite accumulation

In order to determine if the activity observed in the ISCD bench tests was truly due to internally stored carbon denitrification or from endogenous decay, experiments measuring the endogenous rates of the system were set up. Results for the endogenous decay test are shown below in Figure 36, and results from the internally stored carbon denitrification test are in Figure 37 below. The endogenous decay rates by spiking a MLSS sample with nitrate and nitrite after aerating the sample for over 12 hours in order to deplete all internal and external carbon sources. The ISCD rates were determined by also aerating a MLSS sample for over 12 hours, then spiking with COD as acetate. After spiking with COD, the acetate was given time to deplete, then the MLSS was washed to get rid of external carbon, then the ISCD was measured in a following anoxic period.

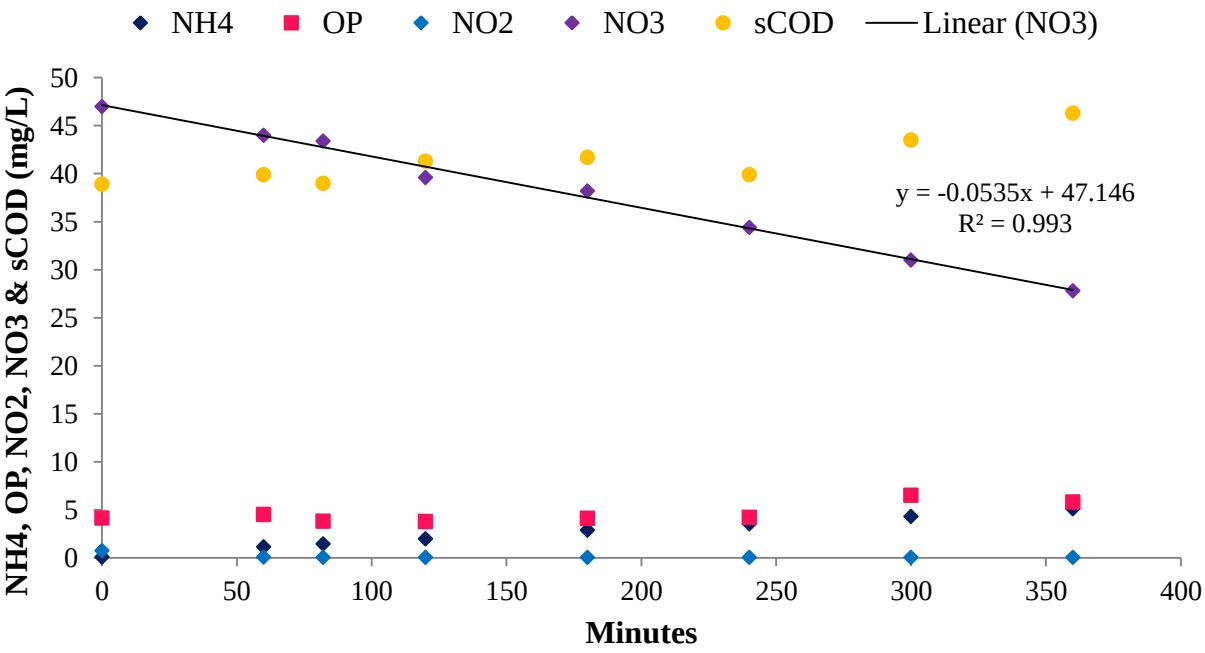

Figure 36: Endogenous decay rates (EA_ANX). The analysis methods for this data are described in section 3.8

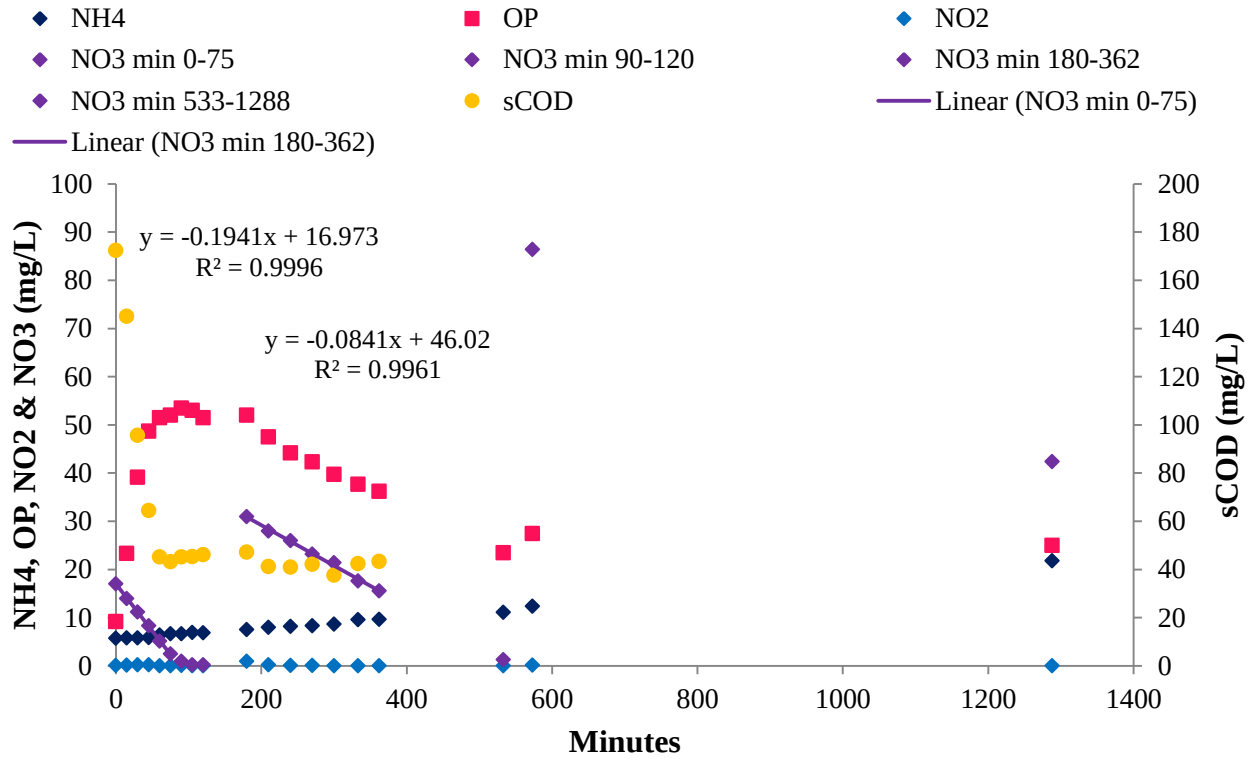

Figure 37: Internally stored carbon denitrification rate (EA_EICD). The analysis methods for this data are described in section 3.8

Based on the MLVSS measured in these tests, and the rates shown above, the differing denitrification rates were calculated. The endogenous rate of the system was calculated to be 0.51 (mgN/gVSS/hr), which is in the normal endogenous denitrification rate range of 0.2-0.6 (mgN/gVSS/hr) that is commonly referenced (Kujawa & Klapwijk, 1999). The rate of denitrification from acetate addition in the anaerobic part of the EA_EICD test was calculated to be 2.95 (mgN/gVSS/hr), and the internally stored carbon denitrification rate during the anoxic part was calculated to be 1.28 (mgN/gVSS/hr). This is an expected internally stored carbon denitrification rate, especially since it is higher than the endogenous rate and lower than the denitrification rate from acetate. It is also slightly higher, but similar, to the post-anoxic denitrification rates of 0.47-1.17 (mgN/gVSS/hr) observed in the Vocks study (Vocks et al., 2005).

The ISCD activity test results shown in Figure 38 below show the change in internally stored carbon denitrification and nitrite accumulation throughout the research duration. When "NO2 removed" is positive that shows that nitrite was increasing during the test, and all highly positive points were observed during result period 2 when nitrite accumulation occurred. These tests show no nitrite accumulation due to internally stored carbon during the operational period 3. When OP released is positive, that means that OP is increasing throughout the test, likely due to release by endogenous decay. In order to show dPAO activity, OP rates would have to be negative, which was never clearly shown. The NO_3^- reduction rates show that denitrification decreased when the fermentate addition decreased around day 385. NO_3^- denitrification rates continued to remain low until increasing again around day 603, which was 121 days after the fermentate addition was added back into the system.

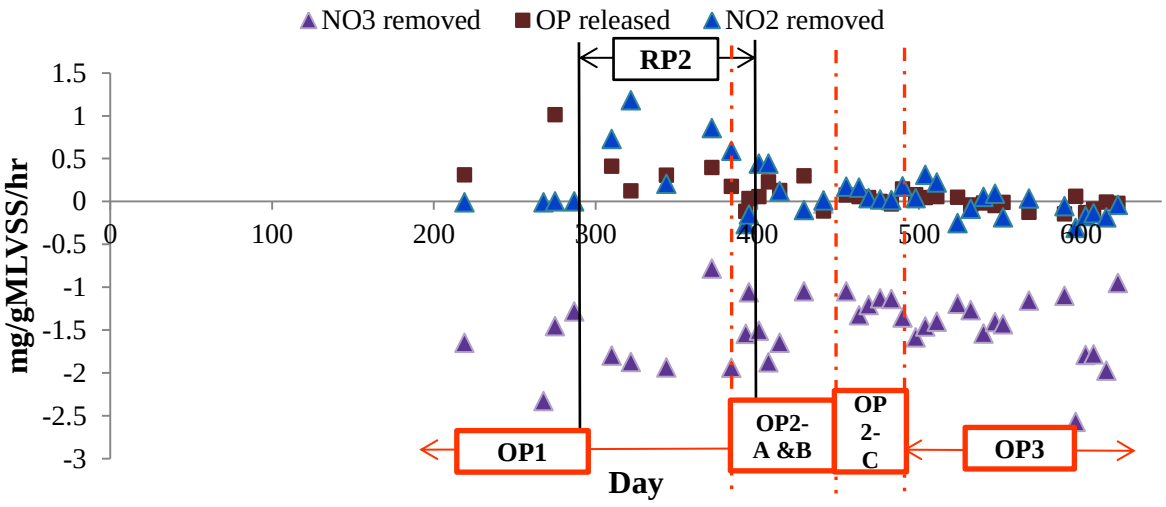

Figure 38: ISCD maximum activity test rates for NO3 removed, OP released, and NO_2^- removed. Result period 2 where effluent NO_2^- >1 (mg NO_2^-/L) are displayed on this graph. The analysis methods for this data are described in section 3.5

The average rates for result period 2 and operational period 3 are displayed in Table 9. There is clear nitrite accumulation at a rate of 0.45 ($mgNO_2/gVSS/hr$) during result period 2, and no nitrite accumulation for the entirety of OP3. The higher NO_x removal rate for operational period 3 than for result period 2 is because of the nitrite accumulation experienced in result period 2 impeding the overall nitrogen removal from the system.

When the ISCD tests rates are compared to the previously measured endogenous rates of the system, all of the N removal rates are above the measured 0.51 (mgN/gVSS/hr) endogenous rate, showing that most of the denitrification measured in this test is done by the use of some amount of internally stored carbon compounds. This is expected because even though fermentate is not added to the SBPR during OP2-C shown in Figure 38 above, the system still had a sidestream anaerobic bio-P zone and a mainstream pre-anaerobic zone the entire time, which enhances post-anoxic denitrification. The ISCD rates are clearly higher before fermentate addition is halted in OP2-C and after fermentate addition is added back in OP3, showing that the VFA from fermentate did contribute to internally stored carbon used for post-anoxic denitrification. When compared to the previously measured system ISCD rates, the average N removal rates for result period 3 and operational period 3 where fermentate was added were close to the measured value of 1.28 (mgN/gVSS/hr) removed. The result period 3 & operational period 3 rates are also similar to the post-anoxic denitrification rates in the Vocks study, 0.47-1.17 (mgN/gVSS/hr) (Vocks et al., 2005). It is clear that these tests show that some amount of denitrification from internally stored carbon compounds is happening post-anoxically in this system, and these rates increase when fermentate is added to the SBPR.

Table 9: ISCD activity rate averages

Averaged values mg/gVSS/hr				
	NO_x	**NO_3^-**	**NO_2^-**	**OP**
RP1	-1.11	-1.56	0.45	0.17
OP3	-1.51	-1.48	-0.03	-0.01

No nitrite accumulation was observed in B-stage or in the ISCD tests for operational period 3 (day 482-632). Since the tCOD added to both the sidestream and mainstream was greater during the operational period 3 than it was during the nitrite accumulation period, the cause of the nitrite accumulation could be more accurately linked to VFA than tCOD. Figure 39 below shows a sharp trend between VFA added (g VFA as acetate/day) and NO_2^-effluent (mg NO_2/L) for the start of the nitrite accumulation period where there was no cyanide interference (days 227-330). The average fermentate VFA addition for this period was 113 ± 24 (g VFA as acetate/day), and the average VFA/OP was 7.7 ± 2.9 (g VFA as acetate/g total OP) which is significantly higher than the average VFA of 91 ± 10 (g VFA as acetate/day) and the average VFA/OP of 5.5 ± 1.3 (g VFA as acetate/g total OP) for operational phase 3 (Shown in Figure 40 below). It is probable

that the VFA addition amount that caused the internal carbon storage needed for partial denitrification leading to nitrite accumulation was between 112-91 (g VFA as acetate/day), or between 5.5-7.7 (g VFA as acetate/g total OP).

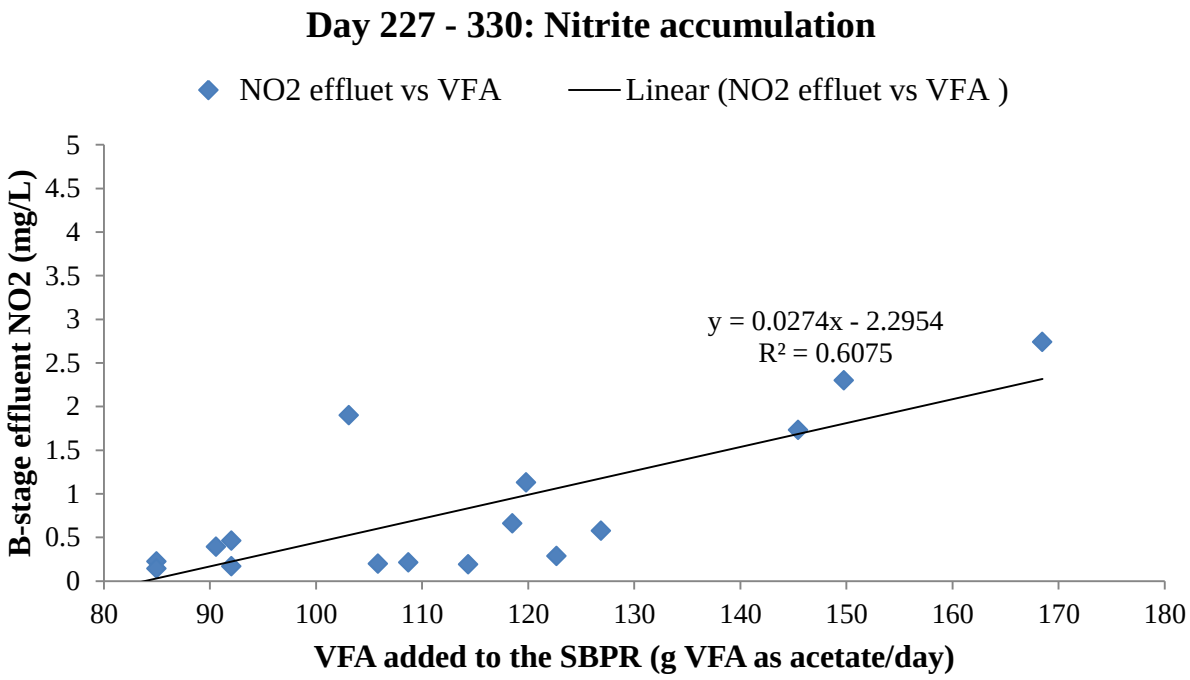

Figure 39: Linear correlation trend between the VFA added to the SBPR (g VFA as acetate/day) and B-stage effluent nitrite (mg NO_2^-/L). The analysis methods for this data are described in sections 3.1 and 3.7

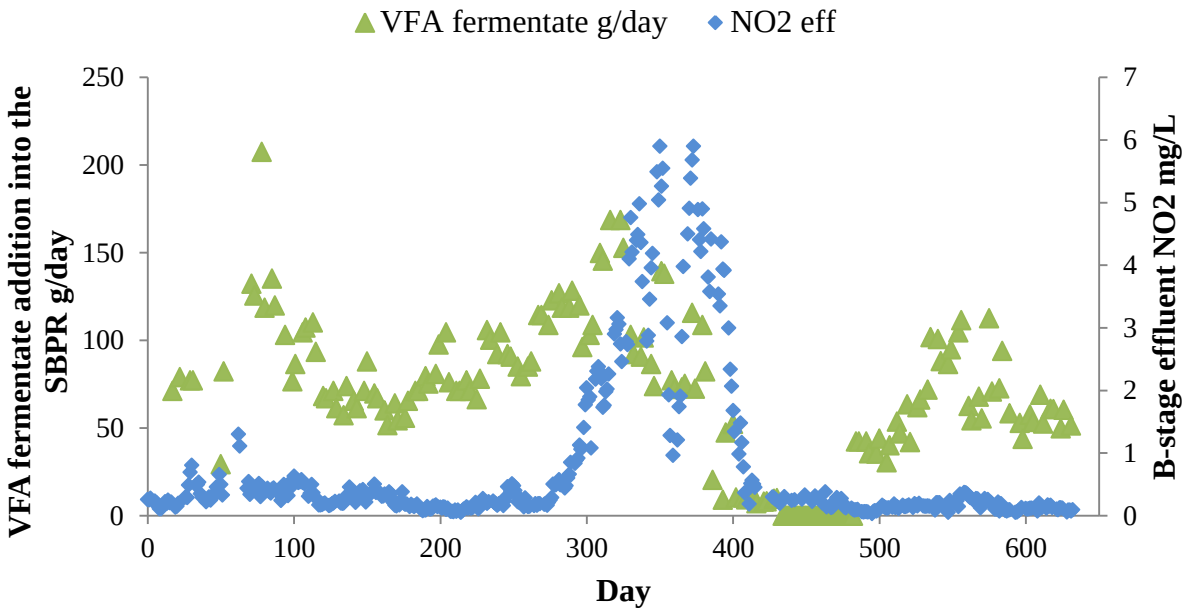

Figure 40: VFA addition to the SBPR (g VFA as acetate/day) and B-stage effluent nitrite (mg NO_2^-/L). The analysis methods for this data are described in sections 3.1 & 3.7

It would make sense if the bacteria responsible for the internally stored carbon denitrification were dGAOs since the nitrite accumulation period also coincided with an unstable bio-P period, and dGAOs would be directly competing with PAOs for VFA. Some studies have linked dGAOs to nitrite accumulation (Rubio-Rincón et al., 2017). However, the ISCD organism could also be any other species of bacteria that is storing the VFA from fermentate internally to be used later for denitrification because these bacteria would also compete with PAOs for VFA. It is possible that hydrolysis of total COD in the SBPR played a role on the bacteria population as well, although it is likely less of a factor then VFA because of the short SRT in the SBPR. It is possible that fermentative PAOs also played a role in the sidestream, either by fermenting and producing VFA themselves or up taking OP (McIlroy et al., 2018b).

4.4.7 AOB & NOB activity

No clear increase in AOB rates over NOB rates that would indicate NOB out-selection are shown throughout the duration of the experiment, displayed in Figure 41 below. There is a clear drop in rates around day 350 for both AOB and NOB, likely due to cyanide inhibition. The aerobic fraction is at its maximum set limit intermittently from day 300 – 600 due to fluctuating cyanine in the influent, which inhibits nitrification and requires more air in B-stage for the AvN ratio to be met. Studies have shown that AOB are more resistant to cyanide inhibition than NOB, which explains the AOB>NOB during the first major cyanide inhibition period around day 350 (Kim, Lee, Park, Park, & Park, 2011). It is clear that NOB rates significantly increased around

the time of operational phase 3, but due to possible cyanide inhibition it is unclear if that is a direct result of the fermentate addition. The difference between NOB – AOB maximum rate was an average of 1.1 ± 23 (mgN/gMLSS/day) up until operational phase 3 (day 0-481) and increased to 23.3 ± 14 (mgN/gMLSS/day) during operational phase 3 (day 482-632), showing a significant increase in NOB over AOB during operational phase 3.

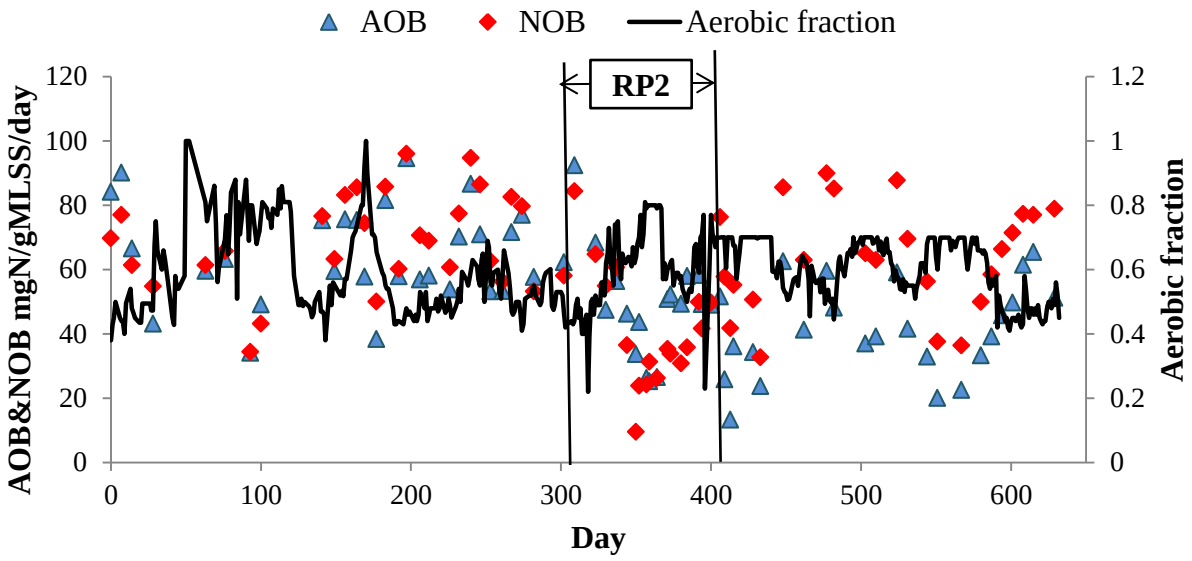

Figure 41: AOB and NOB maximum specific activity rates and B-stage aerobic fraction. Result period 2 where effluent NO_2^- >1 (mg NO_2^-/L) are displayed on this graph. The analysis methods for this data are described in section 3.3

A possible explanation for the failure of NOB out-selection would be the nitrite loop theory, where a consistent carbon load to B-stage could have supplied a nitrite source by partial denitrification that NOB were able to use to thrive (Winkler et al., 2012). It is odd that potentially the nitrite loop would affect NOB rates more during operational phase 3 than in result phase 2, since there was nitrite accumulation and therefor plenty of nitrite for NOB to thrive during result period 2. Nonetheless, it is clear that NOB out-selection was unsuccessful throughout the duration of the experiment.

5. Conclusions

- Nitrite accumulation occurred from days 295 to 401, during operational phase 1, were the B-stage effluent nitrite ranged from 1.1-5.9 (mg NO_2^-/L), referred to in this thesis at result period 2. Profiles, ISCD tests, and AOB/NOB rate tests showed that this nitrite accumulation was due to partial denitrification of nitrate to nitrite by a bacteria using internally stored carbon to as the electron source necessary to denitrify. There is a link between EBPR systems and bacteria that are capable of storing carbon internally to later be used for denitrification, although the bacteria responsible for this were not conclusively identified in this study. Conclusive research should be done on the bacteria responsible for the partial denitrification, and whether the bacteria responsible are dGAOs or not, research needs to be done on how to control and promote these organisms while also promoting PAO activity for OP removal.
- Effluent OP periods below 1 (mg OP/L), referred to in this thesis as result periods 1 & 3, are likely a result of the VFA load to the SBPR (g VFA as acetate/day). This is shown by the linear correlation analysis between OP and the VFA load to the SBPR. The highest r^2 value for result period 1 was $r^2 = 0.183$ for VFA g/day vs effluent OP (mg OP/L), and the highest r^2 value for the result period 3 was $r^2 = 0.646$ for VFA g/day vs OP removed (mg OP/L). Total COD could have had an effect since it presented another high correlation for result period 3 at $r^2 = 0.455$ for fermentate (g total COD/day) vs OP removed (mg OP/L), but the VFA r^2 value is still the highest r^2 value. Result period 1 occurred during a fermentate load of 9.4 ± 3.7 (g VFA as acetate/g total OP), and result period 3 occurred during 5.2 ± 0.7 (g VFA as acetate/g total OP). Based on low effluent OP occurring at different VFA/OP loads, it can be concluded that B-stage effluent OP <1 (mg OP/L) can be achieved between the fermentate loads of 5 - 9 (g VFA as acetate/g total OP).
    - Emphasis should be put on increasing fermentation efficiency to increase VFA production if enhancing bio-P activity is desired. Enhancing fermentation for VFA production intensifies the process because it avoids excess COD addition to the system to achieve bio-P, allowing for smaller tank sizes and less biomass production in a system that combines short-cut nitrogen removal with sidestream bio-P.
- Since nitrite accumulation was not observed in operational phase 3 with an average of 5.5 ± 1.3 (g VFA as acetate/g total OP), the probable VFA load needed to produce enough internal carbon storage to lead to nitrite accumulation in this system is between 5 - 9 (g VFA as acetate/g total OP). Nitrite accumulation via partial denitrification of nitrate to nitrite using internally stored carbon compounds could be a potential source of nitrite for anammox in systems that combine shortcut nitrogen removal and EBPR. More research needs to be done on the amount of VFA needed to promote nitrite accumulation if partial denitrification can be used as a reliable source of nitrite.

References

Al-Omari, A., Wett, B., Nopens, I., De Clippeleir, H., Han, M., Regmi, P., . . . Murthy, S. (2015). Model-based evaluation of mechanisms and benefits of mainstream shortcut nitrogen removal processes. *Water Science and Technology, 71*(6), 840-847. doi:10.2166/wst.2015.022

Anthonisen, A. C., Loehr, R. C., Prakasam, T. B. S., & Srinath, E. G. (1976). Inhibition of Nitrification by Ammonia and Nitrous Acid. *Journal (Water Pollution Control Federation), 48*(5), 835-852.

APHA. (2005). Standard methods for the examination of water and wastewater. (21).

Barak, Y., & Rijn, J. v. (2000). Atypical polyphosphate accumulation by the denitrifying bacterium Paracoccus denitrificans. *Applied and environmental microbiology*(3), 1209.

Barnard, J. L. (1985). A Review of Biological Phosphorus Removal in the Activated Sludge Process. *Water SA, 2*, 139-144.

Barnard, J. L., Dunlap, P., & Steichen, M. (2017). Rethinking the Mechanisms of Biological Phosphorus Removal. In (Vol. 89, pp. 2043-2054).

Bernat, K., & Wonjnowska-Baryla, I. (2007). Carbon course in aerobic denitrification. *Biochemical Engineering Journal, 36*.

Bernat, K., Wonjnowska-Baryla, I., & Dobrzynska, A. (2008). Denitrification with endogenous carbon source at low C/N and its effect on P(3HB) accumulation. *Bioresource Technology, 99*.

Biological Nutrient Removal Processes and Costs. (2007). Retrieved from https://www.epa.gov/sites/production/files/documents/criteria_nutrient_bioremoval.pdf

Blackburne, R., Vadivelu, V. M., Yuan, Z., & Keller, J. (2007). Kinetic characterisation of an enriched Nitrospira culture with comparison to Nitrobacter. *Water Research, 41*(14), 3033-3042. doi:https://doi.org/10.1016/j.watres.2007.01.043

Camejo, P. Y., Owen, B. R., Martirano, J., Ma, J., Kapoor, V., Santo Domingo, J., . . . Noguera, D. R. (2016). Candidatus Accumulibacter phosphatis clades enriched under cyclic anaerobic and microaerobic conditions simultaneously use different electron acceptors. *Water Research, 102*, 125-137. doi:10.1016/j.watres.2016.06.033

Cao, G., Wang, S., Peng, Y., & Miao, Z. (2013). Biological nutrient removal by applying modified four step-feed technology to treat weak wastewater. *Bioresource Technology, 128*, 604-611. doi:10.1016/j.biortech.2012.09.078

Chandran, K., & Smets, B. F. (2000). Single-step nitrification models erroneously describe batch ammonia oxidation profiles when nitrite oxidation becomes rate limiting. *Biotechnology and Bioengineering, 68*(4), 396-406. doi:10.1002/(SICI)1097-0290(20000520)68:4<396::AID-BIT5>3.0.CO;2-S

Chen, H.-b., Yang, Q., Li, X.-m., Wang, Y., Luo, K., & Zeng, G.-m. (2013). Post-anoxic denitrification via nitrite driven by PHB in feast–famine sequencing batch reactor. *Chemosphere, 92*(10), 1349-1355. doi:10.1016/j.chemosphere.2013.05.052

Chesapeake Bay TMDL Document, § 1-14 (2010).

Coats, E. R., Mockos, A., & Loge, F. J. (2011). Post-anoxic denitrification driven by PHA and glycogen within enhanced biological phosphorus removal. *Bioresource Technology, 102*, 1019-1027. doi:10.1016/j.biortech.2010.09.104

Courtens, E. N. P., De Clippeleir, H., Vlaeminck, S. E., Jordaens, R., Park, H., Chandran, K., & Boon, N. (2015). Nitric oxide preferentially inhibits nitrite oxidizing communities with high affinity for nitrite. *Journal of Biotechnology, 193*, 120-122. doi:https://doi.org/10.1016/j.jbiotec.2014.11.021

DeBarbadillo, C. (2018). *Overview of Biological Nutrient Removal.* Paper presented at the Nutrient Removal and Recovery Conference, Raleigh, NC.

Dytczak, M. A., Londry, K. L., & Oleszkiewicz, J. A. (2008). Nitrifying genera in activated sludge may influence nitrification rates. In (Vol. 80, pp. 388-396).

Filipe, C. D. M., Daigger, G. T., & Grady, C. P. L. (2001). pH as a key factor in the competition between glycogen-accumulating organisms and phosphorus-accumulating organisms. In (Vol. 73, pp. 223-232).

Fuhs, G. W., & Chen, M. (1975). Microbiological Basis of Phosphate Removal in the Activated Sludge Process for the Treatment of Wastewater. *Microbial Ecology, 2*(2), 119-138.

George Tchobanoglous, F. B., H. David Stensel. (2003). *Wastewater engineering treatment and reuse* (Vol. 4): Medcalf & Eddy, Inc.

The Godfather of Biological Nutrient Removal. (2011). Retrieved from https://www.waterworld.com/articles/wwi/print/volume-26/issue-2/regulars/international-show-preview-singapore-intern/the-godfather-of-biological-nutrient-removal.html

González-Cabaleiro, R., Curtis, T. P., & Ofiţeru, I. D. (2019). Bioenergetics analysis of ammonia-oxidizing bacteria and the estimation of their maximum growth yield. *Water Research, 154*, 238-245. doi:https://doi.org/10.1016/j.watres.2019.01.054

Grady, C. P. L., Daigger, G. T., Love, N. G., & Filipe, C. D. M. (2011). *Biological Wastewater Treatment*: IWA Publishing.

Hao, X., Wang, Q., Cao, Y., & van Loosdrecht, M. C. M. (2010). Experimental evaluation of decrease in the activities of polyphosphate/glycogen-accumulating organisms due to cell death and activity decay in activated sludge. *Biotechnology and Bioengineering, 106*(3), 399-407. doi:10.1002/bit.22703

Hellinga, C., Schellen, A. A. J. C., Mulder, J. W., van Loosdrecht, M. C. M., & Heijnen, J. J. (1998). The sharon process: An innovative method for nitrogen removal from ammonium-rich waste water. *Water Science and Technology, 37*(9), 135-142. doi:https://doi.org/10.1016/S0273-1223(98)00281-9

Hendriks, A. T. W. M., & Langeveld, J. G. (2017). Rethinking Wastewater Treatment Plant Effluent Standards: Nutrient Reduction or Nutrient Control? *Environmental Science & Technology, 51*(9), 4735-4737. doi:10.1021/acs.est.7b01186

Her, J.-J., & Huang, J.-S. (1995). Influences of carbon source and C/N ratio on nitrate/nitrite denitrification and carbon breakthrough. *Bioresource Technology, 54*(1), 45-51. doi:https://doi.org/10.1016/0960-8524(95)00113-1

Hesselmann, R. P. X., Werlen, C., Hahn, D., Van der Meer, J. R., & Zehnder, A. J. B. (1999). Enrichment, Phylogenetic Analysis and Detection of a Bacterium That Performs Enhanced Biological Phosphate Removal in Activated Sludge. *Systematic and Applied Microbiology*(3), 454.

History of Activated Sludge. (2014). Retrieved from http://www.iwa100as.org/history.php

Houweling, D., Dold, P., & Barnard, J. (2010). Theoretical Limits to Biological Phosphorus Removal: Rethinking the Influent Cod:N:P Ratio. *Proceedings of the Water Environment Federation, 2010*, 7044-7059. doi:10.2175/193864710798207107

Huynh, T. V., Nguyen, P. D., Phan, T. N., Luong, D. H., Truong, T. T. V., Huynh, K. A., & Furukawa, K. (2019). Application of CANON process for nitrogen removal from anaerobically pretreated husbandry wastewater. *International Biodeterioration & Biodegradation, 136*, 15-23. doi:10.1016/j.ibiod.2018.09.010

Jiang, H., Liu, G.-h., Ma, Y., Xu, X., Chen, J., Yang, Y., . . . Wang, H. (2018). A pilot-scale study on start-up and stable operation of mainstream partial nitrification-anammox biofilter process based on online pH-DO linkage control. *Chemical Engineering Journal, 350*, 1035-1042. doi:https://doi.org/10.1016/j.cej.2018.06.007

Johnson, B. R., Goodwin, S., Daigger, G. T., & Crawford, G. V. (2005). A comparison between the theory and reality of full-scale step-feed nutrient removal systems. *Water Science And Technology: A Journal Of The International Association On Water Pollution Research, 52*(10-11), 587-596.

Juretschko, S., Timmermann, G., Schmid, M., Schleifer, K. H., Pommerening-Röser, A., Koops, H. P., & Wagner, M. (1998). Combined molecular and conventional analyses of nitrifying bacterium diversity in activated sludge: Nitrosococcus mobilis and Nitrospira-like bacteria as dominant populations. In (Vol. 64, pp. 3042-3051).

Kim, Y. M., Lee, D. S., Park, C., Park, D., & Park, J. M. (2011). Effects of free cyanide on microbial communities and biological carbon and nitrogen removal performance in the industrial activated sludge process. *Water Research, 45*(3), 1267-1279. doi:https://doi.org/10.1016/j.watres.2010.10.003

Kobylinski, E. D., G.V.; Barnard, J.; Massart, N.; Koh,S. (2008). *How Biological Phosphorus Removal is Inhibited by Collection System Corrosion and Odor Control Practices.* Paper presented at the WEFTEC 2018, Chicago, Il.

Kong, Y., Nielsen, J. L., & Nielsen, P. H. (2005). Identity and Ecophysiology of Uncultured Actinobacterial Polyphosphate-Accumulating Organisms in Full-Scale Enhanced Biological Phosphorus Removal Plants. *Applied and environmental microbiology*(7).

Kornaros, M., Dokianakis, S. N., & Lyberatos, G. (2010). Partial Nitrification/Denitrification Can Be Attributed to the Slow Response of Nitrite Oxidizing Bacteria to Periodic Anoxic Disturbances. *Environmental Science & Technology, 44*(19), 7245-7253. doi:10.1021/es100564j

Kowalchuk, G. A., & Stephen, J. R. (2001). AMMONIA-OXIDIZING BACTERIA: A Model for Molecular Microbial Ecology. *Annual Review of Microbiology, 55*(1), 485. doi:10.1146/annurev.micro.55.1.485

Kuba, T., Van Loosdrecht, M. C. M., Brandse, F. A., & Heijnen, J. J. (1997). Occurrence of denitrifying phosphorus removing bacteria in modified UCT-type wastewater treatment plants. *Water Research, 31*(4), 777-786. doi:https://doi.org/10.1016/S0043-1354(96)00370-3

Kuba, T., VanLoosdrecht, M. C. M., & Heijnen, J. J. (1996). Phosphorus and nitrogen removal with minimal cod requirement by integration of denitrifying dephosphatation and nitrification in a two-sludge system. In (Vol. 30, pp. 1702-1710).

Kujawa, K., & Klapwijk, B. (1999). A method to estimate denitrification potential for predenitrification systems using NUR batch test. In (Vol. 33, pp. 2291-2300).

Laureni, M., Weissbrodt, D. G., Villez, K., Robin, O., de Jonge, N., Rosenthal, A., . . . Joss, A. (2019). Biomass segregation between biofilm and flocs improves the control of nitrite-oxidizing bacteria in mainstream partial nitritation and anammox processes. *Water Research, 154*, 104-116. doi:10.1016/j.watres.2018.12.051

Levin, G. V., Shaheen, D. G., Topol, G. J., & Tarnay, A. G. (1974). Discussion: Pilot Plant Tests for Phosphate Removal Processes. *Journal (Water Pollution Control Federation), 46*(2), 404-408.

López-Vázquez, C. M., Hooijmans, C. M., Brdjanovic, D., Gijzen, H. J., & van Loosdrecht, M. C. M. (2008). Factors affecting the microbial populations at full-scale enhanced biological phosphorus removal (EBPR) wastewater treatment plants in The Netherlands. *Water Research, 42*(10), 2349-2360. doi:https://doi.org/10.1016/j.watres.2008.01.001

Lu, H., Chandran, K., & Stensel, D. (2014). Review: Microbial ecology of denitrification in biological wastewater treatment. *Water Research, 64*, 237-254. doi:10.1016/j.watres.2014.06.042

Lu, H., Oehmen, A., Virdis, B., Keller, J., & Yuan, Z. (2006). Obtaining highly enriched cultures of Candidatus Accumulibacter phosphates through alternating carbon sources. *Water Research, 40*, 3838-3848. doi:10.1016/j.watres.2006.09.004

Marques, R., Santos, J., Nguyen, H., Carvalho, G., Noronha, J. P., Nielsen, P. H., . . . Oehmen, A. (2017). Metabolism and ecological niche of Tetrasphaera and Ca. Accumulibacter in enhanced biological

phosphorus removal. *Water Research, 122*, 159-171. doi:https://doi.org/10.1016/j.watres.2017.04.072

McIlroy, S. J., Onetto, C. A., McIlroy, B., Herbst, F.-A., Dueholm, M. S., Kirkegaard, R. H., . . . Nielsen, P. H. (2018a). Genomic and in Situ Analyses Reveal the Micropruina spp. as Abundant Fermentative Glycogen Accumulating Organisms in Enhanced Biological Phosphorus Removal Systems. *Frontiers in Microbiology*.

McIlroy, S. J., Onetto, C. A., McIlroy, B., Herbst, F.-A., Dueholm, M. S., Kirkegaard, R. H., . . . Nielsen, P. H. (2018b). Genomic and in Situ Analyses Reveal the Micropruina spp. as Abundant Fermentative Glycogen Accumulating Organisms in Enhanced Biological Phosphorus Removal Systems. In (Vol. 9).

Menes, R. J., Viera, C. E., Farías, M. E., & Seufferheld, M. J. (2011). Halomonas vilamensis sp. nov., isolated from high-altitude Andean lakes. *International Journal Of Systematic And Evolutionary Microbiology, 61*(Pt 5), 1211-1217. doi:10.1099/ijs.0.023150-0

Miao, L., & Liu, Z. (2018). Microbiome analysis and -omics studies of microbial denitrification processes in wastewater treatment: recent advances. In (Vol. 61, pp. 753-761).

Mulder, A., Vandegraaf, A. A., Robertson, L. A., & Kuenen, J. G. (1995). ANAEROBIC AMMONIUM OXIDATION DISCOVERED IN A DENITRIFYING FLUIDIZED-BED REACTOR. In (Vol. 16, pp. 177-183).

Nan, X., Ma, B., Qian, W., Zhu, H., Li, X., Zhang, Q., & Peng, Y. (2019). Achieving nitritation by treating sludge with free nitrous acid: The effect of starvation. *Bioresource Technology, 271*, 159-165. doi:10.1016/j.biortech.2018.09.113

Nifong, A., Nelson, A., Johnson, C., & B. Bott, C. (2013). *Performance of a Full-Scale Sidestream DEMON® Deammonification Installation* (Vol. 2013).

O'Shaughnessy, M. (2016). *Mainstream Deammonification*. London, UNITED KINGDOM: IWA Publishing.

Oehmen, A., Teresa Vives, M., Lu, H., Yuan, Z., & Keller, J. (2005). The effect of pH on the competition between polyphosphate-accumulating organisms and glycogen-accumulating organisms. *Water Research, 39*, 3727-3737. doi:10.1016/j.watres.2005.06.031

Park, M. R., & Chandran, K. (2016). *Impact of Hydroxylamine Exposure on Anabolism and Catabolism in Nitrospira Spp.* Paper presented at the WEF/IWA Nutrient Removal and Recovery, Denver, CO.

Regmi, P., Miller, M. W., Holgate, B., Bunce, R., Park, H., Chandran, K., . . . Bott, C. B. (2014). Control of aeration, aerobic SRT and COD input for mainstream nitritation/denitritation. *Water Research, 57*, 162-171. doi:https://doi.org/10.1016/j.watres.2014.03.035

Rubio-Rincón, F. J., Lopez-Vazquez, C. M., Welles, L., van Loosdrecht, M. C. M., & Brdjanovic, D. (2017). Cooperation between Candidatus Competibacter and Candidatus Accumulibacter clade I, in denitrification and phosphate removal processes. *Water Research, 120*, 156-164. doi:https://doi.org/10.1016/j.watres.2017.05.001

Salazar-Benites, G. M. (2017). *Quantifying cyanide inhibition of nitritification and developing cost-effective treatment processes.* Old Dominion University,

Schuler, A. J., & Jenkins, D. (2003). Enhanced Biological Phosphorus Removal from Wastewater by Biomass with Different Phosphorus Contents, Part I: Experimental Results and Comparison with Metabolic Models. *Water Environment Research, 75*(6), 485-498.

Siegrist, H., Salzgeber, D., Eugster, J., & Joss, A. (2008). Anammox brings WWTP closer to energy autarky due to increased biogas production and reduced aeration energy for N-removal. *Water Science and Technology, 57*(3), 383-388. doi:10.2166/wst.2008.048

Sliekers, A. O., Haaijer, S. C. M., Stafsnes, M. H., Kuenen, J. G., & Jetten, M. S. M. (2005). Competition and coexistence of aerobic ammonium- and nitrite-oxidizing bacteria at low oxygen concentrations. *Applied Microbiology & Biotechnology, 68*(6), 808-817. doi:10.1007/s00253-005-1974-6

Tooker, N. B., Barnard, J., Bott, C., Carson, K., Dombrowski, P., Dunlap, P., . . . Gu, A. (2017). *Side-Stream Enhanced Biological Phosphorus Removal As A Sustainable And Stable Approach For Removing Phosphorus From Wastewater.* Paper presented at the WEFTEC.

Vadivelu, V. M., Yuan, Z., Fux, C., & Keller, J. (2006). The Inhibitory Effects of Free Nitrous Acid on the Energy Generation and Growth Processes of an Enriched Nitrobacter Culture. *Environmental Science & Technology, 40*(14), 4442-4448. doi:10.1021/es051694k

Van Loosdrecht, M. C. M., & Henze, M. (1999). Maintenance, endogeneous respiration, lysis, decay and predation. *Water Science and Technology, 39*(1), 107-117. doi:10.1016/S0273-1223(98)00780-X

Vocks, M., Adam, C., Lesjean, B., Gnirss, R., & Kraume, M. (2005). Enhanced post-denitrification without addition of an external carbon source in membrane bioreactors. *Water Research, 39*(14), 3360-3368. doi:https://doi.org/10.1016/j.watres.2005.05.049

Wang, Q., Wang, Y., Lin, J., Tang, R., Wang, W., Zhan, X., & Hu, Z.-H. (2018). Selection of seeding strategy for fast start-up of Anammox process with low concentration of Anammox sludge inoculum. *Bioresource Technology, 268*, 638-647. doi:10.1016/j.biortech.2018.08.056

Welles, L., Tian, W. D., Saad, S., Abbas, B., Lopez-Vazquez, C. M., Hooijmans, C. M., . . . Brdjanovic, D. (2015). Accumulibacter clades Type I and II performing kinetically different glycogen-accumulating organisms metabolisms for anaerobic substrate uptake. *Water Research, 83*, 354-366. doi:https://doi.org/10.1016/j.watres.2015.06.045

Wende, T., Weiguang, L., Hui, Z., & Zheng, Y. (2010, 17-18 July 2010). *Affecting factors and control strategies of the competition of phosphorus accumulating organisms (PAO) and glycogen accumulating organisms (GAO) in enhanced biological phosphorus removal.* Paper presented at the 2010 The 2nd Conference on Environmental Science and Information Application Technology.

Wett, B. (2006). Solved upscaling problems for implementing deammonification of rejection water. In (Vol. 53, pp. 121-128).

Wett, B. (2007). Development and implementation of a robust deammonification process. *Water science and technology : a journal of the International Association on Water Pollution Research*(7).

Wett, B., & Rauch, W. (2003). The role of inorganic carbon limitation in biological nitrogen removal of extremely ammonia concentrated wastewater. *Water Research, 37*(5), 1100-1110. doi:https://doi.org/10.1016/S0043-1354(02)00440-2

Whang, L. M., Filipe, C. D. M., & Park, J. K. (2007). Model-based evaluation of competition between polyphosphate- and glycogen-accumulating organisms. *Water Research, 41*, 1312-1324. doi:10.1016/j.watres.2006.12.022

Winkler, M., Bassin, J., Kleerebezem, R., Sorokin, D., & Loosdrecht, M. (2012). Unravelling the reasons for disproportion in the ratio of AOB and NOB in aerobic granular sludge. *Applied Microbiology & Biotechnology, 94*(6), 1657-1666. doi:10.1007/s00253-012-4126-9

Wu, L., Li, Z., Zhao, C., Liang, D., & Peng, Y. (2018). A novel partial-denitrification strategy for post-anammox to effectively remove nitrogen from landfill leachate. *Science of the Total Environment, 633*, 745-751. doi:10.1016/j.scitotenv.2018.03.213

Yuan, Z., Pratt, S., & Batstone, D. J. (2012). Phosphorus recovery from wastewater through microbial processes. *Current Opinion in Biotechnology, 23*(6), 878-883. doi:10.1016/j.copbio.2012.08.001

Yunhong, K., Nielsen, J. L., & Nielsen, P. H. (2004). Microautoradiographic Study of Rhodocyclus-Related Polyphosphate-Accumulating Bacteria in Full-Scale Enhanced Biological Phosphorus Removal Plants. *Applied & Environmental Microbiology, 70*(9), 5383-5390. doi:10.1128/AEM.70.9.5383-5390.2004

Zeng, R. J., van Loosdrecht, M. C. M., Yuan, Z., & Keller, J. (2003). Metabolic model for glycogen-accumulating organisms in anaerobic/aerobic activated sludge systems. *Biotechnology and Bioengineering, 81*(1), 92-105. doi:10.1002/bit.10455

Zhang, Y., Li, M., Zhang, Q., Sang, W., & Jiang, Y. (2018). Start-up performance of anaerobic/aerobic/anoxic-sequencing batch reactor (SBR) augmented with denitrifying polyphosphate-accumulating organism (DPAO) and their gene analysis. In (Vol. 78, pp. 523-533).

Zhao, J., Wang, X., Li, X., Jia, S., Wang, Q., & Peng, Y. (2019). Improvement of partial nitrification endogenous denitrification and phosphorus removal system: Balancing competition between phosphorus and glycogen accumulating organisms to enhance nitrogen removal without initiating phosphorus removal deterioration. *Bioresource Technology, 281*, 382-391. doi:https://doi.org/10.1016/j.biortech.2019.02.109